

## **General Disclaimer**

### **One or more of the Following Statements may affect this Document**

- This document has been reproduced from the best copy furnished by the organizational source. It is being released in the interest of making available as much information as possible.
- This document may contain data, which exceeds the sheet parameters. It was furnished in this condition by the organizational source and is the best copy available.
- This document may contain tone-on-tone or color graphs, charts and/or pictures, which have been reproduced in black and white.
- This document is paginated as submitted by the original source.
- Portions of this document are not fully legible due to the historical nature of some of the material. However, it is the best reproduction available from the original submission.



**American Science  
and Engineering, Inc.**

955 Massachusetts Avenue  
Cambridge, Massachusetts 02139  
617-868-1600

31 DECEMBER 1974

ASE 3654

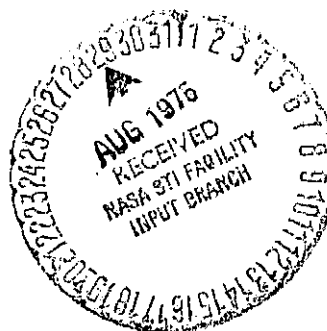
**SMALL ASTRONOMY  
SATELLITE-A,  
UHURU DATA ANALYSIS  
FINAL REPORT**

FINAL REPORT FOR PERIOD  
12 DECEMBER 1970 TO 31 DECEMBER 1974

CONTRACT NO. NAS5-11422

PREPARED FOR :

NATIONAL AERONAUTICS AND  
SPACE ADMINISTRATION  
GODDARD SPACE FLIGHT CENTER  
GREENBELT, MARYLAND 20771



N75-29964

Unclas  
33405

CSCI 03A G3/89

(NASA-CR-144660) SMALL ASTRONOMY  
SATELLITE-A, UHURU DATA ANALYSIS Final  
Report, 12 Dec. 1970 - 31 Dec. 1974  
(American Science and Engineering, Inc.)  
168 p HC \$6.25

SMALL ASTRONOMY SATELLITE-A, UHURU  
DATA ANALYSIS FINAL REPORT

Prepared by:

D. Koch  
American Science and Engineering, Inc.  
955 Massachusetts Avenue  
Cambridge, Massachusetts 02139

31 December 1974

FINAL REPORT for Period 12 December 1970 to 31 December 1974

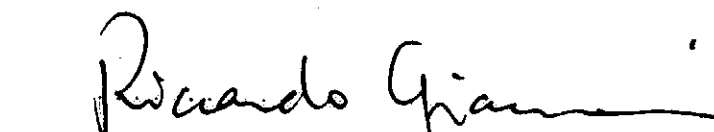
Contract No. NAS5-11422

Prepared for:

National Aeronautics and Space Administration  
Goddard Space Flight Center  
Greenbelt, Maryland 20771

Approved:

  
D. Koch (Project Scientist)

  
R. Giacconi (Principal Investigator)

TECHNICAL REPORT STANDARD TITLE PAGE

1. Report No. 44	2. Government Accession No.	3. Recipient's Catalog No.
4. Title and Subtitle Small Astronomy Satellite A, Uhuru, Data Analysis Final Report		5. Report Date 31 December 1974
		6. Performing Organization Code
7. Author(s) D. Koch	8. Performing Organization Report No. ASE-3654	
9. Performing Organization Name and Address American Science and Engineering, Inc. 955 Massachusetts Avenue Cambridge, Massachusetts 02139		10. Work Unit No.
		11. Contract or Grant No. NAS5-11422
12. Sponsoring Agency Name and Address Mr. Anthony J. Caporale, Code 701.4 NASA, Goddard Space Flight Center Greenbelt, Maryland 20771		13. Type of Report and Period Covered Final Report 12 Dec. 1970-31 Dec. 74
14. Sponsoring Agency Code		
15. Supplementary Notes		
16. Abstract <p>This is the Final Report for NASA Contract NAS5-11422. In broad terms the objectives performed under this contract were to conduct observations with the first satellite entirely devoted to X-ray astronomy and to analyze the results obtained. A catalog of X-ray sources was generated and results of discoveries and further detailed observations of sources were presented in scientific journals and meetings.</p> <p>This report contains a list of the objectives and how they were met, a brief description of the instrument, a selection of significant results, the X-ray catalog and a complete bibliography of results presented under this contract.</p>		
17. Key Words (Selected by Author(s))  X-ray sources X-ray astronomy		18. Distribution Statement
19. Security Classif. (of this report) Unclassified	20. Security Classif. (of this page)	21. No. of Pages 167
22. Price*		



## PREFACE

This is the Final Report for NASA Contract NAS5-11422. In broad terms the objectives performed under this contract were to conduct observations with the first satellite entirely devoted to X-ray astronomy and to analyze the results obtained. A catalog of X-ray sources was generated and results of discoveries and further detailed observations of sources were presented in scientific journals and meetings.

This report contains a list of the objectives and how they were met, a brief description of the instrument, a selection of significant results, the X-ray catalog and a complete bibliography of results presented under this contract.

## CONTENTS

<u>Section</u>	<u>Page</u>
1.0 INTRODUCTION	1-1
2.0 INSTRUMENT DESCRIPTION AND SATELLITE OPERATIONS	2-i
2.1 Instrumentation	2-1
2.2 Operations	2-5
3.0 GALACTIC X-RAY SOURCES	3-1
3.1 Hercules X-1	3-4
3.1.1 Observations	3-4
3.1.2 Discussion	3-17
3.2 Centaurus X-3	3-21
3.3 Cygnus X-1	3-26
3.4 2U 0900-40	3-36
3.4.1 Introduction	3-36
3.4.2 Observations	3-37
3.4.3 Discussion	3-41
3.5 2 U 1700-37	3-45
3.5.1 Introduction	3-45
3.5.2 Observations	3-46
3.5.3 Discussion	3-51
3.6 Cygnus X-3	3-57
3.7 SMC X-1	3-65
3.7.1 Introduction	3-65
3.7.2 Observations	3-65
3.7.3 Discussion	3-71
3.8 Scorpius X-1	3-76
3.9 Cygnus X-2	3-88
4.0 EXTRAGALACTIC X-RAY ASTRONOMY	4-1
4.1 Introduction	4-1
4.2 Identified Sources	4-1
5.0 NEW TECHNOLOGY	5-1
6.0 BIBLIOGRAPHY	6-1
APPENDIX: THE UHURU CATALOG OF X-RAY SOURCES	A-1

## ILLUSTRATIONS

<u>Figure</u>	<u>Page</u>
2-1 Major Elements of the UHURU Instrumentation	2-2
2-2 Band of the Sky Swept by the Two Detectors During One Revolution of the Satellite	2-3
3-1 Hercules 2-6 keV Intensity Data	3-5
3-2 Measurements of the Hercules Heliocentric Pulsation Period in Seconds During Five of the "on" States of the 35-Day Period	3-7
3-3 Hercules Intensity Data During Three "on" States	3-9
3-4a Difference in Days Between the Observed Turn- on Times of the Hercules on States and What Would be Predicted by a Constant 34.88 -Day Trial Period	3-11
3-4b Absolute Range of Each Turn-on Time Plotted as a Function of Orbital Phase	3-11
3-5 Four Counting Rate Spectra Obtained During Different Parts of the 1972 January High State	3-14
3-6 Hercules X-1 Intensity Dips	3-16
3-7 X-ray Variability of Cen X-3	3-22
3-8 Observations of Cygnus X-1 on 10 June 1971	3-27
3-9 X-ray Location of Cygnus X-1	3-28
3-10 Cygnus X-1 Folded Intensity, 17 December 1971 to 21 January 1972	3-30
3-11 16 Months of Observations of Cygnus X-1	3-32
3-12 2 - 6 keV Intensity of 2U 0900-40	3-38
3-13 2 - 6 keV Intensity of 2U 0900-40, March 17, 1971	3-40
3-14 Location of 2U 0900-40	3-42
3-15 2 - 6 keV Intensity of 2U 1700-37	3-47
3-16 Location of 2U 1700-37	3-50
3-17 Observations of Cygnus X-3 from 8 May to 17 May	3-58
3-18 Counting Rate Data for Cygnus X-3	3-59

# ILLUSTRATIONS ( cont'd)

<u>Figure</u>		<u>Page</u>
3-19	Average 2 - 6 keV Intensity for Cygnus X-3 on Various Days from January 1971 until July 1971	3-61
3-20	2 - 6 keV X-ray Intensity for Cygnus X-3 in late August and Early September 1972	3-62
3-21	Intensity of SMC X-1 in Observed Counts/Sec During Eight Days in January and Three Days in June 1971	3-67
3-22	Typical Energy Spectra of Four Binary Sources	3-73
3-23	Simultaneous X-ray, Optical, and Radio Observations for SCO X-1 on 22-25 February 1971	3-77
3-24	Same as Figure 3-23 Except for 26 February-1 March 1971	3-78
3-25	Same as Figure 3-23 Except for 23-26 March 1971	3-79
3-26	Same as Figure 3-23 Except for 27-30 March 1971	3-81
3-27	Sco X-1 Brightness Histogram 23-28 March 1971	3-83
3-28	Simultaneous X-ray-Optical Variability of Sco X-1	3-84
3-29	Temperature Versus X-ray Intensity for Sco X-1	3-85
3-30	X-ray Position of Cygnus X-2	3-89
4-1	The X-ray Sources in the UHURU Catalog	4-2
4-2	Identified Extragalactic X-ray Sources	4-3
4-3	Locations of Two UHURU Sources Identified with Distant Radio Galaxies	4-5
4-4	X-ray Sources in Clusters of Galaxies	4-6
4-5	Sizes and X-ray Luminosities of Extragalactic X-ray Sources	4-8
4-6	Luminosity Versus Velocity Dispersion for X-ray Sources in Clusters	4-9
4-7	Spectra of Extragalactic Sources	4-11
4-8	Centaurus A	4-13

<u>Figure</u>	ILLUSTRATIONS (cont'd)	<u>Page</u>
4-9	Unidentified High Latitude X-ray Sources	4-14
4-10	Galactic Latitude Distribution of Unidentified X-ray Sources	4-15
4-11	Integral Distribution of Number of Sources vs Strength	4-17
4-12	Point to Point Count Rate Differences	4-18
4-13	Contributions to the Diffuse X-ray Background (2 - 6 keV)	4-19

## TABLES

<u>Table No.</u>		<u>Page</u>
3.1	Characteristics of X-ray Binaries	3-2
3.2	Characteristics of X-ray Sources	3-3
3.3	Characteristics of X-ray Binaries	3-54
3.4	Properties of Some X-ray Binaries	3-72

## 1.0 INTRODUCTION

The first satellite entirely devoted to the study of cosmic X-ray sources was placed into orbit on 12 December 1970 from the San Marco launch platform off the coast of Kenya by the Centro Ricerche Aerospaziali. The satellite is the first of a series of small astronomy satellites sponsored by the National Aeronautics and Space Administration. December 12 was the seventh anniversary of the Kenyan Independence, and in recognition of the kind hospitality of the Kenyan people, the operating satellite has been named "Uhuru" (Swahili for "Freedom").

This document is the Final Report for NASA Contract NAS5-11422. The scientific objectives of the original post-launch proposal (ASE-2484) are summarized as follows:

### 1. All-Sky Survey

Systematically survey in a period of about one month the entire sky for sources emitting X-rays in the energy range 2 - 20 keV. Expected location accuracies range from 1 arc minute for stronger sources to 25 arc minutes (radius of position error circle) for sources at the minimum detectable sensitivity of about  $5 \times 10^{-5}$  Sco X-1. At the same time map the cosmic X-ray background with a statistical precision of about 2 percent on a scale of 25 square degrees or 20 percent on a scale of 2.5 square degrees and look for isotropy.

### 2. Time Variations

Study time variations of X-ray sources such as occasional outbursts, changes over hours or days, sudden appearances of a source, rapid fluctuations about a constant mean brightness, slow decay over months, and changes on time scales of seconds or less for strong sources.

### 3. Spectral Measurements

Measure energy spectra of sources out to a maximum energy depending on source strength.

### 4. X-Ray - Visible Correlated Studies

Make X-ray location measurements, communicate the locations to optical astronomers, make reasonably certain optical identifications, schedule and carry out simultaneous X-ray-optical observations.

### 5. Time Correlations (not with optical)

Simultaneous measurements at X-ray and other wavelengths such as radio, IR, XUV, higher energy X-ray and  $\gamma$ -ray.

### 6. Transient Phenomena

Maneuver satellite to observe supernova outbursts. Monitor data for outbursts seen only in X-rays such as Cen XR-2 and Cen XR-4.

### 7. Interpretation of X-Ray Observations

Obtain distributions of sources versus measured parameters such as source temperature, intensity, time variability and location. Construct phenomenological models to explain overall electromagnetic emission of sources.

Everyone of these objectives has been met, in many cases with results far beyond what was anticipated. The following are some of the major findings from the data:

1. A third Uhuru catalog of X-ray Sources has been produced containing 161 sources, with nearly complete sky coverage to 10 counts per second sensitivity. The catalog gives the location, intensity, any unusual properties and indicates correlations in other portions of the electromagnetic spectrum.
2. The discovery of what is probably the first black hole (Cyg X-1) representing the most condensed state of matter possible.



3. The discovery of binary X-ray pulsars, Cen X-3 and Her X-1, which emit pulses of X-rays every few seconds, coupled with other examples of bizarre behavior.
4. The detection of X-ray emission from clusters of galaxies.
5. The detection of X-ray objects at high galactic latitudes with no optical counterpart, hence implying a very high X-ray to optical luminosity and possibly belonging to a new class of objects, "X-Ray Galaxies, " not anticipated prior to the launching of UHURU.

This document contains a description of the instrument, the results on galactic X-ray sources, the results on extragalactic X-ray sources, an Appendix containing a reproduction of The Third Uhuru Catalog of X-ray Sources and a Bibliography containing a list of all the publications made under this contract.

## 2.0 INSTRUMENT DESCRIPTION AND SATELLITE OPERATIONS

Uhuru was launch 12 December 1970 from the San Marco launch platform. Uhuru is in a nearly equatorial circular orbit of about 560 km apogee and 520 km perigee and  $3^{\circ}$  inclination with a period of 96 minutes. The use of large area counters and the long time available for observations permit us to study the X-ray sky with a qualitative improvement upon the sensitivity and completeness achieved by previous rocket and satellite experiments. In addition, the capability to steer the spin axis to a desired orientation in the sky permits us to perform conveniently X-ray measurements on a specific object in conjunction with visible and radio ground observations. In this sense we can consider Uhuru as a true X-ray observatory.

### 2.1 Instrumentation

Figure 2-1 illustrates the major elements of the experimental portion of the satellite containing the X-ray detectors and aspect sensors. The spacecraft spins at a nearly constant rate of one revolution per 720 seconds. On command from the ground the spin axis can be oriented to a particular location on the celestial sphere by means of magnetic torquing. A new orientation of the spin axis can, in general, be achieved in a few orbits. Figure 2-2 shows the band of the sky which is scanned during each spin for any given orientation.

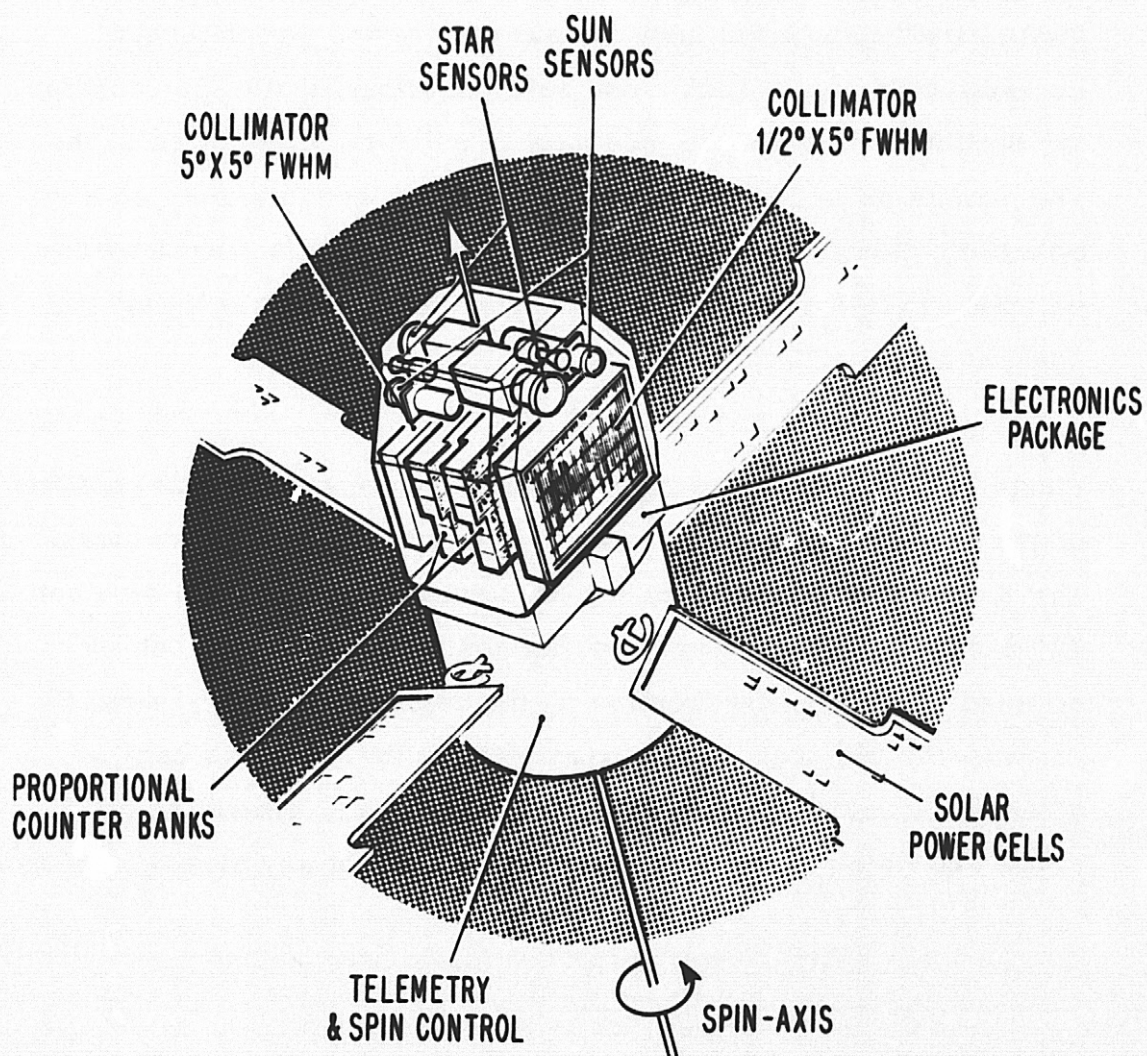


Figure 2-1

Major Elements of the UHURU Instrumentation

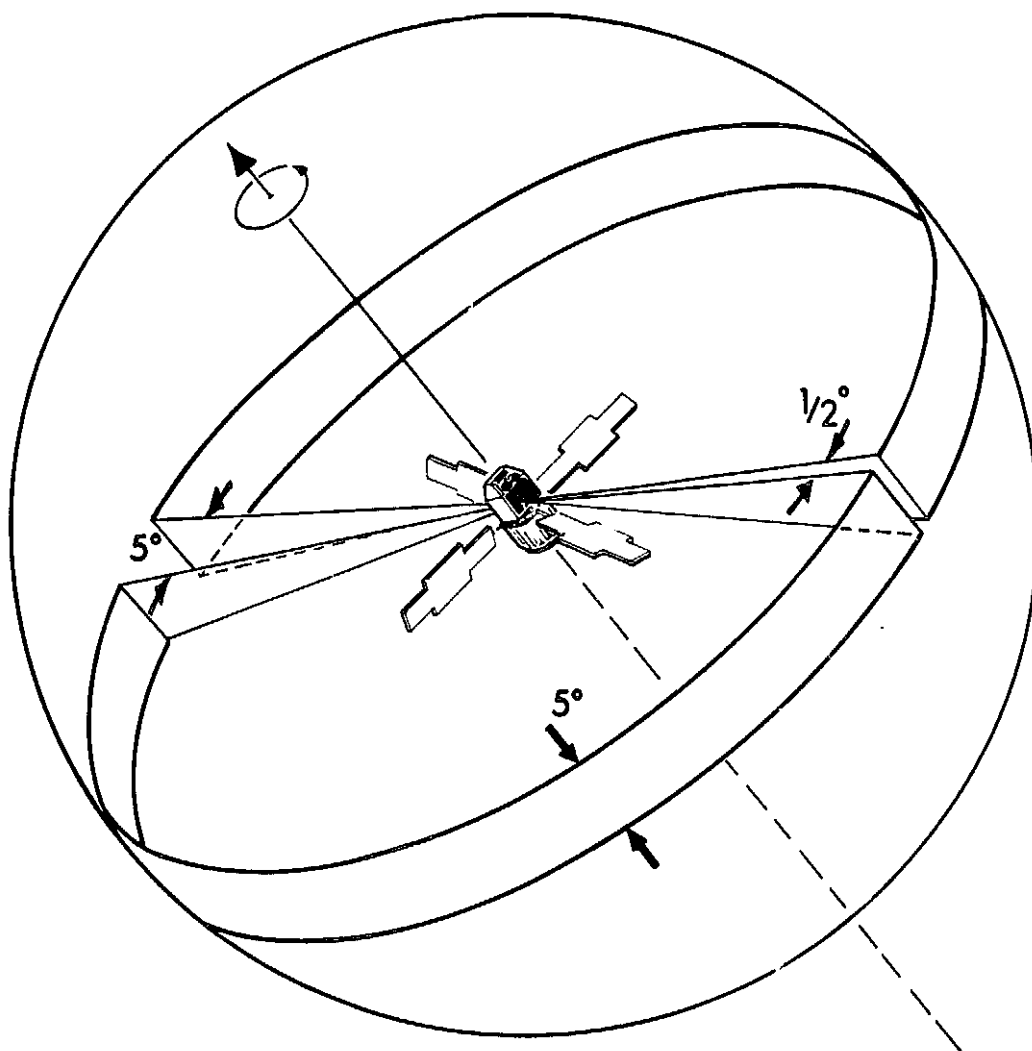


Figure 2-2

Band of the sky swept by the two detectors during one revolution of the satellite. The fields of view indicated are full width at half maximum. The full width of the band of sky scanned, taking into account the offset of detectors and the precise values of the fields of view is of  $12.7^\circ$ .

The X-ray detectors consist of two sets of proportional counters each with about  $840 \text{ cm}^2$  effective area. The counters are sensitive with  $> 10\%$  efficiency to X-ray photons in the 1.7 to 18 keV range. The lower limit is determined by the attenuation of the beryllium windows of the counter plus a thin thermal shroud that is needed to maintain the temperature stability of the spacecraft. The upper limit is determined by the transmission properties of the filling gas. Pulse shape discrimination and anticoincidence techniques are used to reduce the background due to particles and high energy photons. Pulse height analysis in eight channels is used to obtain information on the energy distribution of the incident photons. An in-flight calibration system utilizing X-rays from a  $^{55}\text{Fe}$  radioactive source and fluorescent X-rays from Zr excited by a radioactive  $^{147}\text{Pm}$  source, is used to monitor the efficiency and gain stability of the counters.

The two sets of counters are placed back to back and are collimated to  $0.52^\circ \times 5.2^\circ$  and  $5.2^\circ \times 5.2^\circ$  (full width at half maximum) respectively. The center of the fields of view of the two detector banks are displaced from the equatorial plane of the satellite at respective angles of  $88.9^\circ$  and  $91.2^\circ$  from the spin axis. (The full width of the band in the sky covered by the two detectors during each spin is therefore  $12.7^\circ$ ). This arrangement allows us to evaluate roughly the elevation of isolated sources in a single pass. While the  $1/2^\circ$  detector yields a finer angular resolution, the  $5^\circ$  detector yields high sensitivity for isolated sources. The precise value of the increase in sensitivity depends on the nature and value of the background and on the angular extent of the source.

Two identical and independent visible light star sensors are rigidly mounted to each of the two collimators, as shown in Figure 2-1. Star images are focused onto an "N" shaped slit located in front of a photomultiplier. Traversal of a star results in a triplet of signals whose time sequence is analyzed for two-dimensional aspect information to a typical accuracy of one arc minute. Two sun sensors of similar design are also included to provide

aspect information in the sunlit portion of the orbit.

Data from the  $1/2^\circ$  detector consist of total counts in the energy band 2.4-6.9 keV accumulated during successive sampling intervals of 0.096 seconds. With a scan rate of  $0.5^\circ/\text{sec}$  there are about 10 samples for every  $0.5^\circ$  element of angular resolution. In addition, the counts accumulated in each of eight channels of pulse height from 1.2 to 20 keV are sampled every 0.192 seconds. Data from the  $5^\circ$  detector are obtained in a similar fashion but over sampling intervals of 0.384 seconds. Analog voltage signals from the star sensors are sampled every 0.048 seconds. When the sun is within the field of view, sun sensor data are sampled instead. Data are telemetered in real time at 1 kHz and, in addition, a whole orbit of data is recorded for delayed transmission at 30 kHz while the spacecraft passes over the principal ground receiving station at Quito, Ecuador.

A complete technical description of the instrument is given elsewhere.

N. Jagoda, G. Austin, S. Mickiewicz, R. Goddard. IEEE Trans. NS 19, 579 (1972)

## 2.2 Operations

The X-ray detection portion of Uhuru has operated faultlessly over its entire four year life time, demonstrating the longevity of proportional counters and associated equipment. However, difficulties in data transmission occurred on December 27, 1970, and on January 23, 1971. On the first date telemetry transmission ceased. The temperature of the spacecraft depends on the angle of the spin axis to the Sun and is at a maximum when the spin axis is  $90^\circ$  to the Sun. Since at the time of failure the spacecraft was in its maximum temperature condition (about  $85^\circ\text{F}$ ), it was conjectured that this could have caused the failure. Upon achieving a lower temperature (about  $75^\circ\text{F}$ ) condition with the spin axis at approximately  $30^\circ$  to the Sun, the telemetry transmission was fully restored. Although the cause for this failure was not understood, a recurrence has thus far been avoided by maintaining the spin

axis within a  $30^{\circ}$  cone of the Sun. Hence the pointing capability of the spacecraft has been restricted resulting in a considerable modification of the original observing program.

On January 23, the tape recorder failed making it necessary to rely exclusively on the real time data transmission. Consequently several other receiving stations along the equator have been requested to record data from Uhuru. This extended coverage has allowed the recovery of at least half of the data obtained in each orbit.

The transmitter has continued to be a problem with further fears of total loss occurring in June and July of 1971. In December 1971, after a year of operation, it was found that the star sensors no longer performed satisfactorily, most likely due to damage to the reticle pattern caused by exposure to the Sun. Since the Sun sensors and spacecraft magnetometer are perfectly functional, they will be used in post December 1971 observations requiring a superposition capability. A long radioactive calibration showed the X-ray detectors and electronics still operating with no degradation.

During April 1973 the battery on the spacecraft failed which caused the loss of the rotor (stability was maintained by speeding up the spacecraft spin rate to  $5^{\circ}$ /second) and the loss of the transmitter output stage (resulting in a weak signal receivable only at Quito). By switching to Solar-Only status, daytime data was obtained. The entire month was spent searching for ways to increase the amount of usable data. On April 26, 1973, we oriented the satellite to the galactic plane, and detected the strong galactic sources, thus assuring us that the onboard X-ray detectors were still functional.

### 3.0 GALACTIC X-RAY SOURCES

Of the currently known sources (Giacconi et al., 1974), about 100 are galactic, 33 are tentatively identified (of which 24 are stars), 4 are globular clusters, and 5 are supernova remnants. About 60 are extragalactic, of which 20 are clusters of galaxies, 8 are active galaxies, and 1 or 2 are QSO's. Also, about 30 sources well off the galactic plane are as yet unidentified and may be an entirely new type of object. Of the galactic sources, the properties of the more interesting and well studied sources are given in Tables 3.1 and 3.2. The source SMC X-1 is included even though it is located in another galaxy of the local group since it has many characteristics similar to sources in the Galaxy.



Table 3.1  
**Characteristics of X-ray Binaries**

<u>Source</u>	<u>Binary Period (days)</u> <u>Center of Occultation</u>	<u>Eclipse duration</u> <u>Transition duration</u> <u>(days)</u>	<u>Velocity of x-ray</u> <u>source (Km/sec)</u>	<u>Approximate</u> <u>percentage</u> <u>pulsed, possibly</u> <u>non-periodic</u>	<u>Approximate</u> <u>mass of X-rays</u> <u>source (Mo)</u>
Her X-1	1.700165 $\pm$ 0.000002 1972 Nov. 22.60587	0.24 $\pm$ 0.1 0.025	169.2 $\pm$ 0.4	80%	0.2 - 1.2
Cen X-3	2.08712 $\pm$ 0.00004 1972 Sept. 14.056	0.48 $\pm$ 0.012 0.035 $\pm$ 0.007	415.1 $\pm$ 0.4	70%, variable	0.3 - 0.2
Cyg X-1	5.5999 $\pm$ 0.0009*	none	68.2 $\pm$ 1.7*	< 50%	10 - 20
3U0900 - 40	8.95 $\pm$ 0.02 1972 May 9.04	1.90 $\pm$ 0.05 undefined	26 $\pm$ 6*	$\leq$ 10%	
3U1700 - 37	3.412 $\pm$ 0.002 1972 May 15.64	1.10 $\pm$ 0.07 undefined	23 $\pm$ 5*	$\leq$ 17%	
SMC X-1	3.8927 $\pm$ 0.0010 1971 Jan. 12.99	0.60 $\pm$ 0.04 $\leq$ 0.1	?	$\leq$ 10%	
Cyg X-3	0.199667 $\pm$ 0.000014	The eclipse is not total	unknown		

\* Values derived from observations of the optical candidate. The velocity figure applies not to the X-ray source but to its visible companion.

Table 3.2

## CHARACTERISTICS OF X-RAY SOURCES

Source	Location <u><math>\delta</math></u>	Short-term Variability	Long-term Variability	Power Law Energy Index	Cutoff (keV)	Intensity		Optical Candidate	Peak Luminosity 2 - 10 keV erg/sec
						Max (c/s)	Max. Min.		
Her X-1 (3U1653 + 35)	58.26 38.12	1.23782 sec pulsations	Extended lows $34.85 \pm 1.70$ day period; turn on 1973 March $1.4 \pm 0.1$	-1.3 $\rightarrow$ 0.2	1.5 $\rightarrow$ 3.2	100	$\geq 6$	H $\gamma$ Her 15 - 13 mag.	$1 \times 10^{37}$
Cen X-3 (3U1118 - 60)	292.07 0.36	4.842 sec pulsations	Extended lows	-0.4 $\rightarrow$ +0.6	1.5 $\rightarrow$ 4.2	160	$\geq 20$	?	?
Cyg X-1 (3U1956 + 35)	71.32 3.08	Quasi-periodic pulsations on scales of milliseconds	Single low - energy tran- sition	2.8 $\rightarrow$ 4.1 before tran- sition 0.45 after tran- sition	$\leq 1.5$	1175	5	HDE226868 B01b 9 mag.	$1 \times 10^{37}$ before transition  $3 \times 10^{36}$ after transition
3U0900 - 40 (GX263 + 3)	263.07 3.93	Non-periodic pulsations on times of sec.	No extended lows	-0.2 $\rightarrow$ +0.7	2.5 $\rightarrow$ 4.4	100	10	HD77581 B051b 6 mag.	$4 \times 10^{36}$
3U1700 - 37	347.75 2.19	Non-periodic pulsations on times as short as 0.1 sec.	No extended lows	-0.4 $\rightarrow$ +1.0	2.1 $\rightarrow$ 5.5	102	$\geq 3$	HD153919 B007f 6 mag.	$3 \times 10^{36}$
Cyg X-3 (3U2030 + 40)	79.84 0.71	No pulsations observed on times of sec.	Transitions possibly similar to Cyg X-1	0.4 $\rightarrow$ 1.6	2.9 $\rightarrow$ 4.0	194	$\geq 3$	No optical; Radio and IR source	$6 \times 10^{37}$
SMC X-1 (3U0115 - 73)	300.45 -43.58	Non-periodic on times of min.	Extended lows	0.0 $\rightarrow$ 0.3	1.5 $\rightarrow$ 3.0	28	$\geq 9$	Sk160 B01b 13 mag.	$3 \times 10^{38}$
Sco X-1 (3U1617 - 15)	359.09 -23.77	Non-periodic variations on times of min.	Flaring: 10 - 30 min.	6 - 10; thermal spectrum	variable ? $\sim 0.5$	17000	2.5	Sco X-1 12 - 13 mag.	$1 \times 10^{36}$
Cyg X-2 (3U2142 + 38)	87.32 -11.32	Non-periodic pulsations on times of min.	?	3 - 7; thermal spectrum	variable ? $\sim 0.5$	540	$\leq 2.5$	Cyg X-2 14 mag.	

### 3.1 Hercules X-1<sup>\*</sup>

#### 3.1.1 Observations

Since the original discovery of the periodically pulsating binary X-ray source Her X-1 (Schreier et al, 1972; Tananbaum et al, 1972), intensive studies of its characteristics have continued from the UHURU X-ray observatory. The bulk of the data, which will be discussed here, was obtained in the energy range from 2 to 6 keV. The UHURU instrumentation has been described in a previous Letter (Giacconi et al, 1971).

We have already discussed the periodic pulsation of Her X-1 observed in January 1972 with a period of 1.24 seconds (Tananbaum et al, 1972). We also discussed the sinusoidal variation of this pulse period, occurring in phase with the orbital period of the binary system, which we interpreted as due to Doppler effect. We have now obtained two new results on the 1.24 second pulsations with regard to the pulse shape and the long term variability of the average period.

In a recent rocket experiment (Doxsey et al, 1973) the MIT group studied the pulse shape with fine time resolution. The main pulse was observed to have a double-peaked structure with a dip in the center. The double peak and dip occur in a few hundred milliseconds and the fall of the peak is considerably faster than its rise. The UHURU data, with 0.096-sec resolution, show a pulse shape consistent with the MIT results. Moreover, the data show the average pulse shape to be variable. In Figure 3-1 we show the results of folding data, obtained with 0.096-sec resolution, modulo the 1.24-sec period. The data were acquired in two 60-second intervals separated by about an hour. We observe on one occasion a double-peaked main pulse similar to the MIT data, followed by a very shallow interpulse, but at another time a single broad peak in the main pulse and an enhanced interpulse.

---

<sup>\*</sup>The Astrophysical Journal, 1973, 184, 227. R. Giacconi, H. Gursky, E. Kellogg, R. Levinson, E. Schreier, H. Tananbaum. Reproduced by permission of the University of Chicago Press.

**HERCULES X-1 1972 MAY 1**  
**DATA FOLDED MODULO 1.2378 SEC**

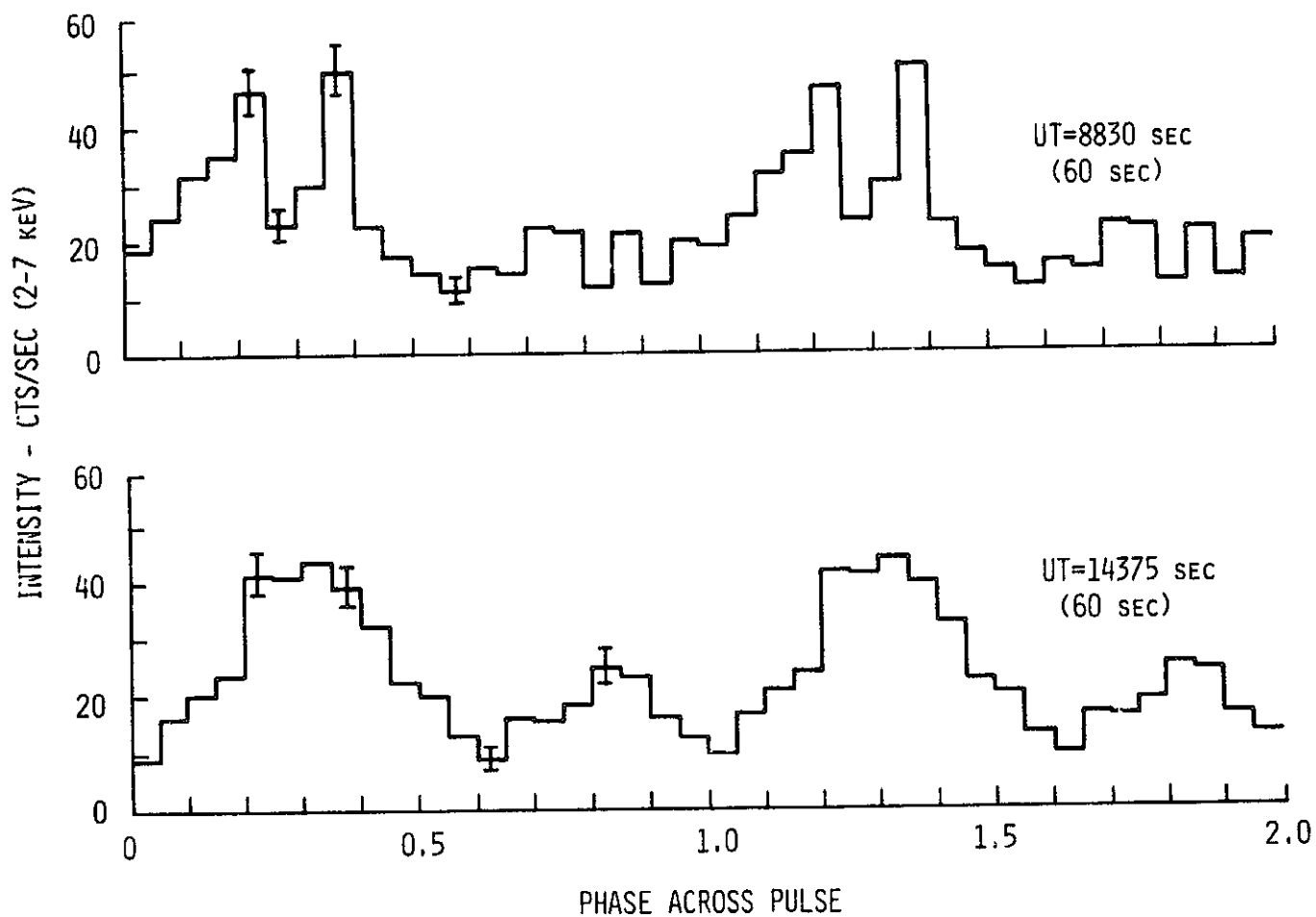


**Figure 3-1** Hercules 2-6 keV intensity data. Two sixty-second passes folded modulo 1.24 seconds.

With regard to long term variations of the average period, we discussed in our previous Letter the procedure we used to determine the best fit of a sinusoidal function to the observed pulsation phases. The parameters for the fit determine the average period during the entire observation time which extends over several days. Thus, very precise values for the average period of pulsation can be derived during each of the "on" states of Her X-1, which occur approximately every 35 days with a typical duration of 11 days. Using this technique, we have obtained the average period of the X-ray pulsation for January 1972, February 1972, March 1972, April 1972, and July 1972. The helio-centric corrected results are shown in Figure 3-2. The  $1\sigma$  error bar associated with each determination is derived from the quality of the fit. The data show that significant changes in the average period of pulsation occur with an overall decrease of about 4.5 microseconds from January to July. We cannot determine from these data alone whether the changes occur gradually or abruptly. We can, however, exclude a linear change with time which would be seen as a constant slope in Figure 3-2. The period decrease gives strong evidence against the possibility that the energy emitted in X-rays results from the loss of rotational kinetic energy of a neutron star, as is believed to be the case in the Crab Nebula pulsar NP0532.

An additional result from the fitting of the sinusoidal function to the observed pulsation phases is that we now have an updated period and phase for the orbit of the binary system. The period is  $1.700165 \pm 0.000002$  days and the phase of the eclipse center is 1972 July 7.8921  $\pm$  0.0001. The new determinations set an upper limit for change of the 1.7-day eclipse period of 1 part in  $10^5$  per year.

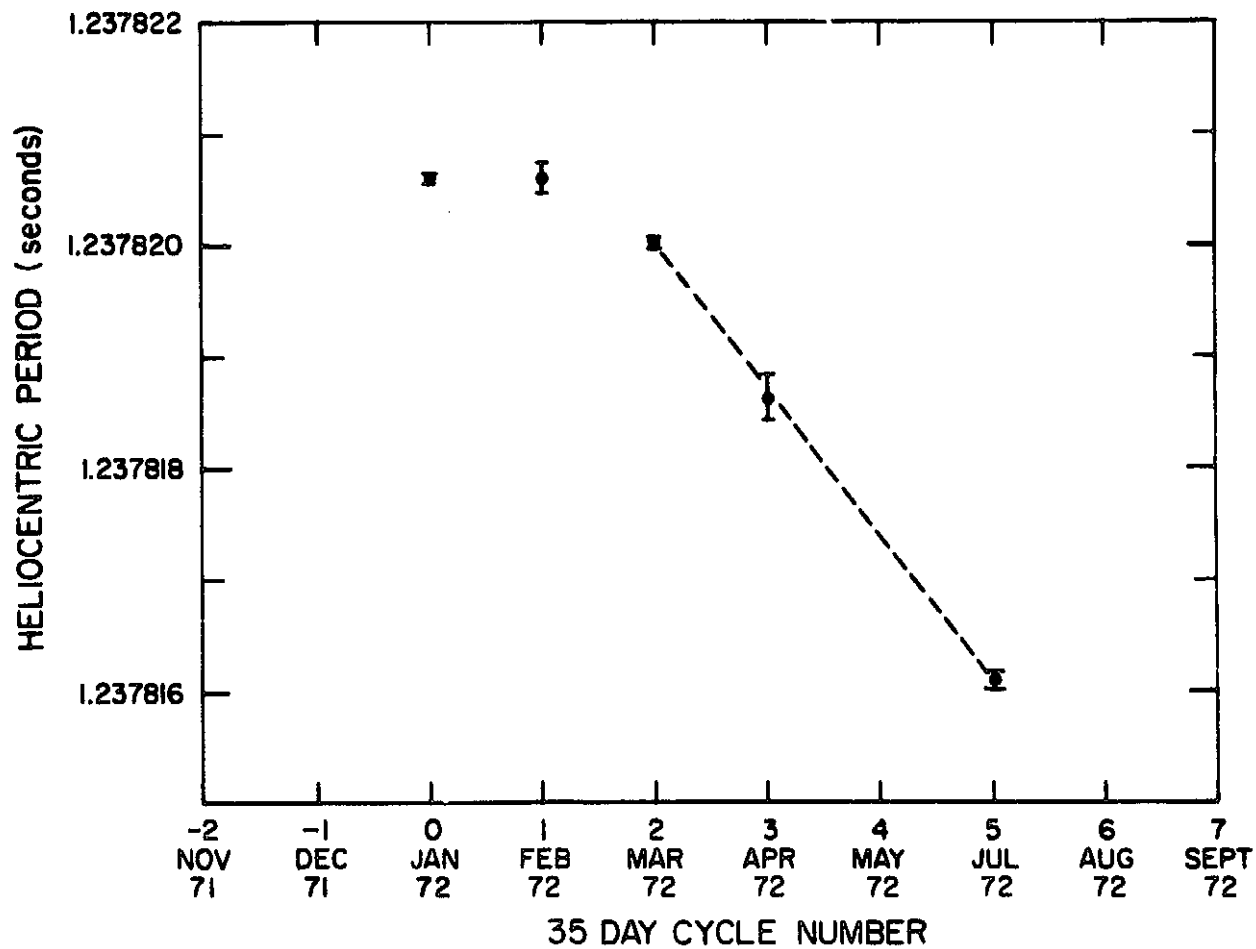


Figure 3-2 Measurements of the Hercules heliocentric pulsation period in seconds during five of the "on" states of the 35-day period.

In addition to the above findings concerning the pulsations, a much more complex picture of the system has emerged from the study of the variations in the average source intensity occurring over time intervals long compared to the pulsation period of 1.24 sec. As previously reported, Her X-1 is observed to be intense and pulsing for 11 or 12 days and below the level of detectability for 24 or 23 days. In addition, it exhibits regular eclipses every 1.7 days, which we had originally thought to be of variable width. We have studied the variation of average intensity in much greater detail by analyzing all available sightings of the source during several "on" states. In Figure 3-3 the behavior during three of these "on" states is shown. Each data point represents the average intensity measured during a single scan of the satellite across the source and is corrected for aspect. Two types of error bars are shown in the figure: (a) the statistical error bar, determined from counting statistics, and applicable when considering variability between adjacent sightings; and (b) the larger error bar which is an estimate of the possible systematic errors associated with the aspect corrections. This last error is applicable when comparing data taken on different days, since the satellite orientation is normally changed on a daily basis. (The rather large error is due to the fact that since the failure of the UHURU star sensors, we depend on sun sensors and magnetometers which yield aspect information to about  $1^\circ$  precision.) The behavior of the source in the three time periods shown in Figure 3-3 is typical of all our observations. Some common qualitative features can immediately be recognized: (1) there is an overall modulation of intensity with a broad maximum and a gradual decrease to below observable levels; (2) the "on" state begins with a fast rise time (less than 90 minutes); (3) "dips" in intensity occur during which the observed flux decreases by factors of 5 to 10; and (4) these "dips" typically occur once per orbit, before the eclipse, and they occur progressively earlier in phase as one approaches the end of the "on" state. It should be emphasized that

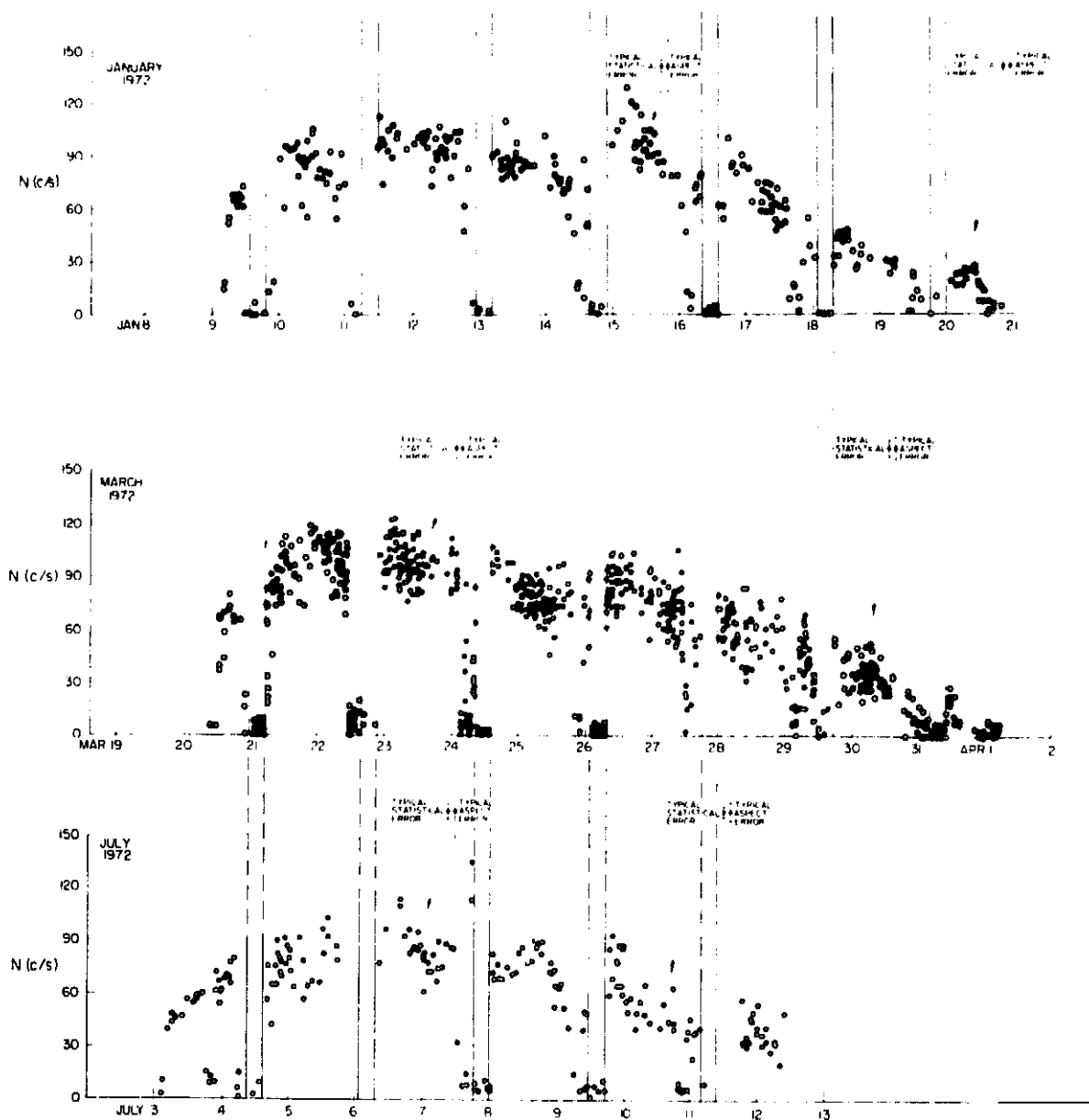


Figure 3-3 Hercules intensity data (2-6 keV) during three "on" states. The vertical lines represent the orbital eclipses, whose positions are determined accurately from the pulsation Doppler analysis. Typical errors appropriate for different groups of data are shown; the statistical error bar is relevant for point-to-point comparisons and the aspect error bar is relevant for day-to-day comparisons. It should be noted that most intensity points below about 10 cts/sec are upper limits.



these four features are observed in every "on" sighting we have studied. We have never observed an "on" state, for instance, which ended with a sharp decrease in intensity, as might be expected for certain special models (Shklovsky, 1972).

For each of the available "on" states, we define two reference times: an abrupt onset time and also a time characteristic of the entire "on" state. Since the intensity maximum is broad (e.g. 1972 January and March), the time of peak intensity is not well defined. The gradual intensity decrease, however, does allow us to fit a straight line to the intensities in the later portion of each on state, and to find the intercept of this fitted line with zero. For each on state, we thus measure the "intercept" time along with an uncertainty, taking into account both statistical and systematic aspect errors. The average time interval between "on" states is then computed by fitting the intercept times with a linear function. We find that the results are consistent with a periodic occurrence of on states with a period of  $34.88 \pm 0.12$  days, although individual points do exhibit large errors.

We then turn to the question of whether the onset times also occur periodically. Since the onset has a relatively fast rise time we can determine its time of occurrence much more precisely. We have plotted in Figure 3-4a the time difference between the actual onset times and those predicted on the basis of the constant 34.88 day period previously determined. It should be noted that the error bars associated with each determination here are absolute limits.

If the turn-on were strictly periodic in time, we would expect all of the data points to lie on a single straight line, which would have zero slope in the event that the period exactly coincided with 34.88 days, our chosen trial period. We find that the onset times can occur at constant time intervals for a few cycles; the first points led to the 35.7-day period we previously reported. Other points, however, define a period close to 34.85 days, and still others are scattered in no apparent systematic way. The last few points are from "quick look" data and their precision may improve when production data are processed. The analysis clearly shows that the turn-on is not periodic.

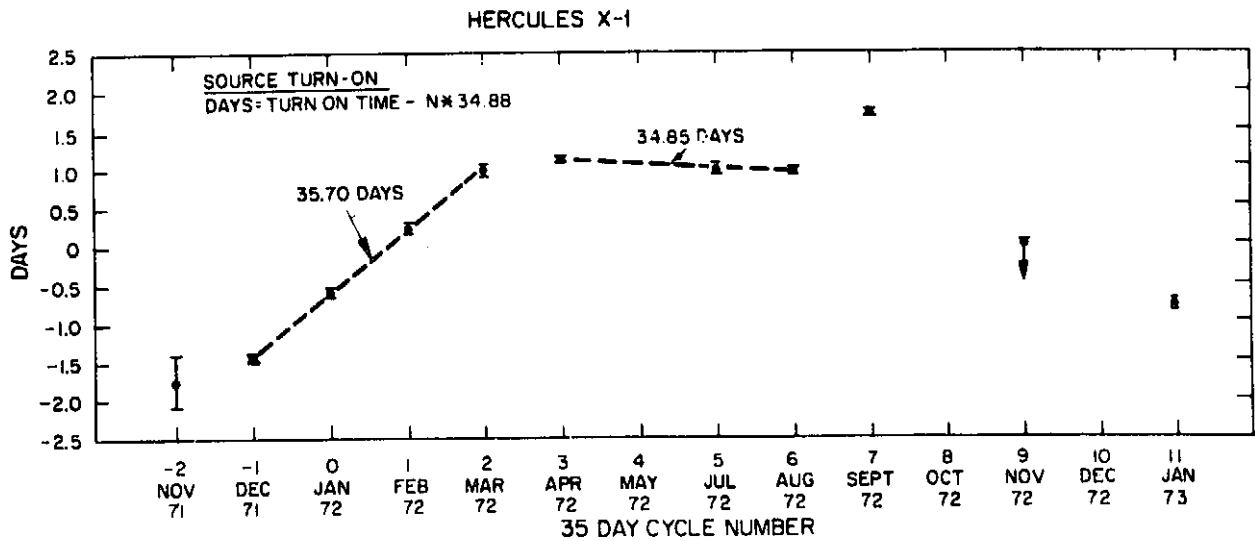


Figure 3-4a The difference in days between the observed turn-on times of the Hercules on states and what would be predicted by a constant 34.88-day trial period. The error bars represent absolute limits on the time during which the turn-on occurred. The dashed lines represent constant periods and show the periodicity in turn-on apparent for a few cycles.

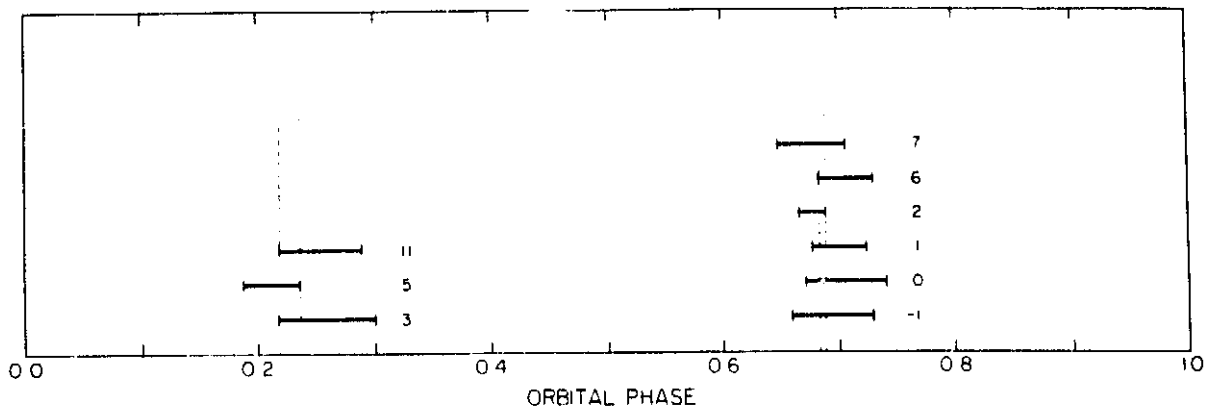


Figure 3-4b The absolute range of each turn-on time is plotted as a function of orbital phase. Phase 0 is the eclipse center. The number associated with each determination refers to the abscissa of Figure 4a. The dashed lines indicate the overlap region of the turn-on phases.

The turn-on times, however, bear a strict relation to the eclipse phase as shown in Figure 3-4b. As previously mentioned, the limit bars associated with each determination are absolute limits rather than statistical errors. The nine turn-on times, which we have measured to better than 0.2 days, occur within two ranges of phase values. The first is from phase 0.19 to phase 0.30; the second, from phase 0.65 to phase 0.74. While it is possible that the turn-on times do, in fact, exhibit a range of values as given above, it should also be noted that all determinations are consistent with two much narrower intervals as defined by the region of overlap of the absolute limits. These intervals are from phase 0.218 to phase 0.235, and from phase 0.682 to phase 0.688. The probability that this clustering is due to a random phenomenon is negligible. The simplest conclusion we can draw is that the X-ray emission is initiated only at specific positions of the X-ray source in its orbit about the companion star.

If we consider now in more detail the intensity variations during the "on" state, we observe, in addition to a large amount of point-to-point variability, the existence of definite decreases in intensity or "dips" outside the well-defined eclipses. We obtain the phase of the eclipse very precisely from the Doppler shift of the pulsation period, and the lines shown in Figure 3-3 defining the eclipse are centered via the null point of the sine curve. The existence of dips occurring in close proximity to the eclipse in the early portions of the "on" state had led us to conclude that the eclipse duration itself was variable. However, if we restrict our attention to eclipses occurring late during the "on" state, we find that their duration is consistent with a constant value of  $0.24 \pm 0.01$  days. The onset and end of the eclipse appear to be extremely sharp. On occasion, we find the transition occurring in less than 700 seconds. (It should be noted, as pointed out by R. Ruffini, that this value implies an absolute upper limit on the dimensions of the X-ray emitting region of about  $10^{10}$  cm.) The X-ray flux from Her X-1 during all eclipses has been below detectable levels.

The dips are qualitatively different from eclipses in some respects and very similar in others. The transition into a dip takes place quite sharply in times as short as tens of minutes, similar to the transitions into eclipse. However, the X-ray flux can have a finite value within the dip, in sharp contrast with what occurs in eclipses. The duration of the dips is on the average of the same order as the eclipse duration, but on one occasion was half as long. We interpret the occurrence of these dips as due to absorption of the radiation by intervening gas. This interpretation stems from the detailed comparison of the spectral content of the radiation from Her X-1 inside and outside the dips. In Figure 3-5 four different spectra each obtained over a few tenths of a day during different portions of the "on" cycle are shown. The spectrum corresponding to the highest intensity was obtained during the central portion of the 11 day "on" state in January 1972 at an orbital phase corresponding to highest flux. The spectrum appears to be very flat, with a best fit power law energy index of 0.0 or with a best temperature fit for an exponential spectrum of  $T > 150 \times 10^6 \text{ K}$ . The cutoff energy  $E_a$  corresponds to less than about 1.5 keV. The second spectrum also obtained at the highest intensity of the eclipse light curve, but near the end of the same "on" state is shown by the dashed line. While the intensity is reduced by a factor of 2.7, the shape of the spectrum is the same within statistics. The third spectrum is obtained in a dip adjacent to the time interval during which the second spectrum was obtained. While the intensity at energies above 10 keV is not too different in the last two cases, a substantial low energy deficit can be observed for the spectrum obtained during the dip. Finally, the fourth spectrum is obtained during the rapid rise at the onset of the January 1972 cycle. We see that the spectral shape is essentially identical to the one observed in the dip, with a large, low energy cutoff of the order of 4 keV. This similarity may have some significance in allowing us to distinguish between different mechanisms that could give rise to the rather abrupt onset of the radiation.

# HERCULES X-1 SPECTRA

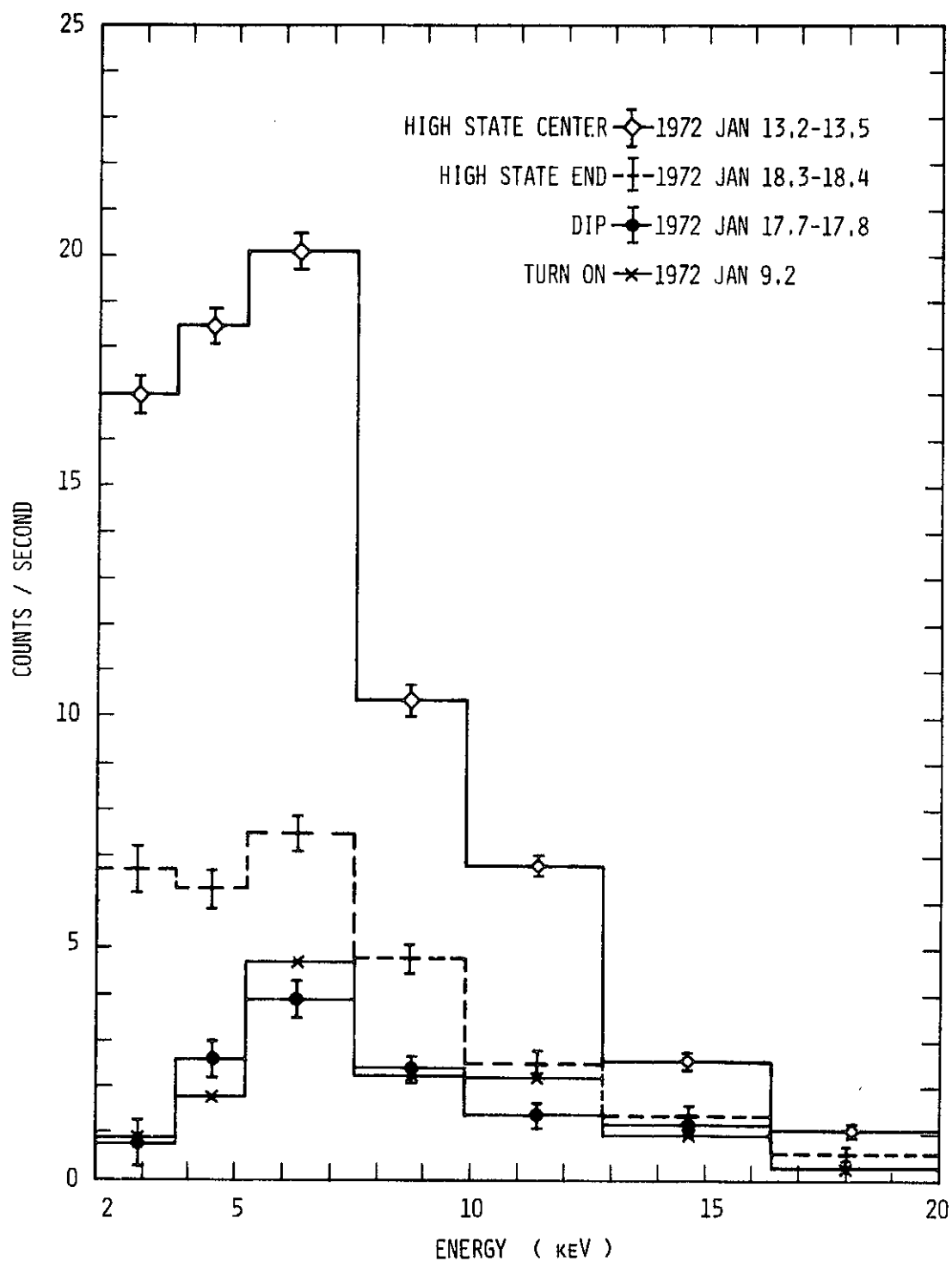


Figure 3-5 Four counting rate spectra obtained during different parts of the 1972 January high state. Counts in each energy channel are plotted with  $1\sigma$  errors.

If we thus interpret the low energy attenuation in the dips as due to absorption by a gas with the standard cosmic abundances (Brown and Gould, 1970), we can derive a typical column density of  $10^{23}$  Hydrogen atoms/cm<sup>2</sup>. With regard to the detailed behavior of the radiation within the dips, we observe a great deal of variability in the flux. The intensity can change by factors of 5 or greater in times as short as 300 seconds. This would suggest that, if indeed the absorption occurs in a gas, this gas does not present a uniform column density.

We wish now to turn our attention to the time of occurrence of the "dips". We find that the dips change their phase with respect to the 1.7 day-eclipses, appearing progressively earlier before each eclipse in a given "on" state. We can define a time of occurrence of the dips by the leading edge of the decrease in intensity. In Figure 3-6 we plot for several different cycles the time difference between the leading edge of each dip and the nearest eclipse center as a function of time. The data sets have been stacked vertically, subtracting an integral number of 34.88 days. The fact that in each "on" state the position of the dips moves regularly with respect to the eclipse center is apparent in the figure. It is also apparent that they do not move at a constant rate. It is clear that the behavior of the dips bears some relation both to the 35-day cycle and to the 1.7-day orbital phase, but we have not yet been able to establish any simple relationship between these phenomena. The picture is also somewhat complicated by the observation of two extra dips which appeared 0.6 days after the source turned on in April 1972 and July 1972. On these two occasions the source turned on at phase 0.23 and the trailing edge of the extra dips mentioned above coincided with phase 0.68.

# HERCULES X-1 INTENSITY DIPS

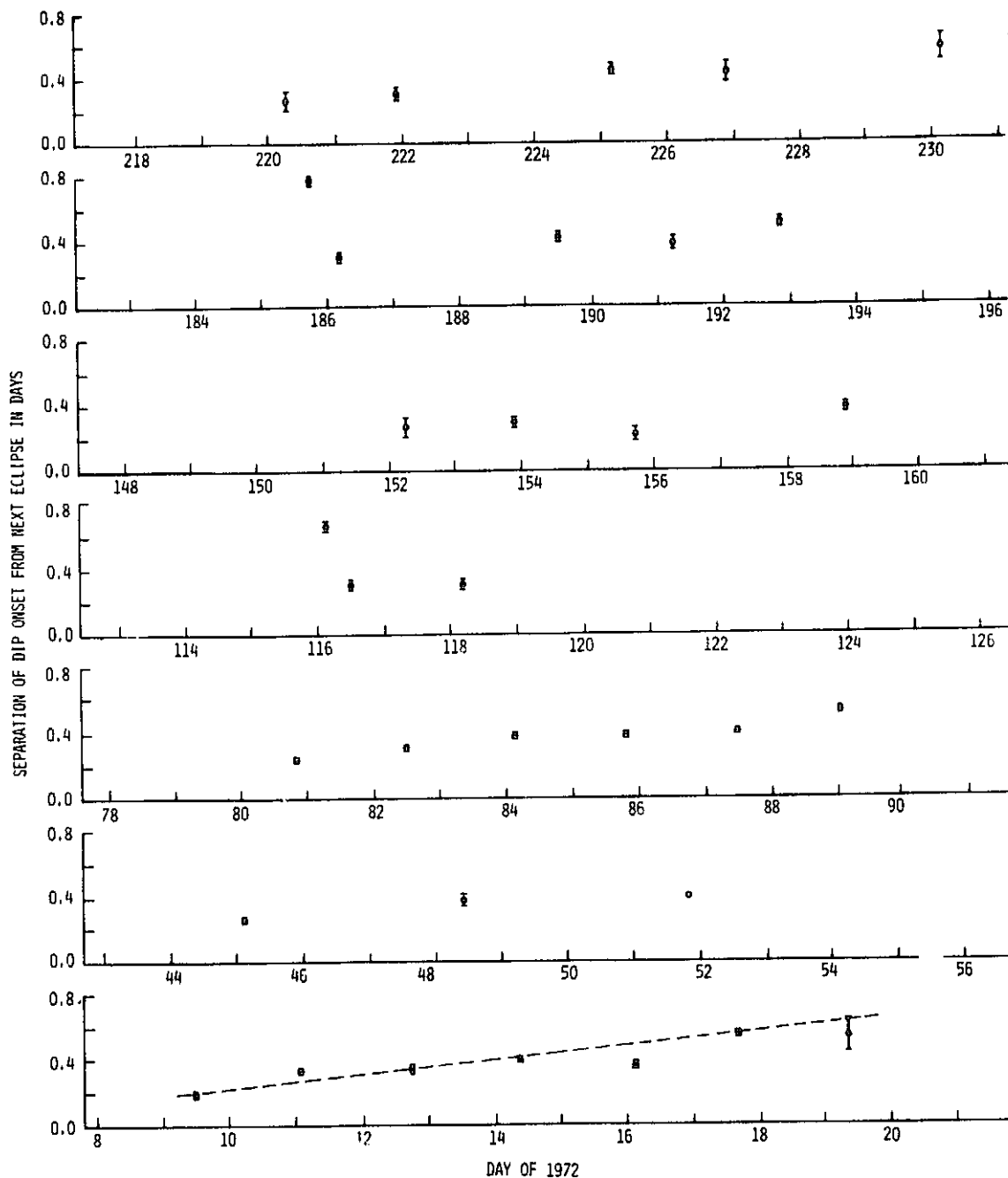


Figure 3-6 Hercules X-1 intensity dips; the separation between the leading edge of a dip and the center of the next eclipse in days is plotted versus day of 1972. The error bars represent absolute limits. The high states studied are stacked modulo the 34.88 day average separation. The roughly monotonic progression of the dips is indicated by the dashed line.

### 3.1.2 Discussion

From the above description it becomes apparent that Her X-1 is a more complex system than originally described. It is, therefore, not surprising that we are not yet able to fully understand all of the details of its X-ray emission. However, from the study of the accretion process by many authors, among them Zeldovich and Novikov (1971), Shklovsky (1967), Cameron and Mock (1967), Prendergast and Burbidge (1968), Schwartzman (1971), Pringle and Rees (1972), Ostriker and Davidson (1972), Lamb, Pethick and Pines (1972), there appears to be convergence toward a model of the Her X-1 binary system which appears to be, qualitatively at least, in agreement with the known observational facts. While this model is not yet generally accepted, even with respect to the choice of a neutron star as opposed to a white dwarf (Brecher and Morrison, 1973) as the X-ray star, we have adopted it at least as a guide to the study of the data and the interpretation of the results.

The star HZ Herculis was identified with Her X-1 by Bahcall and Bahcall (1972) and Forman, Jones and Liller (1972), who demonstrated the existence of periodic intensity variations with the same period and phase as the X-ray eclipses. The optical data indicate that the binary system contains a normal A or F type star and the X-ray data suggest its companion is a magnetic rotating neutron star. Matter is lost from the atmosphere of the normal star and accreted onto the neutron star giving rise to the observed pulsed X-rays. In this view, the energy source for the X-rays ultimately resides in the gravitational energy which is converted during the accretion process. The neutron star is rotating with a 1.24-second period and furnishes the clock mechanism for the short pulsations. The period of rotation of the binary system is 1.7 days and the X-ray eclipse is due to occultation of the neutron star by the normal star. The 1.7-day light curve in the visible is due to absorption of the X-ray radiation by the side of the normal star exposed to the X-ray source and re-radiation of the absorbed energy at  $10^4$ °K.



X-ray emission from the accreting material impinging on the magnetic poles of the neutron star is beamed. This can give rise to the observed pulse shape and can explain the existence of an interpulse. Several authors have discussed the effects on the angular distribution of the X-ray radiation of absorption and scattering in the column of material being funneled into the magnetic pole (Pines, 1972; Ostriker and Davidson, 1972; and Gnedin and Sunyaev, 1972). Depending on the density distribution in the accreting column, these authors have shown that a variety of beaming effects could result, since the emitted photons are allowed to escape only in a hollow cone about the accreting column. The variability of the pulse shape could then be explained on the basis of variations in the column density of accreting matter. The time constants estimated for such changes to occur (tens of seconds) are not in disagreement with the times in which the pulse shape is in fact observed to change.

The rate of change of the 1.24-second period and its sign are consistent with the prediction by Lamb et al (1972), and by Pringle and Rees (1972), who consider the angular momentum transferred to the neutron star by the accreting matter.

Several effects that might cause the 34.88-day precession have been discussed with the simplest picture being torque-free precession of an oblate spheroid neutron star as described by Brecher (1972). Pines (1972) has pointed out that dynamical analysis of the system requires a solid rather than liquid neutron core for the star to account for the observed precessional period.

The sudden onset of the "on" state may be due to a triggering effect of the accreting material piling up at the Alfvén surface (Pines, 1972) until the precession angle becomes such that accretion on one or the other of the magnetic pole regions is no longer prevented by centrifugal and magnetic forces. This effect might explain both the sudden onset and the more periodic nature of the onset time. Hopefully, a detailed model may also account for the specific phases at which the onset can occur.

Finally, the dips are due to absorption by the gas streaming in the system and ultimately being accreted. It should be noted that the energy absorbed by the gas during a dip is a large fraction of the total energy emitted by the source. The absorbing gas is heated to extremely high temperatures and would then act as a secondary X-ray source. Depending on its location in the system, the existence of such a secondary source may have observable effects on the visible light curve.

## REFERENCES

- Bahcall, J. N. and Bahcall, N.A. 1972, Ap. J. (Letters), 178, L1.
- Brecher, K. 1972, Nature, 239, 325.
- Brecher, K. and Morrison, P. 1973, Ap. J. (Letters), 180, L121.
- Brown, R. and Gould, R. 1970, Phys. Rev. D1, 2252.
- Cameron, A.G.W. and Mock, M. 1967, Nature, 215, 464.
- Doxsey, R., Bradt, H.V., Levine, A., Murthy, G.T., Rappaport, S. and Spada, G. 1973, Ap. J. (Letters), to be published.
- Forman, W., Jones, C.A. and Liller, W. 1972, Ap. J. (Letters), 177, L103.
- Giacconi, R., Kellogg, E., Gorenstein, P., Gursky, H., and Tananbaum, H., 1971, Ap. J. (Letters), 165, L27.
- Gnedin, Yu. N. and Sunyaev, R.A., 1972, preprint.
- Lamb, F.K., Pethick, C.J. and Pines, D. 1972, preprint.
- Ostriker, J.P. and Davidson, K. 1972, IAU Symposium #55, X- and Gamma-ray Astronomy.
- Pines, D. 1972, Sixth Texas Symposium on Relativistic Astrophysics
- Prendergast, K.H. and Burbidge, G.R. 1968, Ap. J. (Letters), 151, L83.
- Pringle, J.E. and Rees, M.J. 1972, Astron. and Astrophys., 21, 1
- Schreier, E., Levinson, R., Gursky, H., Kellogg, E., Tananbaum, H. and Giacconi, R. 1972, Ap. J. (Letters), 172, L79.
- Schwartzman, V.F. 1971, Sov. Astron. A. J., 15, 377.
- Shklovsky, I. 1967, Ap. J. (Letters), 148, L1.
- Shklovsky, I. 1972, private communication.
- Tananbaum, H., Gursky, H., Kellogg, E.M., Levinson, R., Schreier, E., and Giacconi, R. 1972, Ap. J. (Letters), 174, L143.

### 3.2 Centaurus X-3

This was the first X-ray source observed to be pulsing periodically, (Giacconi, et al. 1971) and the first found to be a binary (Schreier et al. 1972). Based on the X-ray data alone, it is known that the bulk of the observed X-ray power is in the form of a periodic signal with a period of 4.84239 sec. Furthermore, we know that the source is in a binary system; the X-ray emission is eclipsed every 2.08707 days; but more important, the period of the emission is observed to vary sinusoidally with the same two day period. This variation in period has a direct interpretation as a Doppler shift of 415 km/sec corresponding to the motion of the X-ray source around a central star. Furthermore, the center of the eclipse occurs when the Doppler velocity change is zero, consistent with a binary system. The X-ray variations are illustrated in Figure 3-7.

There are many details of the X-ray emission which clearly relate to the nature of the source of the system in which it is imbedded, but which do not lend themselves to such a clean interpretation. The pulsed portion of the X-ray emission disappears for periods of many days in an apparently erratic fashion. During this time and during the eclipse, continuous X-ray emission is observed whose intensity is about 10% of the peak intensity of the pulsed portion. It can not be determined whether this portion of the radiation is present during the time of the pulsing; however, its presence during the eclipse implies that it is produced independently of the pulsed portion.

The transition into and out of the eclipse requires about 0.8 hrs; spectral variations (deficiency of low energy photons) during this period indicate that the X-ray flux is being absorbed rather than being cutoff by a sharp edge; i. e., the source appears to be "setting"

\*From H. Gursky, *Les Astres Occlus*, Les Houches 1972, p. 295, Ed. DeWitt and DeWitt, reproduced by permission of Gordon and Breach Science Publishers

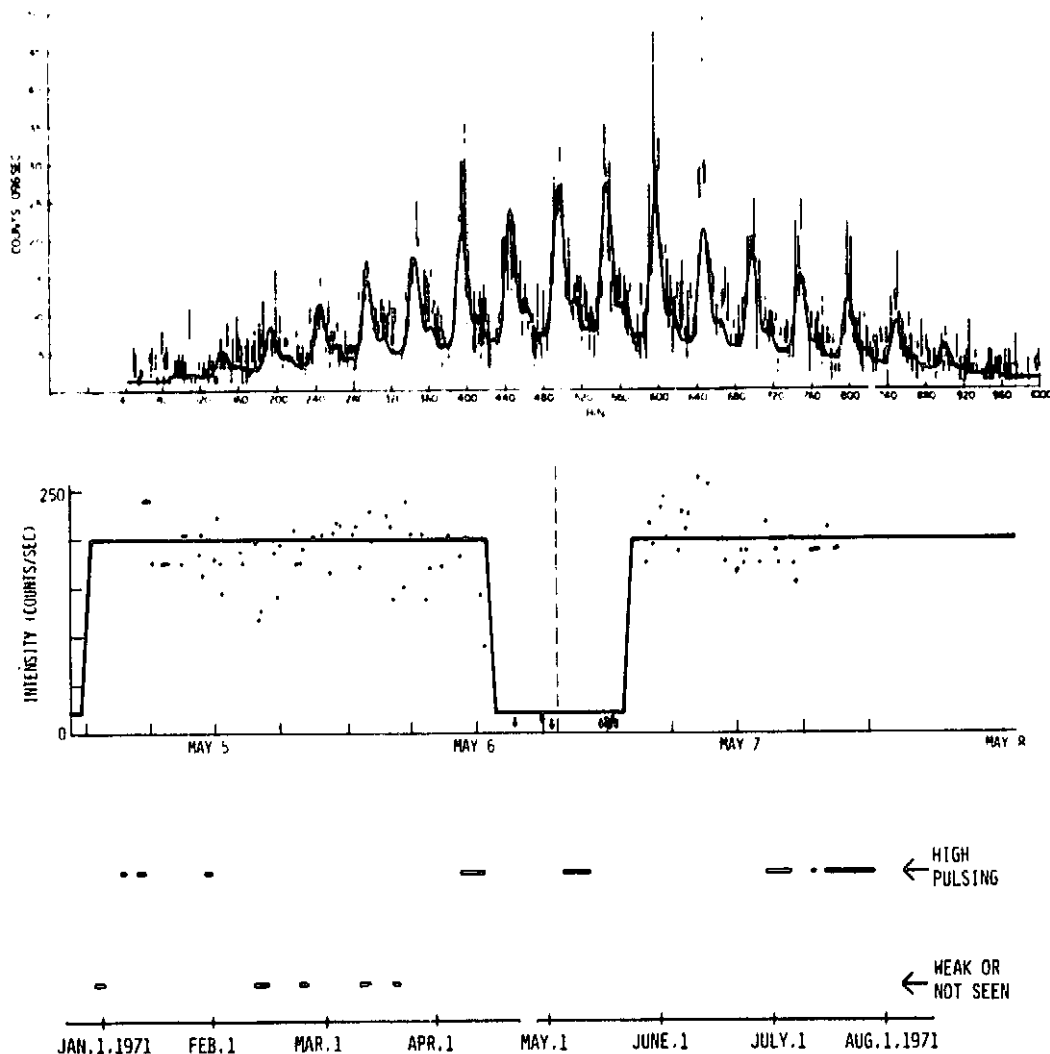


Figure 3-7. X-ray variability of Cen X-3. The upper curve shows the 4.8 seconds pulsations as they appear in the raw data (each bin is 0.096 sec). The fitted curve is the result of a fourier analysis. The middle curve is the average intensity folded modulo the eclipse period of 2 days. The period and phase of the eclipse were obtained from the Doppler velocity variations of the pulsing. The lower curve is the time variability on a scale of months and shows extended periods (e. g. , February - April) when the source is weak or absent when it was predicted to be seen.

into an atmosphere before going behind the central star. Also, the time of the transition varies by an hour or more, indicating that the "atmosphere" is not steady.

There is no optical candidate available for this object; however, it is located right on the galactic plane in the direction of a spiral arm. Thus, it may be badly obscured optically.

Assuming this to be a binary system, the picture that emerges is of a close binary system of radius  $6 \times 10^{11}$  cm ( $\approx 8 R_{\odot}$ ). The separation between the edge of the occulting disk and the X-ray source is only about  $10^{11}$  cm. Based on the Doppler velocity, the mass function is 15  $m_{\odot}$ . The minimum mass of the secondary is 15  $m_{\odot}$ . However, if one accepts the view that this is a mass-exchange binary system in which the unseen object ( $m_s$ ) fills its Roche Lobe, an independent relation arises between the ratio of the radii and the masses; which in turn allows placing limits on the masses. However, there is some controversy here. Wilson (1972) argued that the eclipse duration required a central star that was tidally distorted and derived an upper limit for the mass of the X-ray source of about 0.2  $m_{\odot}$ . Van den Heuvel and Heise (1972), on the other hand, derive an upper limit of 0.7  $m_{\odot}$  for the object based on the central star filling its Roche Lobe. Ruffini and Leach (1972) have derived somewhat higher masses; the main point, insofar as the present discussion is concerned, is that the mass is within the acceptable limits for neutron stars; i.e., one is not compelled to make the X-ray source a black hole. Based on the value of the mass function the other star is the order of 15  $m_{\odot}$ .

It is generally believed that the X-ray emission from Cen X-3 originates from a rotating, magnetic, neutron star based on the similarity to NP0532. The period of 4.8 seconds of the pulsations is within the range of permissible rotation for a white dwarf; how-

ever, the only other X-ray source of this kind we know of, Hercules X-1, has a period of 1.24 seconds which is below the limit of stability for the rotation of normal White Dwarfs.

The shape of the pulse is not consistent with rotation of a source of radiation on the surface which emits isotropically; the pulse is too sharp. The most natural explanation is that it is produced by the same process as is making the X-rays in NP0532. If this is the case, the radiation is beamed, which has important consequences regarding the average luminosity and number of sources of this type.

## REFERENCES

1. R. Giacconi, H. Gursky, E. Kellogg, S. Murray, E. Schreier, and H. Tananbaum, Ap. J. (Letters) 167 L67, 1971.
2. R.W. Leach and R. Ruffini, "X-ray Sources -- A Transient State from Neutron Stars to Black Holes", Preprint, August 1972.
3. E. Schreier, R. Levinson, H. Gursky, E. Kellogg, H. Tananbaum, and R. Giacconi, Ap. J. (Letters) 172, L79, 1972.
4. E. Van den Heuvel and J. Heise, Nature, 1972.
5. R. Wilson, Ap. J. (Letters) 174, L27, 1972.



### 3.3 Cygnus X-1\*

Perhaps the most significant of the UHURU results for the galactic X-ray sources has been the discovery of pulsations from Cygnus X-1. These data led to further study of this object and to the present belief that we are dealing with a black hole. I would like to present the data we have on this object and consider the status of the black hole identification. Figure 3-8 contains data showing substantial variations in X-ray intensity on time scales from 100 milliseconds to 10's of seconds. Some 80 seconds of data are shown here summed on 4 time scales from 100 msec up to 14 sec. I should point out that similar X-ray variability also reported by Rappaport et al. (1971a), Holt et al. (1971) and Shulman et al. (1971) compels us to consider a source region of  $10^9$  cm or less. Figure 3-9 shows the X-ray location obtained from an MIT rocket flight (Rappaport et al., 1971 b) and from UHURU which led to the discovery of a radio source by Braes and Miley (1971) and by Hjellming and Wade (1971). It is this precise radio location that led to the optical identification by Webster and Murrin (1972) and by Bolton (1972a) of Cygnus X-1 with the 5.6 day spectroscopic binary system HDE 226868. The central object of this system is a 19th magnitude star, most likely a B0 supergiant and first mass estimates for the primary led to a mass in excess of  $3 M_{\odot}$  for

\*From "Stellar X-ray Sources" H. Tananbaum, 1973 IAU Symp. No. 60, Galactic Radio Astronomy, D. Reidel Publishing Co.

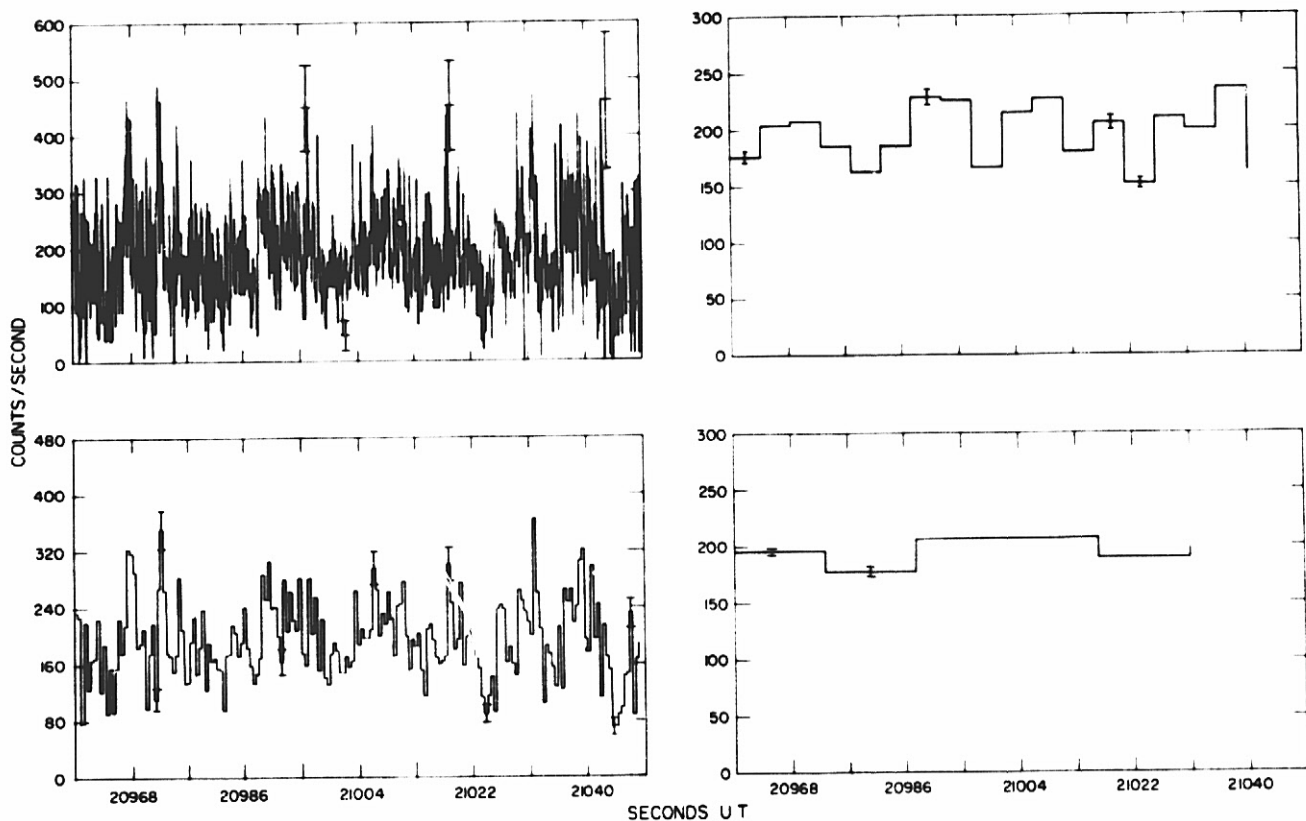
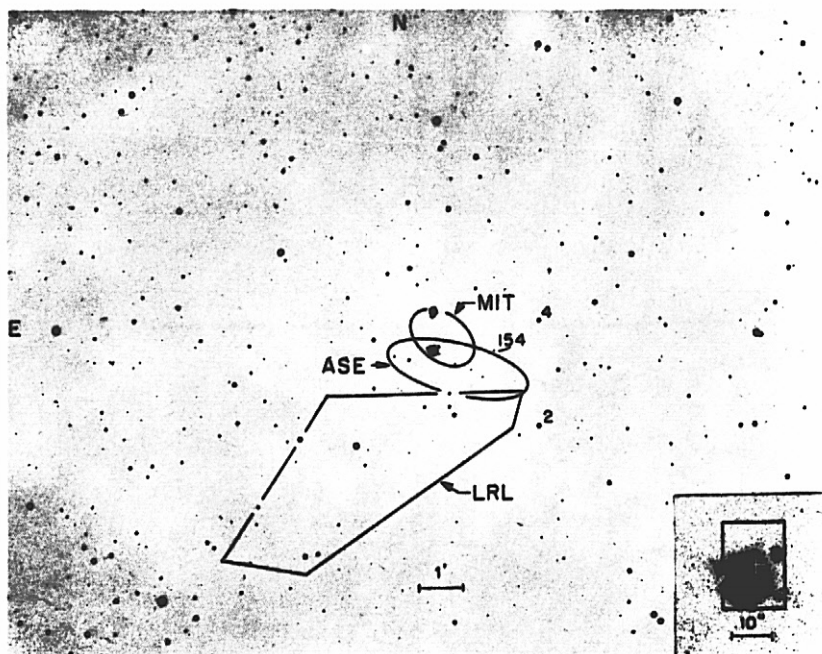


Figure 3-8. Observations of Cygnus X-1 on 10 June 1971. Data have been corrected for the triangular collimator response. Data are summed over 0.096s, 0.48s, 4.8s, and 14.4s intervals. Typical  $1\sigma$  error bars are shown.



S-4058

Figure 3-9. X-ray location of Cygnus X-1. HDE226868 is the bright star in the overlap between the MIT and ASE error boxes. The insert shows the radio location which was reduced to an uncertainty of less than 1 arc second after this figure was drawn and is coincident with HDE226868.

the unseen companion. This came from the mass function determined from the absorption line velocities

$$\frac{M_{\text{sec}}^3 \sin^3 i}{(M_{\text{sec}} + M_{\text{BO}})^2} \approx 0.2.$$

Even at  $i=90^\circ$ , which gives a minimum value of the mass of the secondary,

$$M_{\text{BO}} = 20 \rightarrow M_{\text{sec}} = 5 M_{\odot}$$

If the secondary is the compact X-ray source, then it could well be a black hole, a point to which we will return shortly.

We attempted to confirm the identification of the X-ray source with HDE226868 by looking for a 5.6 day effect on the X-ray light curve. In December 1971 and January 1972 we observed Cygnus X-1 continuously for 35 days. We folded the X-ray data with many different periods including 5.6 days and the results are shown in Figure 3-10. 2-6 keV data are shown folded modulo 3.0, 5.6, and 6.2 days; the average is indicated by the dotted lines, and  $2\sigma$  error bars are indicated by the solid lines. We conclude that there is no evidence for a 5.6 day eclipse here, and believe that previous reports from balloon observations of such an effect at higher energies were caused by the large scale time variability and not by a 5.6 day effect. The report by Professor Boyd at Sydney of a possible 5.6 day effect at energies below 3 keV may be due to a real effect or may be due to the variability of the source and the presence of only two data points. In any case, the absence of a 5.6 day effect does not rule out the identification and can be

# **CYGNUS X-1 FOLDED INTENSITY** **2-6 keV Dec. 17, 1971 to Jan. 21, 1972**

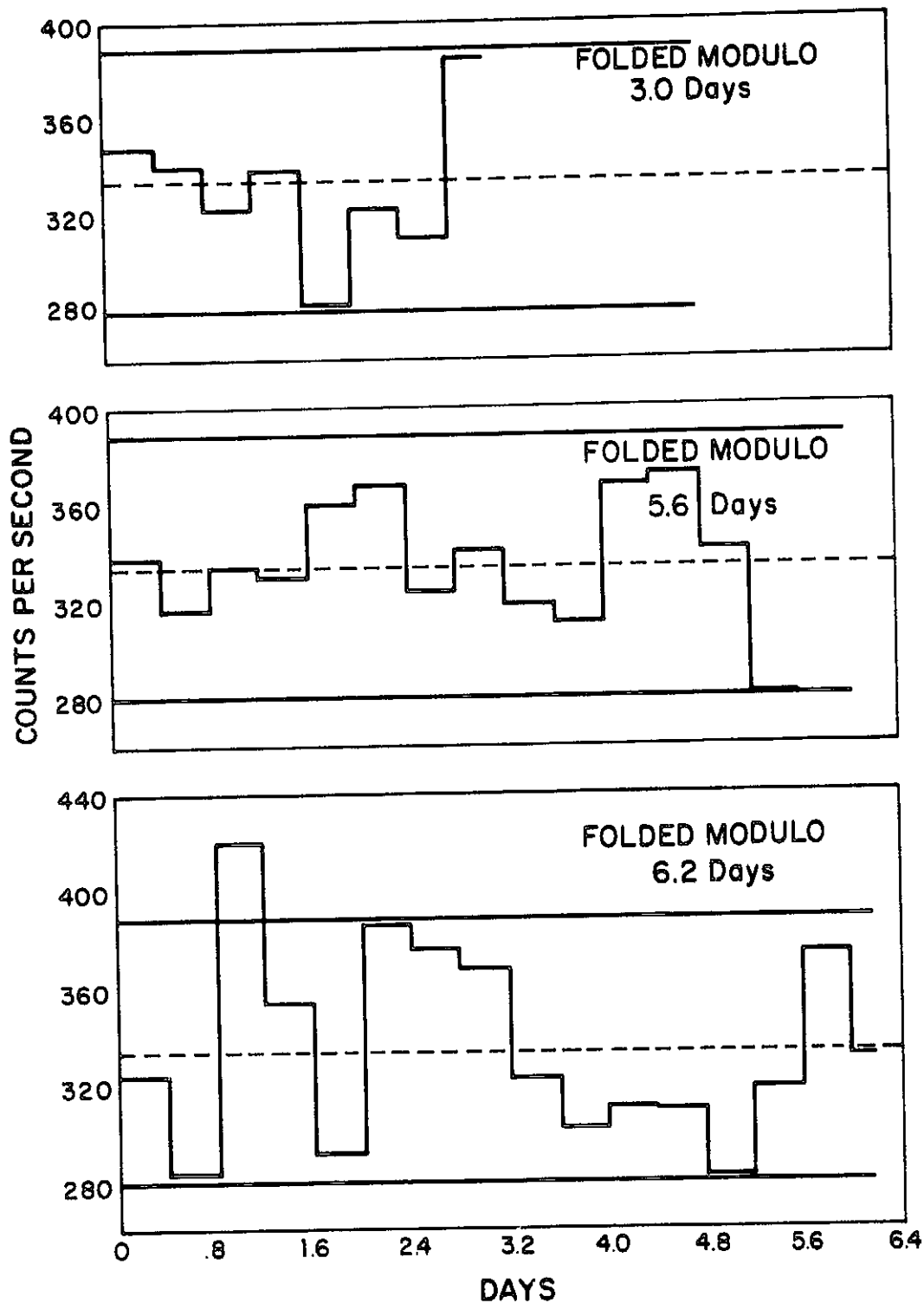


**Figure 3-10.** Cygnus X-1 folded intensity, 17 December 1971 to 21 January 1972. 35 days of 2-6 keV data are shown folded modulo 3.0, 5.6, and 6.2 days. The dotted lines give the average intensity and the solid lines are  $2\sigma$  error bars.

understood in terms of an appropriate inclination angle for the orbital plane of the binary system.

With the use of UHURU as an observatory, we have analyzed 16 months of data on Cygnus X-1 which are shown in Figure 3-11. We have plotted the 2-6 keV intensity vs. day of 1970. The vertical lines for a given day are not error bars, but rather show the range of variability observed on that day. For some days we have only the average intensity shown by a dash available in our analyzed results. We see that a remarkable transition occurred in March and April 1971, with the source changing its average 2-6 keV intensity level by a factor of 4. We have also indicated in the figure the 6-10 keV and 10-20 keV X-ray intensities and see that the average level of the 10-20 keV flux increased by a factor of 2. The figure also shows that at the same time the X-ray intensity changed, a weak radio source appeared at the Cyg X-1 location and was detected by the Westerbork and NRAO groups. Hjellming (1973) has recently reported analysis of additional radio data which shows the radio source first appeared some time between March 22 and March 31, essentially the time during which the 2-6 keV X-ray intensity first headed downward. This correlated X-ray radio behavior is the major evidence in addition to the positional data that Cyg X-1 is in fact identified with the optical and radio object.

With respect to the arguments concerning the mass of the secondary and thereby the possibility of Cygnus X-1's being a black hole, there are three recent papers that approach the question. One paper by Bolton (1972 b) uses the absorption line velocities, the He II 4686 emission line velocities and the 2.2 Kpc distance derived from the observed reddening and the equivalent width and velocity of the interstellar lines to determine values of  $20 M_{\odot}$  for the primary,  $13 M_{\odot}$  for the secondary, and an inclination angle of  $26^{\circ}$ .

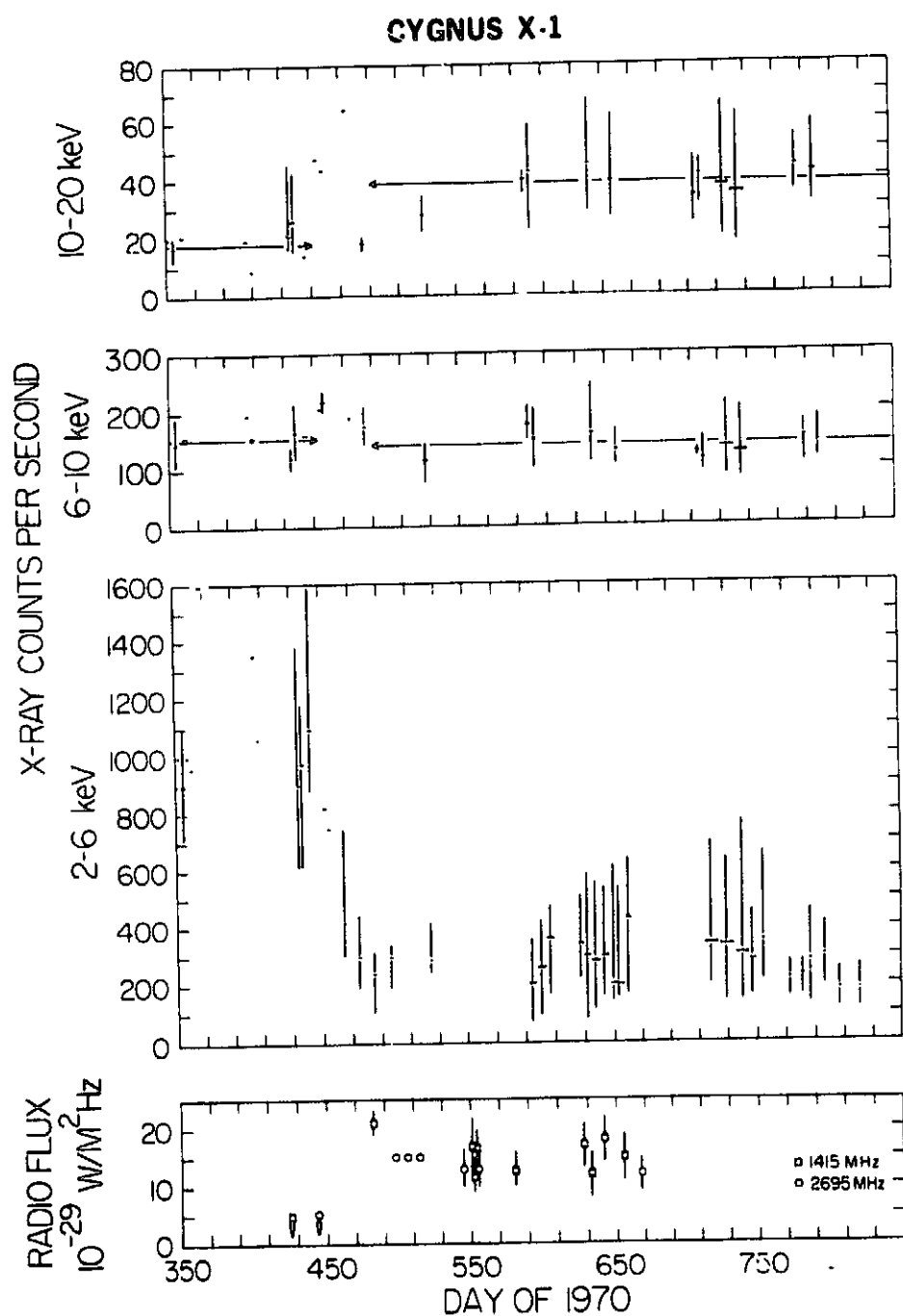


Figure 3-11. 16 months of observations of Cygnus X-1. X-ray data are shown for 3 energy bands, 2-6 keV, 6-10 keV, and 10-20 keV plotted vs. day of 1970. The transition discussed in the text occurred near day 450. The radio data are shown at the bottom of the figure to which should be added the additional positive sighting on day 455 reported by Hjellming (1973).

Cherepashchuk, Lyutiy and Sunyaev (1973) use the absorption line velocities, the He II emission line velocities with some allowance that the emission region may not belong to the X-ray star, but may lie between the two stars (the possible flaw in Bolton's work), and the photoelectric observations showing 0.07 magnitude changes due to a tidally distorted system. Then taking into account limb darkening and gravity darkening, and making the not necessarily correct assumption that the primary fills its Roche lobe they determine a primary mass between 10.7 and 22  $M_{\odot}$ , a secondary mass between 7.8 and 17  $M_{\odot}$ , and a distance of order 5 Kpc -- although they appear to have neglected interstellar absorption effects and could therefore have overestimated the distance by a factor of 2. H. Mauder (1973) uses the mass function determined from the absorption line velocities, the possible distances allowed by the observed reddening and the absence of a bright infrared source which would be produced by an absorbing circumstellar shell around the source, the absence of any substantial reflection effects as demonstrated by the photoelectric observations and the X-ray to visible light energy ratio, and the photoelectric observations plus the assumption that the star cannot be any larger than its Roche lobe. He determines a self consistent set of parameters that gives for a distance of 2 Kpc, a primary mass of 25  $M_{\odot}$  and a secondary mass between 6.0 and 7.3  $M_{\odot}$ .

What is the point of this rather lengthy, yet sketchy description. Since we are talking about the first possible observation of a black hole, we want to consider all the possibilities. The first optical papers suggested a mass of  $\sim 20 M_{\odot}$  for the primary star based on a B0Ib spectral typing. Among others, Trimble, Rose and Weber (1973), and Faulkner (1973) pointed out that a helium burning star of much less mass could give a temperature and effective surface gravity identical to that observed. Since such a source would



be at a distance of 1 Kpc at most, a knowledge of the distance is crucial for deciding the masses of the stars. Now the recent distance measurements that have been made by Bregman et al. (1973) and Margon et al. (1973) rule out the more exotic helium stars, determine that the primary is a massive supergiant, and thereby yield masses from 6 to 22  $M_{\odot}$  for the secondary.

There are 3 links in the chain of arguments leading to our conclusion about Cygnus X-1 -- (1) the identification where location agreement plus the X-ray-radio correlation suggest the HDE226868 secondary is the X-ray source; (2) the compactness where the short time variations, accretion as an energy source, and the absence of substantial visible light emission from the secondary indicate that this object is compact; and (3) the mass estimates of  $\geq 6 M_{\odot}$  which therefore indicate that Cygnus X-1 is a black hole.

In the way of future work on this source, we have the promise of a 1 arc second X-ray location from the HEAO-B X-ray telescope in the late 1970's to make the identification absolute, the large area NRL experiment planned for the HEAO-A mission to study the intensity variations on very short time scales to pursue the compactness, and the continuing optical efforts to confirm the distance measurements.

## REFERENCES

1. Bolton, C.T., 1972a, Nature, 235, 271.
2. Bolton, C.T., 1972b, Nature Phys. Sci., 240, 124.
3. Braes, L. and Miley, G.K., 1971, Nature, 232, 246.
4. Bregman, J., Butler, D., Kemper, E., Koski, A., Kraft, R.P., and Stone, R.P.S., 1973, preprint.
5. Cherepashchuk, A.M., Lyutiy, V.M., and Sunyaev, R.A., 1973, Astron. Zhur., 50, 3.
6. Faulkner, J., 1973, Tucson Workshop on Compact X-ray Sources.
7. Hjellming, R.M., 1973, Astrophys. J. (Letters), 182, L29.
8. Hjellming, R.M. and Wade, C.M., 1971, Astrophys. J. (Letters), 182, L29.
9. Hjellming, R.M. and Wade, C.M., 1971, Astrophys. J. (Letters), 168, L21.
10. Margon, B., Bowyer, S., and Stone, R., 1973, Astrophys. J. (Letters), to be published.
11. Mauder, H., 1973, Astron. and Astrophys., to be published.
12. Parsignault, D.R., Gursky, H., Kellogg, E.M., Matilsky, T., Murray, S., Schreier, E., Tananbaum, H., Giacconi, R., and Brinkman, A.C., 1972, Nature, 239, 123.
13. Rappaport, S., Doxsey, R., and Zaumen, W., 1971a, Astrophys. J. (Letters), 168, L43.
14. Rappaport, S., Zaumen, W., and Doxsey, R., 1971b, Astrophys. J. (Letters), 168, L17.
15. Shulman, S., Fritz, G., Meekins, J., and Friedman, H., 1971, Astrophys. J. (Letters), 168, 449.
16. Trimble, V., Rose, W.K., and Weber, J., 1973, M.N.R.A.S., 162, 1.
17. Webster, B.L., and Murdin, P., 1972, Nature, 235, 37.

### 3.4 2U 0900-40\*

#### 3.4.1 Introduction

The X-ray source 2U 0900-40 (Vela XR-1, GX263+3) was first detected by Chodil et al. (1967) and subsequently the position was refined by Gursky, Kellogg, and Gorenstein (1968). Based upon first Uhuru observations, Kellogg and Murray (1971) and Bradt and Kunkel (1971) suggested HD77581, a BO.5Ib star (Morgan, Code, and Whitford 1955) of visual magnitude 6.9 (Hogg 1958) as an optical candidate for the X-ray source. This star had been observed by Feast, Thackeray, and Wesselink (1956) to have a variable radial velocity which Brucato and Kristian (1972) interpreted as caused by a binary with a period of less than ten days. Hiltner, Werner and Osmer (1972) reported HD77581 to be a spectroscopic binary with a period of approximately seven days. Most recently Ulmer et al. (1972) have reported periodic intensity fluctuations of  $8.7 \pm 0.2$  days in the 7 - 26 keV flux from 2U 0900-40, which they interpret in terms of an eclipsing binary system.

In this letter we report X-ray observations of 2U 0900-40 from the X-ray observatory Uhuru which confirm the observations reported by Ulmer et al. and yield an improved period of  $8.95 \pm 0.02$  days. An improved location for 2U 0900-40, with an area of 4 square minutes of arc, contains the optical candidate HD77581. The 2 - 20 keV energy spectrum and the variability of the source are also discussed.

---

\*The Astrophysical Journal 1973, 182, 1103

W. Forman, C. Jones, H. Tananbaum, H. Gursky, E. Kellogg, and R. Giacconi  
Reproduced by permission of the University of Chicago Press

© 1973. The American Astronomical Society. All rights reserved. Printed in U.S.A.

### 3.4.2 Observations

The discovery of the binary nature of HD77581, the bright star in the error box of 2U 0900-40, prompted us to undertake a detailed study of the X-ray source and to look for evidence of periodic occultations. The low average intensity and the large variability of the X-ray source greatly complicated the search for occulting phenomena. With the Uhuru satellite, 2U 0900-40 was monitored between May 8 and June 30, 1972. These continuous observations show regular intensity variations consistent with a period of  $8.95 \pm 0.10$  days. Analysis of these same data eliminates other periods from fractions of a day up to 8.95 days. Aside from multiples of 8.95 days, these data eliminate any possible periodicities less than about 30 days. Figure 3-12 shows these data folded modulo 8.95 days. The data clearly show the high and low intensity states for the source. In addition to the periodic lows, there are occasional times less than half a day long, when the source is not observed above the background. Although these data are not corrected for aspect, the X-ray detectors were well-centered on the source during all of the X-ray lows so that the upper limits shown do not result from the source's being out of the field of view.

We have studied earlier observations of 2U 0900-40 from Uhuru. On 1971 December 18 - 19 an occultation and subsequent turn-on was observed which agree with data presented by Ulmer et al. for the same two days. The source was also observed for about one day on each of 13 different occasions between 1970 December and 1971 July, while the Uhuru star sensors were operational. In all but two intervals average intensities corrected for aspect ranged from 10 to 75 counts/second, while on 1971 February 5 - 7 and April 18 - 19 the source was not observed above the X-ray background with  $3-\sigma$  upper limits of 3 counts/second. Combining all Uhuru data

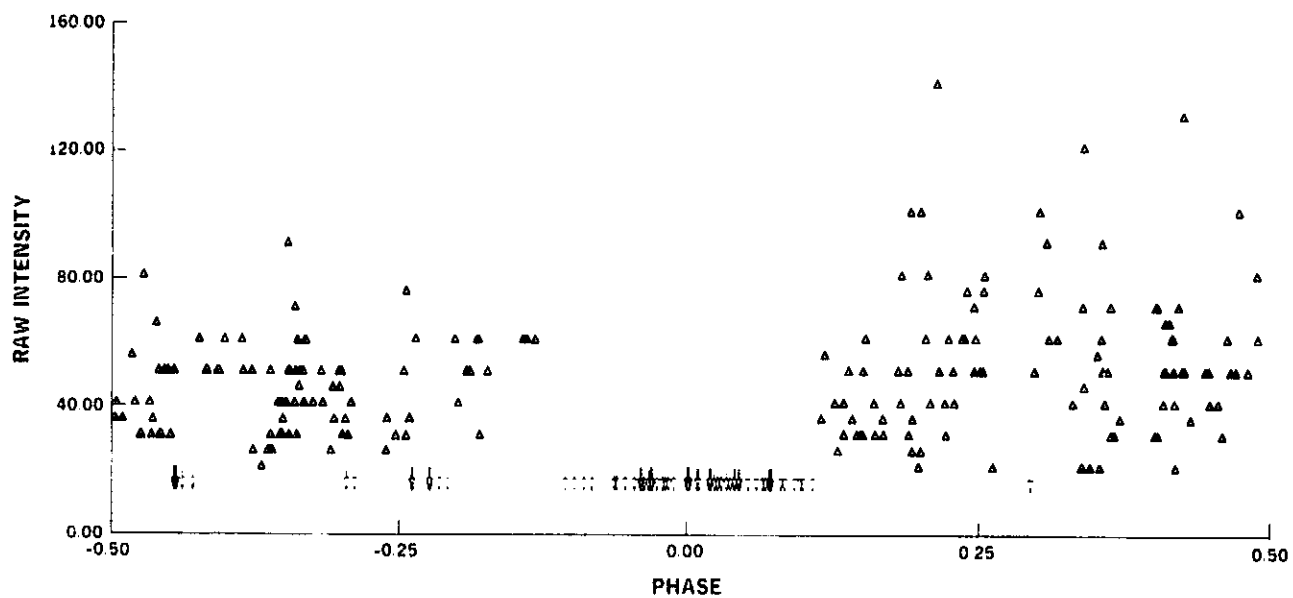


Figure 3-12. The 2 - 6 keV intensity of 2U 0900-40 is shown. The data are from May - July 1972 and are folded modulo the 8.95-day period. The data are not corrected for aspect.

on the source from 1970 December to 1973 January we have been able to determine a unique period of  $8.95 \pm 0.02$  days. The phase of the period as defined by the center of the occultation is UT 1972 May 9.04  $\pm$  0.07. The duration of the occultation is  $1.90 \pm 0.05$  days. However, for 1971 February 5 - 7 the source was not detected for a longer time than the normal eclipse duration. This behavior may result from a variable occultation duration or it may be an interval of low intensity, as was observed occasionally during the high state in the May - June 1972 data. The source has exhibited no extended low intensity states lasting several times the orbital period, such as have been observed for Her X-1, Cen X-3, and SMC X-1.

In addition to the observed occultations, 2U 0900-40 shows a remarkable degree of variability on shorter time scales. Figure 3-13 shows the 2 - 6 keV intensity corrected for aspect during half a day of observations in March 1971. The X-ray luminosity changed by a factor of 30 in about two hours. Flares of this intensity are rare, but irregular variability is the rule as is illustrated by the remainder of the data in the figure. We have observed intensities above 100 cts/sec for at least one pass on three of the 13 days for which star aspect was available. During these 13 days the overall average intensity was about 40 cts/sec.

Observations taken during the peak of the flare, shown in Figure 2, exhibit short time-scale fluctuations. During one 20-second pass the intensity of the source increased by  $24 \pm 4\%$  in less than 0.4 seconds. The intensity remained at the higher value for three seconds before returning to the original level. Fourier analyses of several observations of 2U 0900-40 did not reveal any short term periodicities such as are seen in Her X-1 and Cen X-3. We can set a  $3-\sigma$  upper limit of

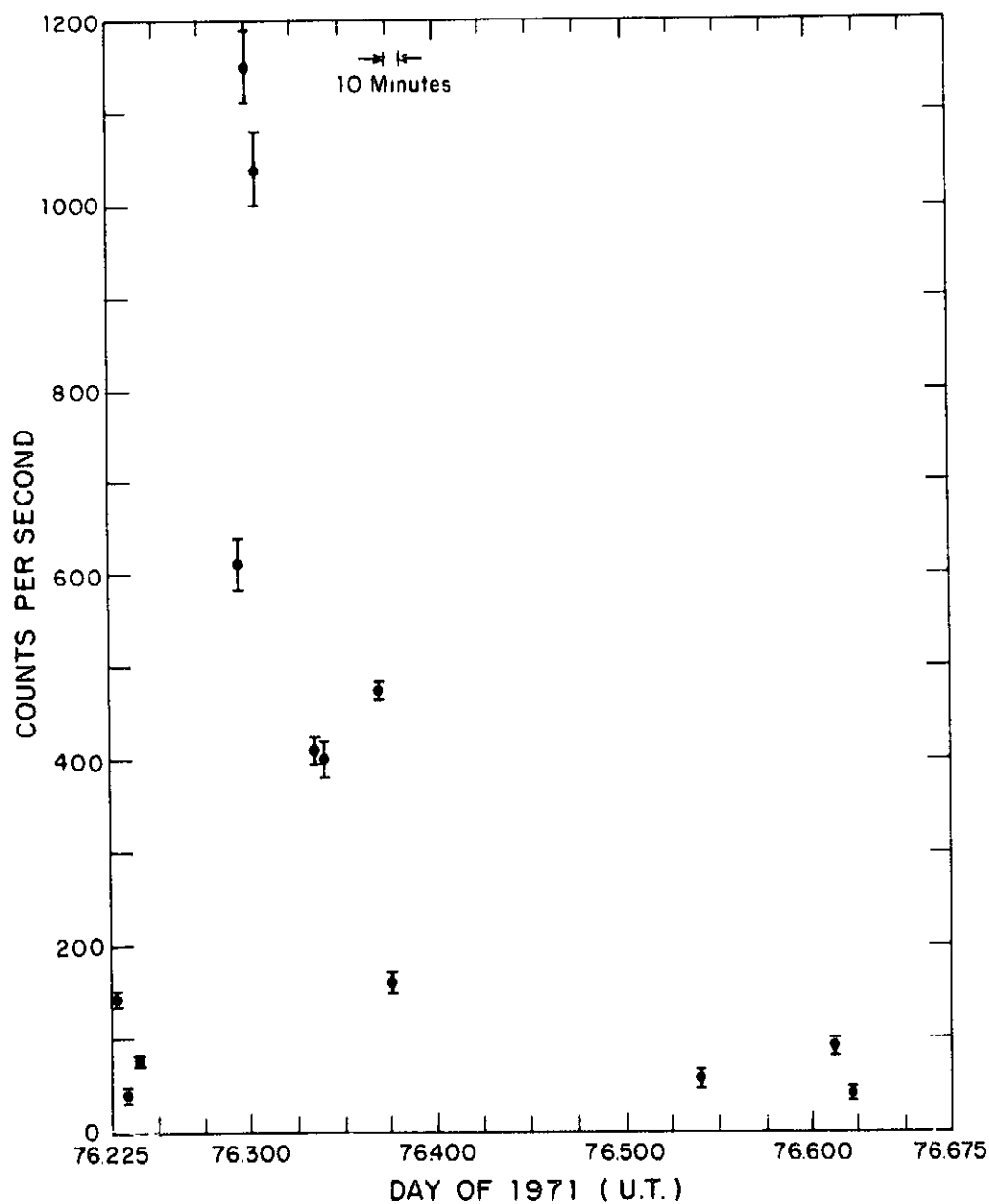


Figure 3-13. The 2 - 6 keV intensity of 2U 0900-40 on March 17, 1971 is shown corrected for aspect with  $\pm 1 \sigma$  error bars (including both aspect and statistical errors). In two hours the intensity of the source increased by a factor of about 30. Other significant intensity variations are also present.

10% on the flux that is periodically pulsed for periods between 0.1 and 10 seconds.

Although the 2 - 20 keV energy spectrum of 2U 0900-40 is somewhat variable, it is always flat with a large amount of low energy absorption. For a power law energy spectrum the low energy cutoff varies between 2.2 and 4.4 keV and the spectral index ranges from -0.2 to +0.7. Thermal spectra with  $T > 20 \times 10^7 \text{ }^\circ\text{K}$  and a low energy cutoff greater than 2.2 keV are also consistent with much of the data.

Using data obtained after the completion of the 2U catalogue, we have refined the source location from an area of 25 square minutes of arc to 4 square minutes of arc. Figure 3-14 shows both the old and the new positions. The star HD77581 remains well within the reduced error box, which is centered at:

$$\alpha (1950) = 9^{\text{h}} 00^{\text{m}} 15.0^{\text{s}} \quad \delta (1950) = -40^{\circ} 21' 40''$$

with corners of the 90% region located at:

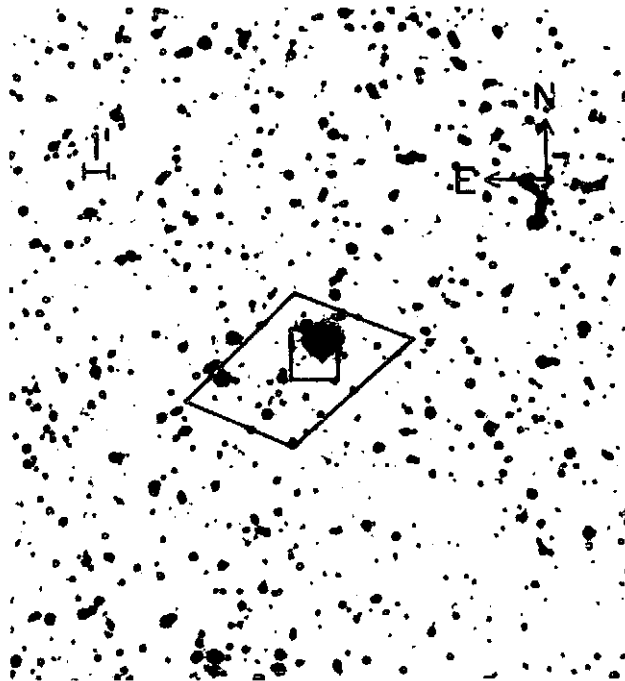
$$\begin{array}{cccc} \alpha = 9^{\text{h}} 00^{\text{m}} 19.7^{\text{s}} & 9^{\text{h}} 00^{\text{m}} 19.7^{\text{s}} & 9^{\text{h}} 00^{\text{m}} 10.3^{\text{s}} & 9^{\text{h}} 00^{\text{m}} 10.3^{\text{s}} \\ \delta = -40^{\circ} 22' 34'' & -40^{\circ} 20' 46'' & -40^{\circ} 20' 46'' & -40^{\circ} 22' 34'' \end{array}$$

### 3.4.3 Discussion

Jones et al. (1973) have recently discussed the similarities among the binary X-ray sources. Most notably, the five known occulting X-ray sources, including 2U 0900-40, have flat spectra with variable low energy cutoffs. The observed range in cutoffs observed in 2U 0900-40 implies hydrogen column densities between  $3.7 \times 10^{22}$  and  $3.2 \times 10^{23} \text{ atoms/cm}^2$  (Brown and Gould 1970). The total HI column density determined from 21-cm emission observations in the direction of 2U 0900-40



## LOCATION OF 2U0900-40



PT-099

Figure 3-14. The location of 2U 0900-40 is shown on an enlargement of the Palomar Sky Survey print. Both the old location from the 2U Catalog and a newer Uhuru position are shown. The bright star in the small error box is HD77581.

is approximately  $6 \times 10^{21}$  atoms/cm<sup>2</sup> (Daltabuit 1972). Therefore, the high absorption observed in the X-ray spectrum is intrinsic to the source, as is confirmed by the variability of the cutoff. Intrinsic cutoffs lend further support to the model in which X-rays are produced by accretion onto a compact object from a circumstellar cloud or disk with the accretion material originating from a binary companion.

The 8.95-day periodicity observed in 2U 0900-40 disagrees with the seven-day periodicity reported by Hiltner et al. for HD77581, the star that is the prime candidate for the optical counterpart to the X-ray source. However, as Hiltner (1972) has pointed out, the optical data are consistent with a 8.95-day period if the observation of 1972 February 13 is put on the descending rather than the ascending branch of the radial velocity curve. Observations indicate 2U 0900-40 is a member of a binary system and the star HD77581, located within the small X-ray error box, has been observed to have a binary period consistent with that determined for the X-ray object. Thus it is possible that 2U 0900-40 and HD77581 are members of the same binary system. Further optical observations of HD77581 are now most important to resolve this question.

### REFERENCES

- Bradt, H. and Kunkel, W. 1971, private communication.
- Brown, R. L. and Gould, R. J. 1970, Phys. Rev., D1, 2252.
- Brucato, R. J. and Kristian, J. 1972, Ap. J. (Letters), 173, L105.
- Chodil, G., Mark, H., Rodrigues, R., Seward, F. D. and Swift, C. D. 1967, Ap. J., 150, 57.
- Daltabuit, E. 1972, preprint.
- Feast, M. W., Thackeray, A. D., and Wesselink, A. J. 1968, Mem. R. A. S., 68, 1.
- Gursky, H., Kellogg, E. M., and Gorenstein, P. 1968, Ap. J. (Letters), 154, L71.
- Hiltner, W. A., private communication, 1972.
- Hiltner, W. A., Werner, J., and Osmer, P. 1972, Ap. J. (Letters), 175, L19.
- Hogg, A. R. 1958, Mount Stromlo Mimeo, 2.
- Jones, C., Forman, W., Tananbaum, H., Schreier, E., Gursky, H., Kellogg, E., and Giacconi, R. 1973, Ap. J. (Letters), 181, L33.
- Kellogg, E. M. and Murray, S. 1971, private communication.
- Morgan, W. W., Code, A. D. and Whitford, A. E. 1955, Ap. J. Suppl., 2, 41.
- Ulmer, M. P., Baity, W. A., Wheaton, W. A., and Peterson, L. E. 1972, Ap. J. (Letters), 178, L121.

### 3.5 2U 1700-37\*

#### 3.5.1 Introduction

The X-ray source 2U 1700-37 was first detected by the Uhuru satellite in December 1970. Observations have shown the source to have periodic occultations every 3.4 days, indicating a binary nature. The source is highly variable on short time scales but exhibits no periodic short-term pulsations such as are seen in the X-ray binaries Cen X-3 and Her X-1 (Giacconi et al. 1971; Schreier et al. 1972a; Tananbaum et al. 1972a). The energy spectrum of 2U 1700-37 is flat and cut off at low energies, similar to the spectra of other reported X-ray binaries (Schreier et al. 1972a; Tananbaum et al. 1972a; Schreier et al. 1972b; Forman et al. 1972). On the basis of close positional agreement and its similarity to other stars associated with X-ray sources (Gursky 1972), the star HD153919 is suggested as an optical candidate.

\*The Astrophysical Journal 1973, 181, L43

C. Jones, W. Forman, H. Tananbaum, E. Schreier, H. Gursky, E. Kellogg, and R. Giacconi, Reproduced by permission of the University of Chicago Press

© 1973. The American Astronomical Society. All rights reserved. Printed in U.S.A.

### 3.5.2 Observations

The most extensive Uhuru observations of 2U 1700-37 were made in May 1972. The 2 to 6 keV intensity measured for seven days during this set of observations is shown in Figure 3-15. These data show two complete cycles of the source. Transitions from the high-intensity state to the low state are clearly visible on May 11.7 and May 15.1. Two upward transitions from states of low intensity to states of high intensity are seen on May 12.8 and May 16.2. Combining these observations with others ranging over a year and a half, we have determined a period of  $3.412 \pm 0.002$  days. The occultation is centered on U. T. 1972, May 15.64  $\pm$  0.04 (J. D. = 2441454.14)

We have examined data for 70 days on which 2U 1700-37 was surveyed between December 1970 and May 1972 and have determined that its behavior is always consistent with the derived period and phase. Observations obtained over this time are shown in Figure 3-15 folded with the 3.412-day period. The data are plotted twice for illustration. We conclude that there are no extended times of low intensity during which the source is not observed.

The eclipse duration determined from the data in Figure 3-15 is  $1.10 \pm 0.07$  days. We can set a  $3-\sigma$  upper limit of 6 counts/second on the intensity observed during the occultation of 2U 1700-37. At times the occultation appears to be somewhat longer than 1.10 days, as in the first cycle in Figure 3-15. It is possible that the large variability in intensity described below could account for this behavior or that the eclipse duration actually does vary.

The data in Figure 3-15 also show a second minimum at phase 0.5. When all the available sightings are folded with the 3.412-day period and averaged into 25

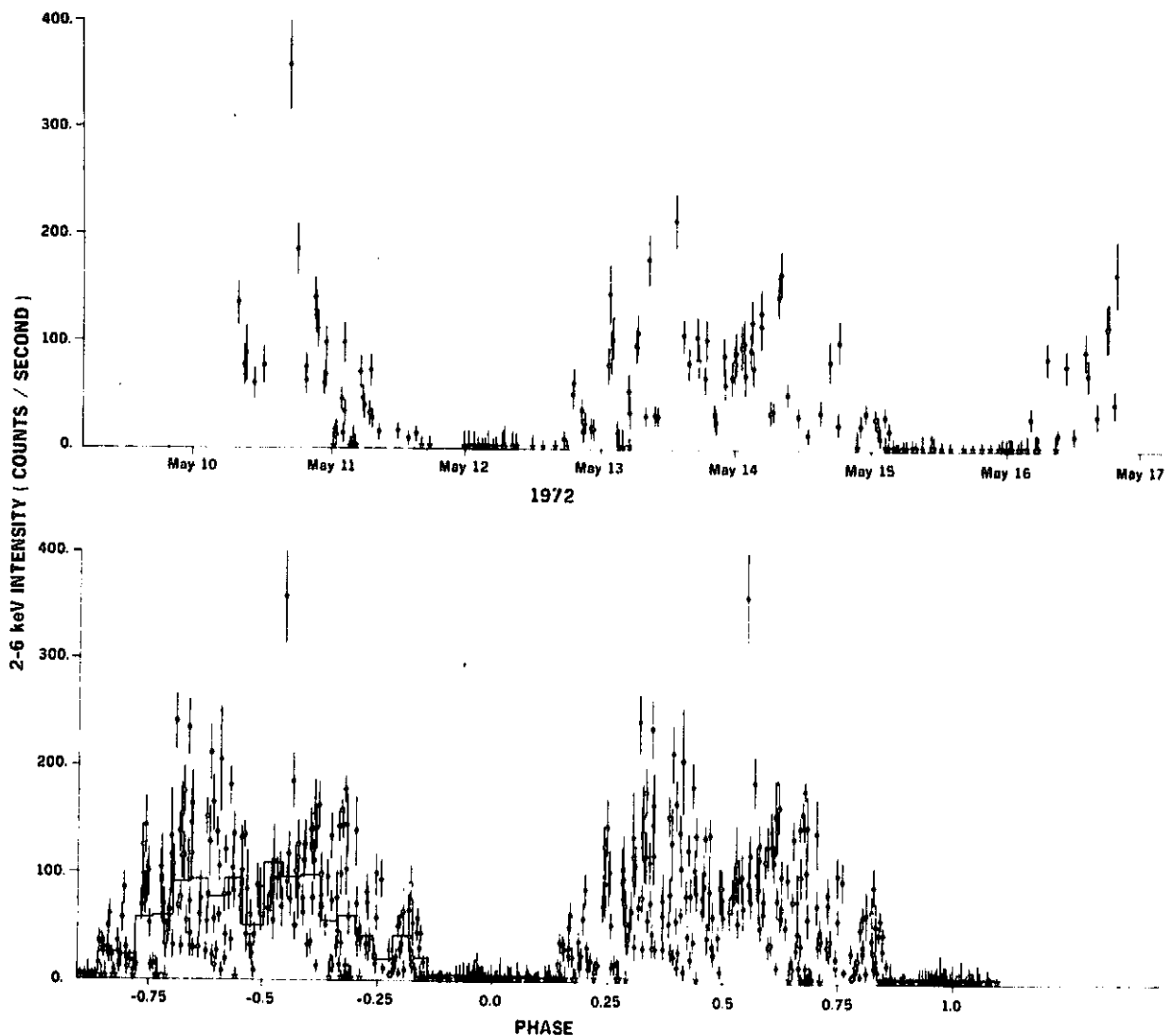


Figure 3-15 The 2 - 6 keV intensity of 2U 1700-37 corrected for elevation in the field of view and shown with  $\pm 1\sigma$  error bars. The upper portion shows seven days of data from May 1972. Plotted below are observations obtained between December 1970 and May 1972 folded with the 3.412-day period. A histogram of the intensity averaged in 25 equal intervals is also shown.

intervals, the average intensity in the center bin of the high state is half that of the adjacent bins. The intensity at phase 0.5 is ten standard deviations below that of the bins on either side, although it is not particularly meaningful to consider the difference in terms of standard deviations since statistically significant fluctuations in intensity are so prevalent in the data. There are, however, no substantial upward fluctuations yet observed at phase 0.5. The intensity averages without error bars are shown in the lower portion of Figure 3-15.

There is a large degree of variability in the intensity during the 2.3-day "on" time, as can be seen in Figure 3-15. Since the data in the top portion of Figure 3-15 were obtained after the failure of the Uhuru star sensors, only rough aspect information was available to correct the source intensity for the location of the source within the collimator field of view, so that the error bars on the intensities are necessarily large. However, the large uncertainties do not mask the fluctuations in which the intensity changes by as much as a factor of four in times of ten minutes. Variability on the time scale of seconds also has been observed. On several occasions the intensity has more than doubled from one second of observations to the next. All of this variability has also been detected during observations made when the Uhuru star sensors yielded good aspect information.

Rapid intensity changes on time scales of a tenth of a second are also present in the 2U 1700-37 data. These fluctuations are not so striking as those seen in Cyg X-1, perhaps owing to the lower intensity of 2U 1700-37. However, even when no significant flares on times of seconds are visible, the fits of the data to a constant intensity are not good, implying that there is variability on even shorter

time scales. When the intensities are averaged over a few tenths of a second the fit is improved for about half the cases. For example, analysis of the center seven seconds of one 30-second pass with the data taken every tenth of a second gave a  $\chi^2$  per degree of freedom of 1.47 with a sigma of 0.16; the same measurement summed in 0.3-second bins gave a  $\chi^2$  per degree of freedom of 1.04 with a sigma of 0.28. We interpret these results as indicating that the rapid changes occurred on times of a tenth of a second or less. We have Fourier-analyzed and performed autocorrelations on several 20 - 30 second observations of 2U 1700-37 with a time resolution of 0.096 seconds to search for a periodicity in the short-term variability. We can set a  $3-\sigma$  upper limit of 17 percent on the percentage of the flux that is periodically pulsed with a period ranging from 0.1 to about 10 seconds.

The 2 to 20 keV spectrum of 2U 1700-37 is flat and shows a large amount of low-energy absorption. The spectrum is variable with a power law energy index ranging from -0.4 to +1.0 and a cutoff varying between 2.1 and 5.5 keV, corresponding to hydrogen densities of  $4 \times 10^{22}$  and  $4 \times 10^{23}$  atoms/cm<sup>2</sup> (Brown and Gould 1970). Thermal spectra with temperatures greater than  $10^8$  °K and substantial low-energy cutoffs are also consistent with many of the observations.

The position of the X-ray source (90% confidence level contours) is shown in Figure 3-16. The large box is the position from the 2U catalog and the small box is a new position obtained from additional source sightings not included in the 2U catalog. The new box has an area of 0.009 square degrees and is centered at  $\alpha(1950) = 17^{\text{h}} 00^{\text{m}} 29^{\text{s}}$  and  $\delta(1950) = -37^{\circ} 46'.4$ , with the corners located at



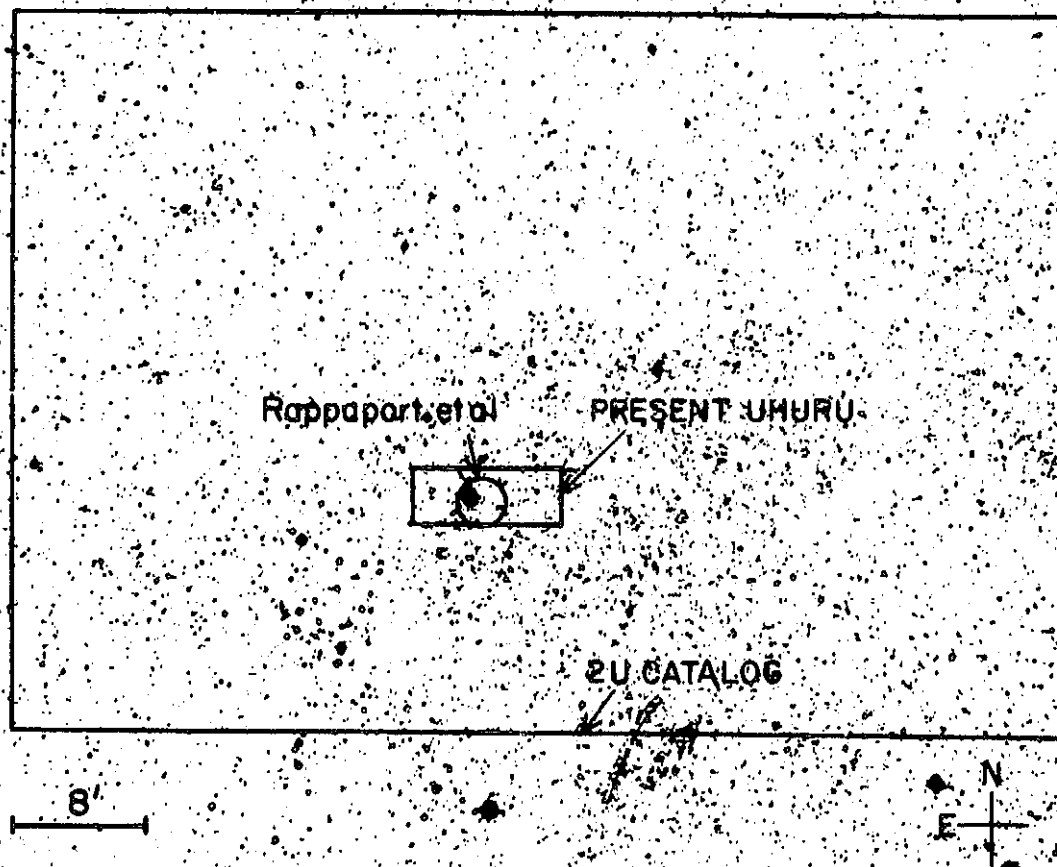


Figure 3-16 The location of 2U 1700-37 is shown on an enlargement from the Palomar Sky Survey. Both the old location from the 2U catalog and the new Uhuru position are shown. In addition, a location recently determined by Rappaport et al. (1972) is given. The bright star contained within all three location determinations is HD153919, the suggested optical candidate.

$\alpha(1950)$	$\delta(1950)$
$17^h 00^m 51^s$	$-37^\circ 48'.0$
$17^h 00^m 51^s$	$-37^\circ 44'.7$
$17^h 00^m 6^s$	$-37^\circ 44'.7$
$17^h 00^m 6^s$	$-37^\circ 48'.0$

### 3.5.3 Discussion

The most conspicuous object at the new X-ray location is a 6.6 magnitude O7f (Crampton 1971) star HD153919 ( $\alpha_{1950} = 17^h 00^m 32^s.7$   $\delta_{1950} = -37^\circ 46' 29''$ ). Rappaport et al. (1972) have communicated that data from a rocket flight on 1971 May 1 have yielded an independent X-ray location for 2U 1700-37. Their observations with a modulation collimator show a  $4\sigma$  peak centered at  $\alpha(1950) = 17^h 00^m 29^s.5$  and  $\delta(1950) = -37^\circ 46' 44''$  with a radius of uncertainty of  $1'.5$  (90% confidence). This position, which includes the candidate star, is also shown in Figure 3-16.

The high correlation of bright stars in X-ray error boxes noted by Gursky (1972) provides further reason for considering this star as the optical candidate. Also Heap (1971) has found that compared to O stars, Of stars have low surface gravities, which would fit well with a model in which X-rays result from the accretion of mass from the binary companion, in this case the O7f star, onto the compact X-ray source. Compactness is inferred from the short time-scale pulsations. Spectra recently obtained on this star (Koo 1972; Liller and Forman 1972) show interesting features that appear to come and go on time scales less than ten minutes. Further optical observations of HD153919 are needed to test the identification with the X-ray source.

Henry (1972) has suggested that for binary systems containing X-ray sources, the amount of X-ray radiation absorbed by the optical companion and reradiated at UV and optical frequencies is proportional to the duration of the X-ray eclipse. For 2U 1700-37, the maximum observed X-ray luminosity from 2 to 10 keV is  $3 \times 10^{36}$  ergs/second, based on a distance of 1.7 kpc to the optical candidate. However, the luminosity of the optical candidate is about  $10^{38}$  ergs/second so that even if a large fraction of the X-ray energy were absorbed and reradiated, there would be only a small ( $\leq 1\%$ ) effect on the observed optical luminosity.

Six X-ray sources--Cen X-3, Her X-1, SMC X-1, Cyg X-1, 2U 0900-40 and 2U 1700-37--are now believed to belong to binary systems. Of the six, all except Cyg X-1 show X-ray occultations. As for the other occulting binaries, the energy spectrum of 2U 1700-37 is flat and has a large low-energy cutoff. Interstellar absorption cannot account for the large cutoff and certainly not for the variability observed in the amount of absorption. In fact, this source has the greatest amount of absorption of any of the X-ray binaries observed so far. The eclipse duration of 2U 1700-37 is also the longest of any of the six binaries, lasting about 30 percent of the entire period. Schreier et al. (1972b) have suggested that the large low-energy cutoff observed in occulting X-ray binaries is due to an accretion disk or circumbinary matter concentrated in the orbital plane. Also the presence of a second intensity minimum, when combined with the compactness required by the time variability and the parameters of the system that might be determined from an optical identification, could be very important in understanding the nature of the emission process.

A comparison of some of the properties of 2U 1700-37 with those of the other X-ray binaries is given in Table 3.3. For the power law energy index and the low-energy cutoff, the extremes in variability are given for each source. In several respects, in addition to their both being in binary systems, 2U 1700-37 is similar to Cyg X-1. For both sources the X-ray energy is pulsed on short time scales requiring compactness of the X-ray source, although neither shows periodic pulsations. Neither source exhibits extended lows during which it is not observed above the X-ray background. In addition, the peak X-ray luminosities of 2U 1700-37 and Cyg X-1 (post transition) are about the same if the optical identifications and hence the distances are correct. The close similarity in the X-ray properties of Cyg X-1 and 2U 1700-37 suggests that 2U 1700-37 might be a black hole, as has been advocated for Cyg X-1 (Webster and Murdin 1972; Bolton 1972a, b; Tananbaum et al. 1972b). In that case, as for Cyg X-1, the mass of the X-ray source would be considerable and the mass ratio therefore would not be very different from unity. Hence a search for radial velocities in the proposed optical candidate could prove most informative.

Table 3.3

## CHARACTERISTICS OF X-RAY BINARIES

<u>Source</u>	<u>Binary Period (Days)</u>	<u>Short Term Variability</u>	<u>Long Term Variability</u>	<u>Power Law Energy Index</u>	<u>Cutoff (keV)</u>	<u>Optical Candidate</u>	<u>Distance (kpc)</u>	<u>Peak Luminosity (<math>2 - 10</math> keV ergs/sec)</u>
2U1700-37	$3.412 \pm 0.002$	Non-periodic pulsations as short as 0.1 sec	No extended lows	$-0.4 \rightarrow +1.0$	$2.1 \rightarrow 5.5$	HD153919	1.7	$3 \times 10^{36}$
2U0900-40 (GX263+3)	$8.96 \pm 0.05^{a,b}$	Non-periodic <sup>a</sup> pulsations on times of secs	No extended lows <sup>a</sup>	$-0.2 \rightarrow +0.7^a$	$2.5 \rightarrow 4.4^a$	HD77581 <sup>c,d,e,t</sup>	$1.3^{d,e}$	$4 \times 10^{36}$
SMC X-1 (2U0115-73)	$3.8927 \pm 0.0010^f$	Non-periodic <sup>f</sup> pulsations on times of mins	Extended lows <sup>f</sup>	$0.0 \rightarrow 0.3^f$	$1.5 \rightarrow 3.0^f$	Sanduleak <sup>u</sup> No. 160	$61^f$	$3 \times 10^{36}$
Her X-1 (2U1702+35)	$1.700167 \pm 0.000006^{g,h}$	$1.23782 \text{ sec}^{g,h}$ pulsations	Extended lows <sup>g,h</sup> average cycle of 35.3 days	$-1.3 \rightarrow +0.2$	$1.5 \rightarrow 3.2$	hZ Her <sup>i,j,k</sup>	$5.9^k$	$1 \times 10^{37}$
Cen X-3 (2U1119-60)	$2.08712 \pm 0.00004^l$	$4.842 \text{ sec}^l$ pulsations	Extended lows <sup>l</sup>	$-0.4 \rightarrow +0.6$	$1.5 \rightarrow 4.2$	None	?	?
Cyg X-1 (2U1956+35)	$5.600 \pm 0.003$ from <sup>m,n,o</sup> optical. Not observed in X-ray	Quasi-periodic <sup>p,q,r</sup> pulsations as short as 50 millisec	Single low-energy <sup>s</sup> transition	$2.8 \rightarrow 4.1$ before transition $0.45$ after transition	$\leq 1.5$	HDE226868 <sup>m,n</sup>	$2^{n,o}$	$1 \times 10^{37}$ before transition $3 \times 10^{36}$ after transition

a. Forman et al. 1972

b. Ulmer et al. 1972

c. Kellogg and Murray 1971

d. Brucato and Kristian 1972

e. Hiltner, Werner, and Osmer 1972

f. Schreier et al. 1972b

g. Tananbaum et al. 1972a

h. Giacconi et al. 1972

i. Liller 1972a

j. Bahcall and Bahcall 1972

k. Forman, Jones, and Liller 1972

l. Schreier et al. 1972a

m. Bolton 1972a

n. Webster and Murdin 1972

o. Bolton 1972b

p. Rappaport et al. 1971

q. Oda et al. 1971

r. Schreier et al. 1971

s. Tananbaum et al. 1972b

t. Bradt and Kunkel 1971

u. Liller 1972b

## REFERENCES

- Bahcall, J., and Bahcall, N. 1972, preprint.
- Bolton, C. T. 1972a, Nature, 235, 271.
- Bolton, C. T. 1972b, preprint.
- Bradt, H., and Kunkel, W. 1971, private communication.
- Brown, R. L., and Gould, R. J. 1970, Phys. Rev. D 1, 2252.
- Brucato, R. J., and Kristian, J. 1972, Ap. J. (Letters), 173, L105.
- Crampton, D. 1971, Astron. J., 76, 260.
- Forman, W., Jones, C., and Liller, W. 1972, Ap. J. (Letters), 177, L103.
- Forman, W., Jones, C., Tananbaum, H., Kellogg, E., Gursky, H., and Giacconi, R. 1972, in preparation.
- Giacconi, R., Gursky, H., Kellogg, E., Schreier, E., and Tananbaum, H. 1971, Ap. J. (Letters), 167, L67.
- Giacconi, R., Gursky, H., Kellogg, E., Levinson, R., Schreier, E., and Tananbaum, H. 1972, in preparation.
- Gursky, H. 1972, Ap. J. (Letters), 175, L141.
- Heap, S. 1971, Astr. and Ap., 15, 77.
- Henry, J. P. 1972, private communication.
- Hiltner, W. A., Werner, J., and Osmer, P. 1972, Ap. J. (Letters), 175, L19.
- Kellogg, E., and Murray, S. 1971, private communication.
- Koo, D. 1972, private communication.
- Liller, W. 1972a, IAU Circ. #2415.
- Liller, W. 1972b, IAU Circ. #2469.
- Liller, W. and Forman, W. 1972, private communication.
- Oda, M., Gorenstein, P., Gursky, H., Kellogg, E., Schreier, E., Tananbaum, H., and Giacconi, R. 1971, Ap. J. (Letters), 166, L1.

- Rappaport, S., Doxsey, R., and Zaumen, W. 1971, Ap. J. (Letters), 168, L43.
- Rappaport, S., Doxsey, F., and Zaumen, W. 1972, private communication.
- Schreier, E., Gursky, H., Kellogg, E., Tananbaum, H., and Giacconi, R. 1971, Ap. J. (Letters), 170, L21.
- Schreier, E., Levinson, R., Gursky, H., Kellogg, E., Tananbaum, H., and Giacconi, R. 1972a, Ap. J. (Letters), 172, L79.
- Schreier, E., Giacconi, R., Gursky, H., Kellogg, E., and Tananbaum, H. 1972b, Ap. J. (Letters), to be published.
- Tananbaum, H., Gursky, H., Kellogg, E., Levinson, R., Schreier, E., and Giacconi, R. 1972a, Ap. J. (Letters), 174, L143.
- Tananbaum, H., Gursky, H., Kellogg, E., Giacconi, R., and Jones, C. 1972b, Ap. J. (Letters), 177, L5.
- Ulmer, M. P., Baity, W. A., Wheaton, W. A., and Peterson, L. E. 1972, Ap. J. (Letters), to be published.
- Webster, B. L. and Murdin, P. 1972, Nature, 235, 37.

### 3.6 Cygnus X-3\*

If we now turn to Cygnus X-3, we find a different looking X-ray picture. Figure 3-17 shows the 2-6 keV Uhuru observation of Cygnus X-3 for 9 days in May 1972. The error bars contain both the statistical and systematic uncertainties. The data show intensity variations of about a factor of two with a period of 4.8 hours first reported by Parsignault et al. (1972). Figure 3-18 shows the 9 days data in three different energy bands from 1.8 to 10.0 keV plotted folded with the 4.8-hour period. We see that the minimum is observed in all three energy bands and that the intensity variations across the 4.8-hour cycle are essentially independent of energy. Thus, the minimum is not due to photoelectric absorption which would show a strong energy dependence,  $\exp \left[ (-E_a/E)^{8/3} \right]$ . Among the possible models still being considered for this 4.8-hour light curve are a binary system with a 4.8-hour orbital period and intensity variations caused either by geometrical obstruction or by different optical depths in different viewing directions due to only weakly energy dependent Compton scattering in a hot-ionized cloud, an idea suggested by Gursky (1973). Compton scattering calculations by Tucker (1973) suggest an emitting region that would be of order  $10^8$  cm, a size consistent with short time scale fluctuations now observed on at least some occasions, indicating a compact component of the source. Other possibilities for the 4.8-hour cycle would be pulsation or rotation of a single star.

For the 4.8-hour cycle we have a new, tentative period of  $0.1996515 \pm 0.0000032$  days constant from December 1970 through June 1971 and a period of  $0.1996787 \pm 0.0000012$  from June 1971 to May 1972, an  $8\sigma$  statistical difference. A word of caution concerning this  $1$  part in  $10^4$  increase in the period is in order. The method used to

---

\* From "Stellar X-ray Sources" H. Tananbaum, 1973 IAU Symp. No. 60-Galactic Radio Astronomy, D. Reidel Publishing Co.



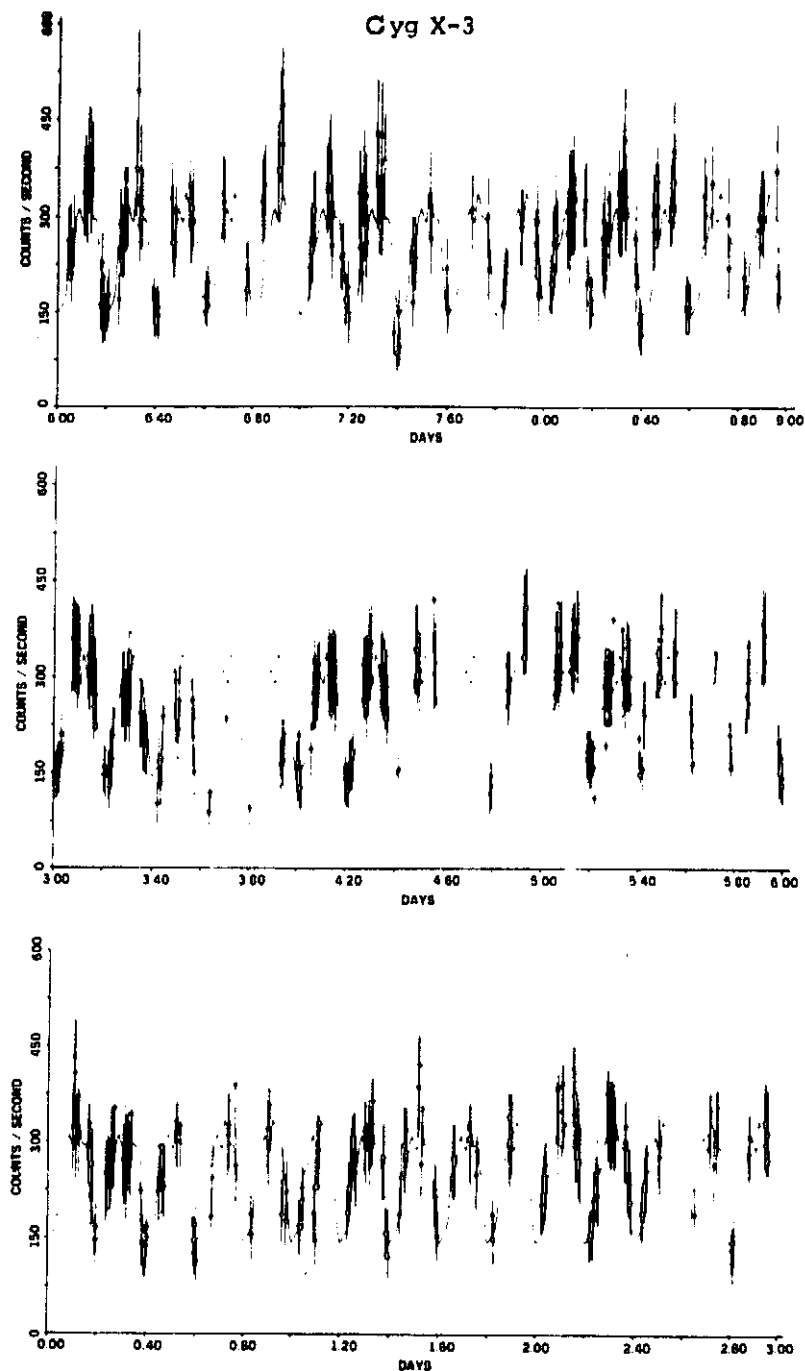


Figure 3-17. Observations of Cygnus X-3 from 8 May to 17 May are plotted as a function of time. The 2-6 keV intensities are given in counts/sec and have been corrected for aspect; errors bars include both statistical error and systematic error and systematic error due to aspect correction. Also shown is the average light curve obtained by folding all the data modulo 4.80 hours and finding the average intensity every 0.24 hours.

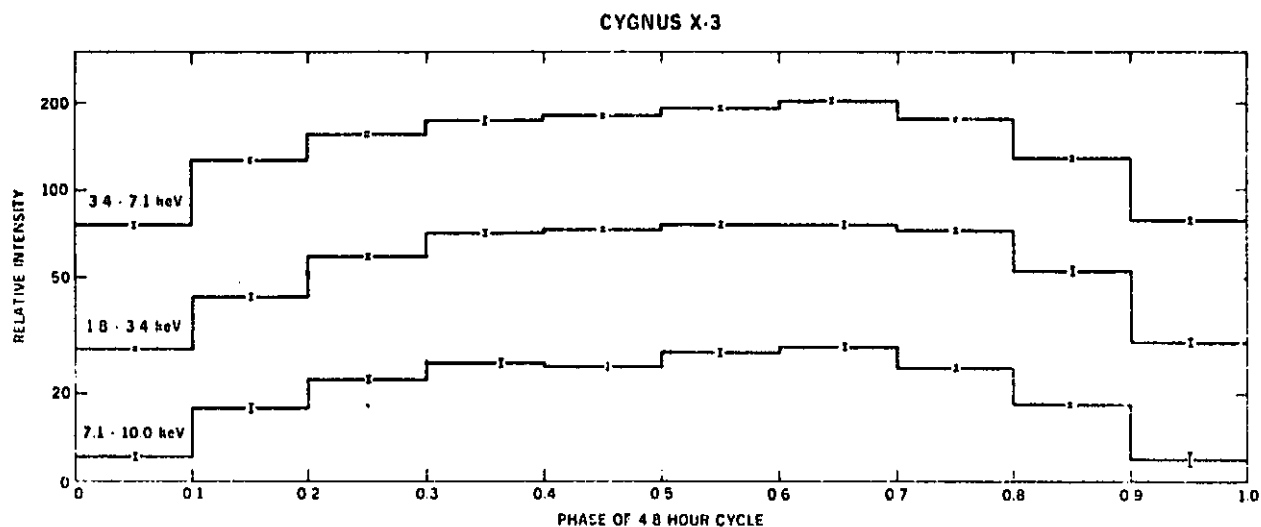


Figure 3-18. Counting rate data for Cygnus X-3 for the same 9 days in May 1972 folded modulo 4.8 hours for 3 energy bands. The intensity scale is logarithmic and the data show that the 4.8 hour intensity variation are essentially energy independent.

determine the phase of the minimum consists of fitting a sine function to the intensity variations. The period is then determined by dividing the time between minimum phases by the appropriate integer number of periods. Canizares et al. (1973) have reported evidence for changes in the shape of the light curve and we must investigate the effects of such a change on our analysis technique before considering the period change as definite. Changes in this period could prove very important in choosing among various models for the 4.8-hour cycle.

Figure 3-19 shows several points over a 1 1/2 year period where we have determined the average intensity of Cygnus X-3. The points with the smallest error bars are data for which the average intensity was determined by the sine fitting technique; other points are obtained as daily averages of randomly selected points or as averages of selected quick look data points at various phases of the 4.8-hour cycle. The data suggest the Cyg X-3 may have average intensity levels which persist for times of months with transitions between levels sometimes observed. Average intensity levels of 60c/s, 125c/s, and 230c/s, are seen at various times. This picture is somewhat similar to that observed for Cygnus X-1 and suggests that the radio data be checked against the X-ray observations if possible, for possible long term correlated changes in average intensity.

Figure 3-20 shows new results for the X-ray intensity for 6 days at the time of the first September 1972 radio flare. We now include production data whereas our earlier report of no significant X-ray changes was based on quick look data only. We see that there are several points of high intensity on September 1, the day before the radio flare was first reported, although the radio data allow for the possibility of an earlier start up since the flare was first observed already in progress. The presence of X-ray intensities of at least

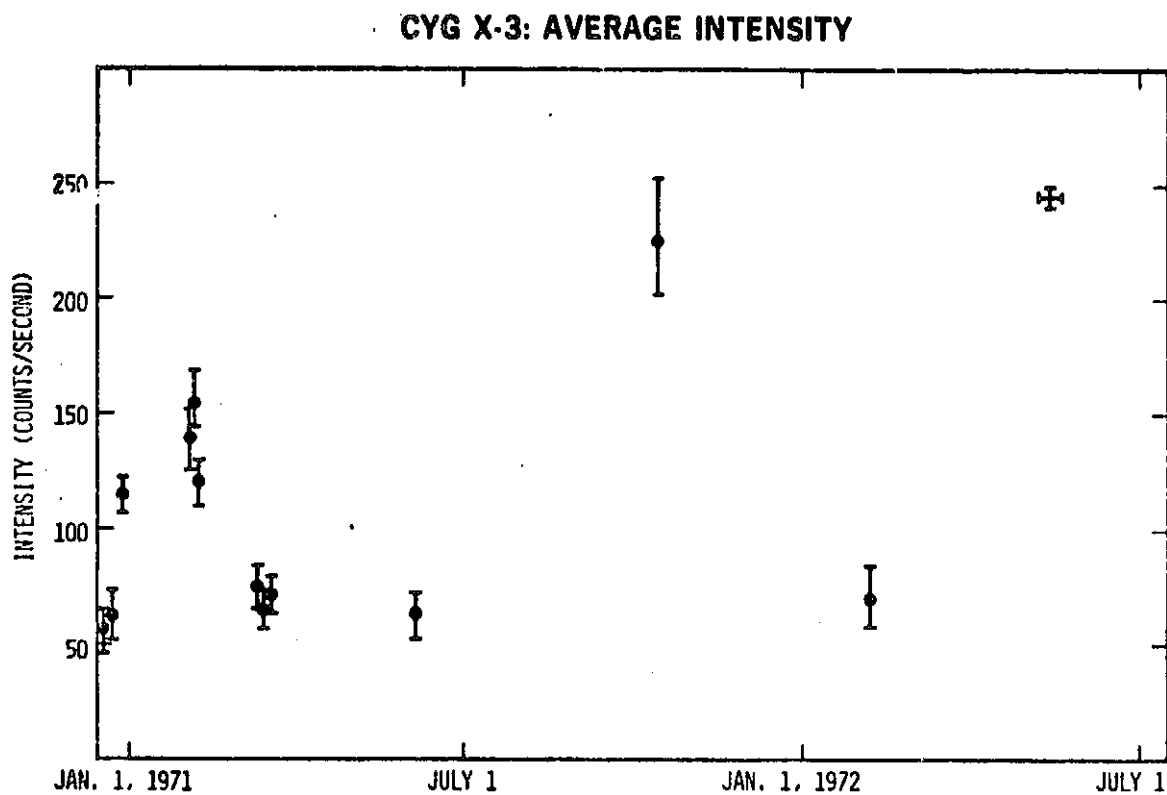


Figure 3-19. Average 2 - 6 keV intensity for Cygnus X-3 on various days from January 1971 until July 1971. Data are corrected for aspect and the concept of "average" is discussed in the text.

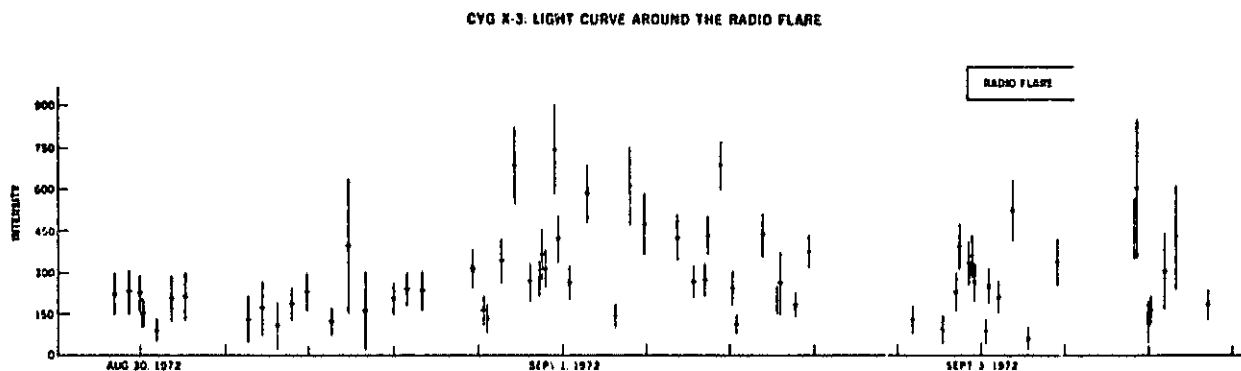


Figure 3-20. 2 - 6 keV X-ray intensity for Cygnus X-3 in late August and early September 1972. The time of the first observation of the giant radio flare is indicated at 220 on September 2. Note the difference in the X-ray behavior around September 1 compared to the preceding days.

600 cts/sec, an intensity greater than ever previously observed for Cygnus X-3 and at least a factor of 2 higher than any intensities measured on August 30 and 31 indicates a connection between the X-ray and radio behavior. This is also supported by preliminary observations of higher temperature energy spectra for the high intensity data points. This observation is important since it confirms the X-ray radio identification previously only suggested by positional coincidence of a few arc minutes. This identification is also confirmed as reported by Professor Boyd at the IAU General Assembly in Sydney by the very recent observation by Becklin et al. (1973) of a 4.8-hour period in the infrared object identified with the Cyg X-3 radio source, with the infrared minimum in phase with the X-ray minimum.

Wallace Tucker and I have performed some very rough, back of the envelope calculations to see what the parameters of a system might be in which  $10^{38}$  ergs/sec is produced in a synchrotron process X-ray flare and  $10^{33}$  ergs/sec is produced in a radio flare. We basically have a model in which the electrons are injected and first produce X-rays in a small region with an intense magnetic field and then expand into a larger region with smaller B and produce the radio emission. We assume an X-ray emitting region of order  $10^9$  cm and a radio emitting region of order  $10^{15}$  cm.

Assuming a radio lifetime of 10 days we find as already determined by Gregory et al. (1972) a magnetic field of  $\leq 5$  gauss in the radio emitting region; we now can determine a magnetic field of  $5 \times 10^9$  gauss in the X-ray region, electron energies of  $\sim 10$  MeV, and number densities of  $\sim 5 \times 10^{-2}/\text{cm}^3$  for the radio emitting region and  $\sim 5 \times 10^3/\text{cm}^3$  for the X-ray region.

## REFERENCES

1. Becklin, E.E., Hawkins, F.J., Mason, K.O., Matthews, K., Neugebauer, G., Sanford, P.W., and Wynn-Williams, C.G., 1973, preprint.
2. Canizares, C.R., McClintock, J.E., Clark, G.W., Lewin, W.H.G., Schnopper, H.W., and Sprott, G.F., 1973, Nature Phys. Sci., 241 .
3. Gregory, P.C., Kronberg, P.P., Seaquist, E.R., Hughes, V.A., Woodsworth, A., Viner, M.R., and Retallack, D., 1972, Nature Phys. Sci., 239, 440.
4. Gursky, H., 1973, Private communication.
5. Parsignault, D.R., Gursky, H., Kellogg, E.M., Matilsky, T., Murray, S., Schreier, E., Tananbaum, H., Giacconi, R., and Brinkman, A.C., 1972, Nature, 239, 123.
6. Tucker, W., 1973, Private communication.

### 3.7 SMC X-1\*

#### 3.7.1 Introduction

Observations from UHURU have previously determined the presence of a discrete, highly variable X-ray source, SMC X-1, in the direction of the Small Magellanic Cloud (Leong et al. 1971). This source came under further scrutiny with the discovery that several variable X-ray sources seen from UHURU are binary systems (Schreier et al. 1972, Tananbaum et al. 1972a, Tananbaum et al. 1972b). Analysis of further data has demonstrated that SMC X-1 is indeed a binary object with occultations visible every 3.9 days. Except for the lack of regular pulsations, other aspects of its behavior are also consistent with those of the previously reported occulting binaries Cen X-3 and Her X-1. There is variability on time scales of hours as well as evidence for extended low states. Furthermore, its energy spectrum is both flat and cut off at low energies. If we follow Leong et al. in putting the source at the distance of the SMC, then the source is emitting in excess of  $10^{38}$  ergs/sec in the energy range 2 - 6 keV.

#### 3.7.2 Observations

The X-ray source in the Small Magellanic Cloud SMC X-1 (2U0115-73) was observed by UHURU on numerous occasions from 1970 December through 1972 April. As previously reported (Leong et al. 1971) the source was seen to be variable; its intensity (2-6 keV) changed by a factor of about twenty in four hours on 1971 January 12.

\*The Astrophysical Journal, 1972, 178, 171

E. Schreier, R. Giacconi, H. Gursky, E. Kellogg and H. Tananbaum  
Reproduced by permission of the University of Chicago Press



Upon analyzing further data, we have found that this intensity change was neither unique nor random, but represented a transition between two levels. The lower part of Figure 3-21 shows the intensity of the source between 1971 January 11.5 and January 19.5. The reported transition between a level of approximately 20 counts/sec and one of less than a few counts/sec is clearly visible on January 12.7; other transitions can also be seen on January 13.4, 16.6 and 17.2. The data are corrected for aspect and summed over several adjacent spins of the satellite. The one-sigma error bars include both statistical and elevation correction errors. The two regions with relatively large errors represent scans when the source was near the edge of the field of view; the source was completely out of the field of view for an interval on January 18, causing the data gap seen. Significant intensity fluctuations on the time scale of a few hours are seen in the data. In addition, there is evidence for similar variations on the scale of minutes.

The data shown are suggestive of the periodic occulting behavior already determined for Cen X-3 and Her X-1 (Schreier et al. 1972, Tananbaum et al. 1972a). The period can be determined from these data as  $3.895 \pm 0.045$  days, with a "low" state of duration  $0.60 \pm 0.04$  days. When we searched the analyzed UHURU data for further SMC X-1 extended sightings, we found a three day period from 1971 June 9.0 to June 12.3 which contains one other complete occultation of duration  $0.63 \pm 0.06$  days as also shown in

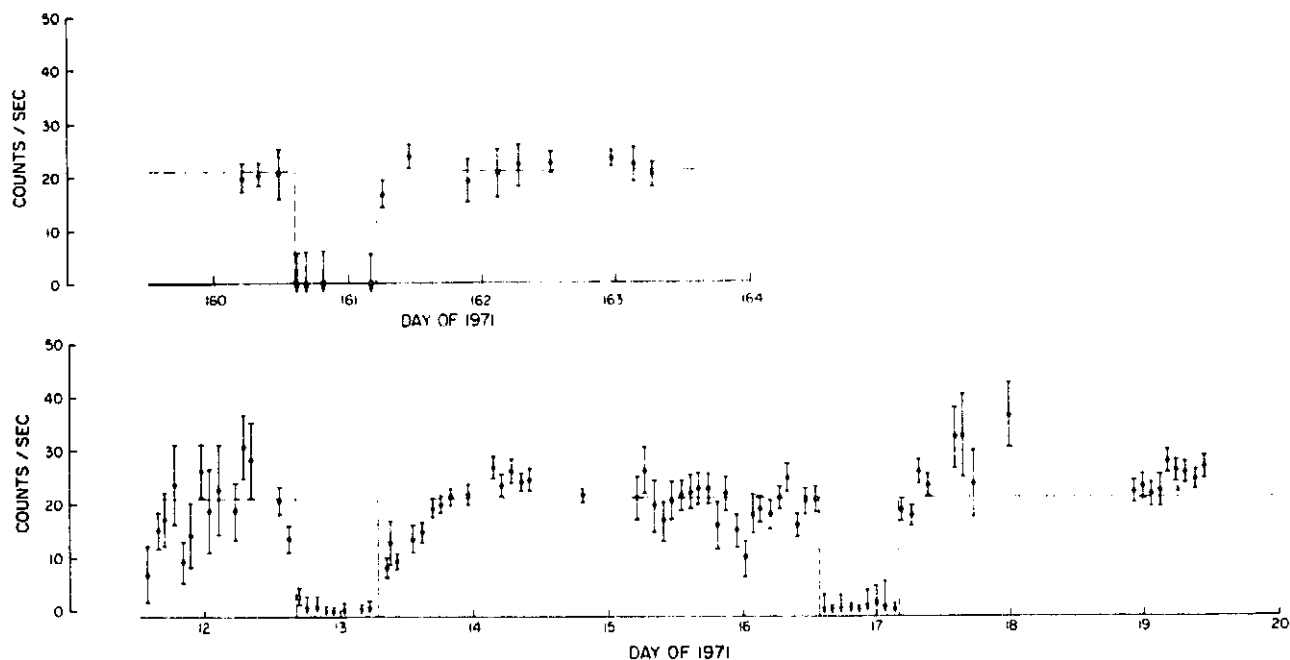


Figure 3-21 The intensity of SMC X-1 in observed counts/sec during eight days in January and three days in June 1971. Data has been corrected for elevation in the field of view; one-sigma error bars include both statistical and elevation correction errors.

Figure 3-21. If we fit a constant period to the data in January and June we can refine the period to  $3.8927 \pm 0.0010$  days. The average low state duration of  $0.60 \pm 0.03$  days is consistent with the three individual determinations. At the present time, the duration of the transition is only determined to be  $\lesssim 0.1$  days. The phase of the period as defined by the center of the low state is  $1971 \text{ January } 12.99 \pm 0.02$ . The dashed line in the figure shows a single periodic light curve extrapolated over the two sightings.

In the remainder of the analyzed UHURU data, there are several times in 1970 December, 1971 January, March, April and May and 1972 March and April when the satellite was oriented so that SMC X-1 was in the field of view. During the 1972 observations, the source was in its "high" state as predicted by the periodicity established above. However, in the remainder of the data there were definite times when the source was seen at or below a few counts per second during predicted high states. Also, in 1971 April, there were at least two occasions when the source was seen at an intermediate level of between 5 and 10 cts/sec during predicted high states. However, we know of no instances in which the source is seen above  $\sim 3$  cts/sec when a low state is predicted. It should also be noted that the intensity of the SMC seen by Price et al. (1971) in 1970 September is comparable to the UHURU "high state"; this observation agrees with our predicted X-ray light curve. If we compare the long term behavior of SMC X-1 with that of Cen X-3 or Her X-1 we

find similarity with Cen X-3. There is no simple regular cycle on the time scale of a month as is known for Her X-1 (Tananbaum et al. 1972a). If one does exist, it must be at least four or five months long. Further continuous observations are planned to study the longer time scale behavior.

The behavior of SMC X-1 on time scales of seconds is harder to determine due to its low counting rate. The two types of behavior we considered were those associated with known X-ray binaries; the periodic pulsations characteristic of Cen X-3 or Her X-1, and the random or quasi-periodic pulsations observed from Cyg X-1.

Simulations were done in which actual UHURU observations of Cen X-3 and Cyg X-1 were scaled down to counting rates comparable to that of SMC X-1, added on to a typical background rate, and randomized according to Poisson statistics. These simulations demonstrated that the pulsations of a Cen X-3 type source could be easily seen even at counting rates lower than that of SMC X-1 by studying a few hundred seconds of data. Fourier analysis and auto-correlations of actual SMC X-1 data showed no evidence of such periodicity. We can place a  $3 - \sigma$  upper limit of 10% on the percentage pulsed in the range of periods from a few tenths of a second to about ten seconds. However, we cannot rule out Cyg X-1 type behavior from the simulations. The short pulse trains often seen in Cyg X-1 data (Schreier et al. 1971) would wash out in the length of data necessary for analysis. Aperiodic fluctuations would not be apparent over statistical fluctuations in a source as weak as SMC X-1, due to the much lower signal-to-noise ratio.

The energy spectrum of SMC X-1 is extremely flat above a few keV, but has a significant low energy cutoff. The best fit power law energy spectral index is  $0.15 \pm 0.10$ ; a thermal bremsstrahlung spectrum with  $kT \gtrsim 30$  keV would fit equally well. The spectrum appears to show variability, especially in respect to the low energy cutoff which has been measured in the range of 1.5 to 2.5 keV, corresponding to a hydrogen column density of about  $2 \times 10^{22}$  atoms/cm<sup>2</sup>. We emphasize that the qualitative behavior of the energy spectrum is the same as that of the other known occulting X-ray sources, Cen X-3 and Her X-1.

The position of SMC X-1 (2U0115-73) has been improved since the 2U catalog and is centered at:

$$\alpha (1950) = 01^{\text{h}} 15^{\text{m}} 24^{\text{s}}$$

$$\delta (1950) = -73^{\circ} 41' 49''$$

with the corners of a 90% region given by

$\alpha = 1^{\text{h}} 14^{\text{m}} 51^{\text{s}}$	$\delta = -73^{\circ} 40' 19''$
$14^{\text{m}} 35^{\text{s}}$	$41' 38''$
$15^{\text{m}} 58^{\text{s}}$	$43' 19''$
$16^{\text{m}} 11^{\text{s}}$	$41' 53''$

Due to the low density of X-ray sources detected by UHURU in this region of the sky (Giacconi et al. 1972), we believe that the location of this source in the direction of the Small Magellanic Cloud is not coincidental. If we assume that the source is indeed in the Small Magellanic Cloud, then the accepted distance of 61 kpc shows that the source is emitting in excess of  $10^{38}$  ergs/sec in the range 2 - 6 keV.

### 3.7.3 Discussion

We may summarize the principal observations as follows: (1) SMC X-1 occults with a period of 3.8927 days; (2) the energy spectrum is cut off at low energies and flat; (3) there is no large amplitude periodic pulsation. In addition, there exists variability at least on time scales of from minute through months. The presence of occultations leads us to compare the properties of SMC X-1 with those of the other known or probable X-ray binaries as shown in Table 3.4. It is evident that in all major respects other than (3) above, SMC X-1 is qualitatively the same as Cen X-3. Indeed, the correlation most apparent in the table appears between occultation and low energy cutoff; they are both present for the first three sources, and neither appears with Cyg X-1 (Figure 3-22). We offer the tentative explanation that occultation requires the observer to be close to the plane of the orbit, and that most of any matter being transferred between the members of the binary system (e.g. an accretion disk) as well as any circumbinary material would be concentrated also in the orbital plane. Thus, low energy cutoff caused by absorption near the source would be most pronounced in the orbital plane and be greatest for occulting sources.

We also note that the luminosity of over  $10^{38}$  ergs/sec makes the binary source SMC X-1 comparable in strength to both the stronger galactic sources and the discrete sources in the Large Magellanic Cloud (Leong et al. 1971). This fact permits the interpretation that even the strongest X-ray sources may be binaries. The high intrinsic luminosities of many galactic sources

Table 3.4  
Properties of Some X-ray Binaries

<u>Source</u>	<u>Occultation</u>	<u>Spectrum</u>	<u>Periodic Pulsation</u>	<u>Long Term Variability</u>
SMC X-1	3.8927 days	Flat, cutoff at 1-3 keV	No large amplitude	Extended lows
Cen X-3 <sup>(a)</sup>	2.08712	Flat, cutoff at 1-4 keV	4.84 sec	Extended lows
Her X-1 <sup>(b)</sup>	1.70017	Flat, cutoff at 1-3 keV	1.24 sec	Extended lows (period = 35 days)
Cyg X-1 <sup>(c)</sup>	None	Flat, no cutoff	None (quasi-periodic)	Single transition (at low energies)

References for Table:

- (a) Schreier et al, 1972
- (b) Tananbaum et al, 1972a
- (c) Schreier et al, 1971  
Tananbaum et al, 1972b and references therein

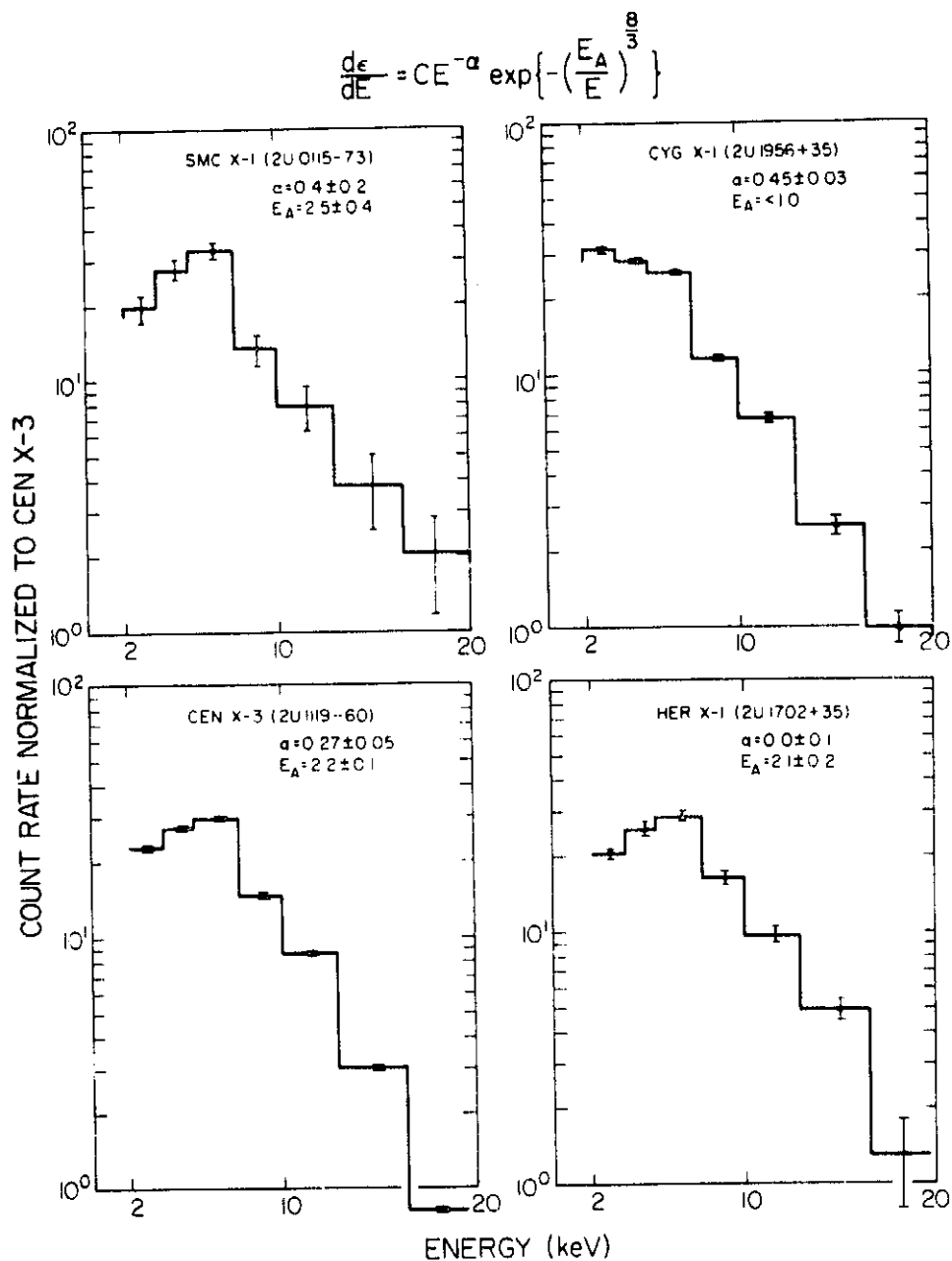


Figure 3-22 Typical energy spectra of four binary sources. Data shown represent relative counting rates with one-sigma errors in seven PHA channels. The data have been normalized by setting the total intensity (2-20 keV) equal to that of Cen X-3. The parameters shown represent the best fits to the data of the power law expression shown on top; exponential spectra with  $kT \gtrsim 25$  keV could fit as well. Also note that since variability is seen in the spectra, any given sighting might differ from the representative spectra shown.



are therefore not in contradiction to the idea that most galactic X-ray sources are binary systems. For such sources, accretion is the obvious energy source, whether the matter is supplied by a stellar wind or by overflow of the Roche lobe of the companion star. The fact that the luminosity of many sources seems to come close to the Eddington limit of  $10^{38} \left( \frac{M}{M_{\odot}} \right)$  ergs/sec imposed by radiation pressure (Pringle and Rees 1972, Ostriker and Davidson 1972, Shakura 1972) strengthens the hypothesis that accretion is indeed the energy source.

## REFERENCES

- Giacconi, R., Murray, S., Gursky, H., Kellogg, E., Schreier, E., and Tananbaum, H. 1972, The UHURU Catalog of X-ray Sources, Ap. J. (to be published).
- Leong, C., Kellogg, E., Gursky, H., Tananbaum, H., and Giacconi, R. 1971, Ap. J. (Letters) 170, L67.
- Ostriker, J. and Davidson, K. 1972, Proceedings of IAU Symposium #55.
- Price, R. E., Groves, D. J., Rodrigues, R. M., Seward, F., Swift, C. D., and Toor, A. 1971, Ap. J. (Letters), 168, L7.
- Pringle, J. and Rees, M. 1972, preprint.
- Schreier, E., Gursky, H., Kellogg, E., Tananbaum, H., and Giacconi, R. 1971, Ap. J. (Letters) 170, L21.
- Schreier, E., Levinson, R., Gursky, H., Kellogg, E., Tananbaum, H., and Giacconi, R. 1972, Ap. J. (Letters) 172, L79.
- Shakura, N. I. and Sunyaev, R. A. 1972, preprint.
- Tananbaum, H., Gursky, H., Kellogg, E., Levinson, R., Schreier, E., and Giacconi, R. 1972a, Ap. J. (Letters) 174, L143.
- Tananbaum, H., Gursky, H., Kellogg, E., Giacconi, R., and Jones, C. 1972b, Ap. J. (Letters) to be published.

Turning to Sco X-1 we have considerably more detailed observations, particularly those obtained by collaborative efforts of a number of radio and optical observers together with UHURU in February and March 1971.

Figure 3-23 shows the X-ray intensity in  $\text{cts/cm}^2 - \text{sec}$ , the blue-magnitude, and the radio intensity observed at NRAO and Westerbork in milliflux units. The radio source is relatively quiet and weak on February 23, 24 and 25; the optical intensity is relatively bright and variable on February 23 and the X-ray source is also highly variable. On February 24 and 25 the blue-magnitude is fainter than 13th and the X-ray emission is relatively low and quiet.

Figure 3-24 shows a continuation of this optical and X-ray behavior on February 26, with an enormous radio flare beginning around 18 hours on February 26. Unfortunately, the X-ray and optical observations are notably absent on the 2nd half of February and on February 27, except for 3 hours of relatively faint blue observations. When the radio data resume at 12 hours on February 27, the flare has totally subsided, and then the X-ray and optical data for February 28 show low intensity and not much variability. Data such as these have been used to infer that the radio behavior is not related to the optical and X-ray emission, but the scarcity of X-ray and optical observations during much of the time on February 26 and 27 makes this conclusion unwarranted.

In Figure 3-25 we pick up Sco X-1 on March 23, 1971. Much of the data for March 23 and 24 show the blue-magnitude brighter than 12.6 and the X-ray source intense and varying (although there are some quiet X-ray times). When the data are picked up on

\*From "Stellar X-ray Sources" H. Tananbaum, 1973 IAU Symp. No. 60-  
"Galactic Radio Astronomy" to be published by D. Reidel Publishing Co.  
3-76

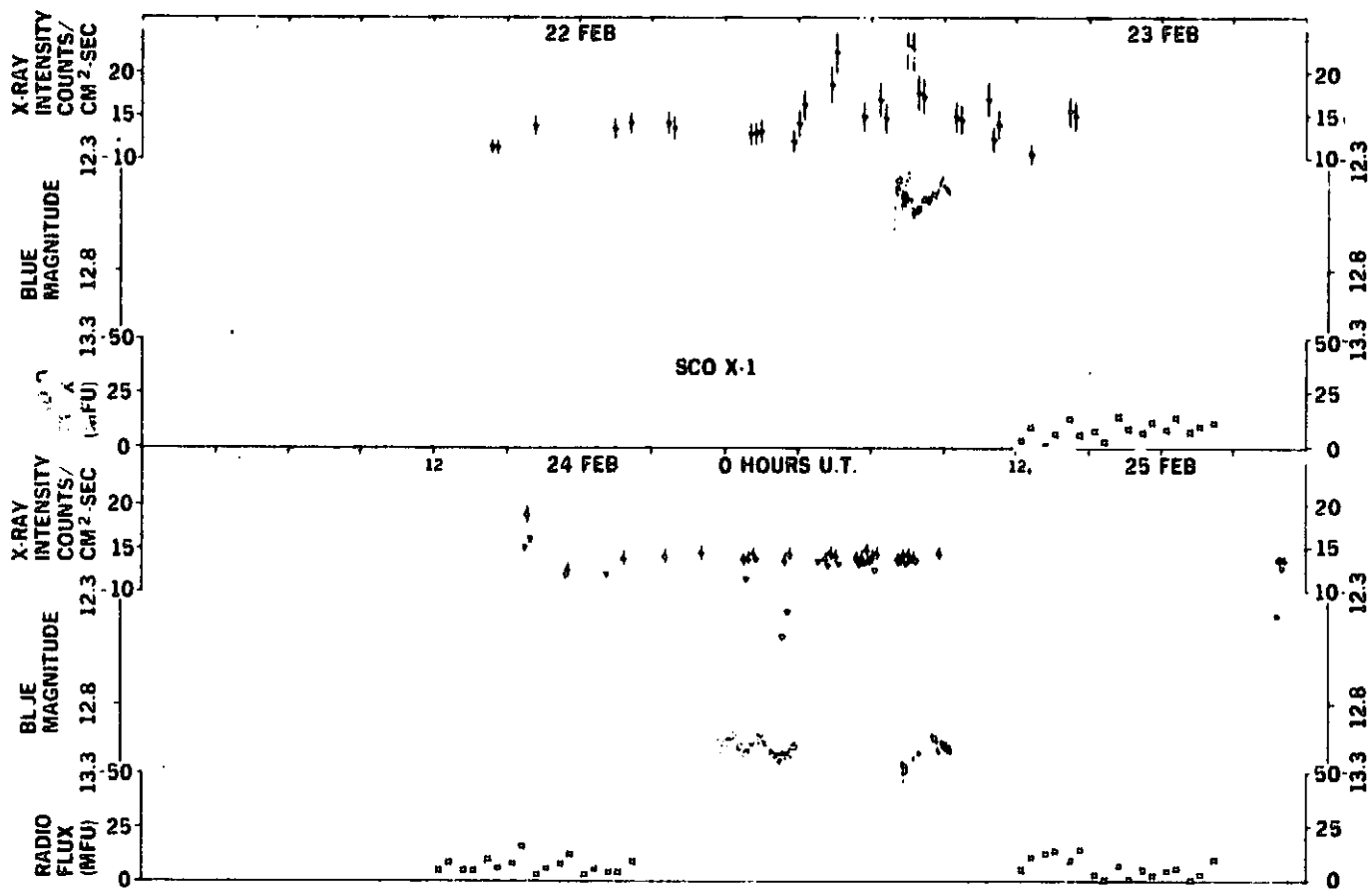


Figure 3-23. Simultaneous X-ray, optical, and radio observations for Sco X-1 on 22 - 25 February 1971. The data are discussed in the text.

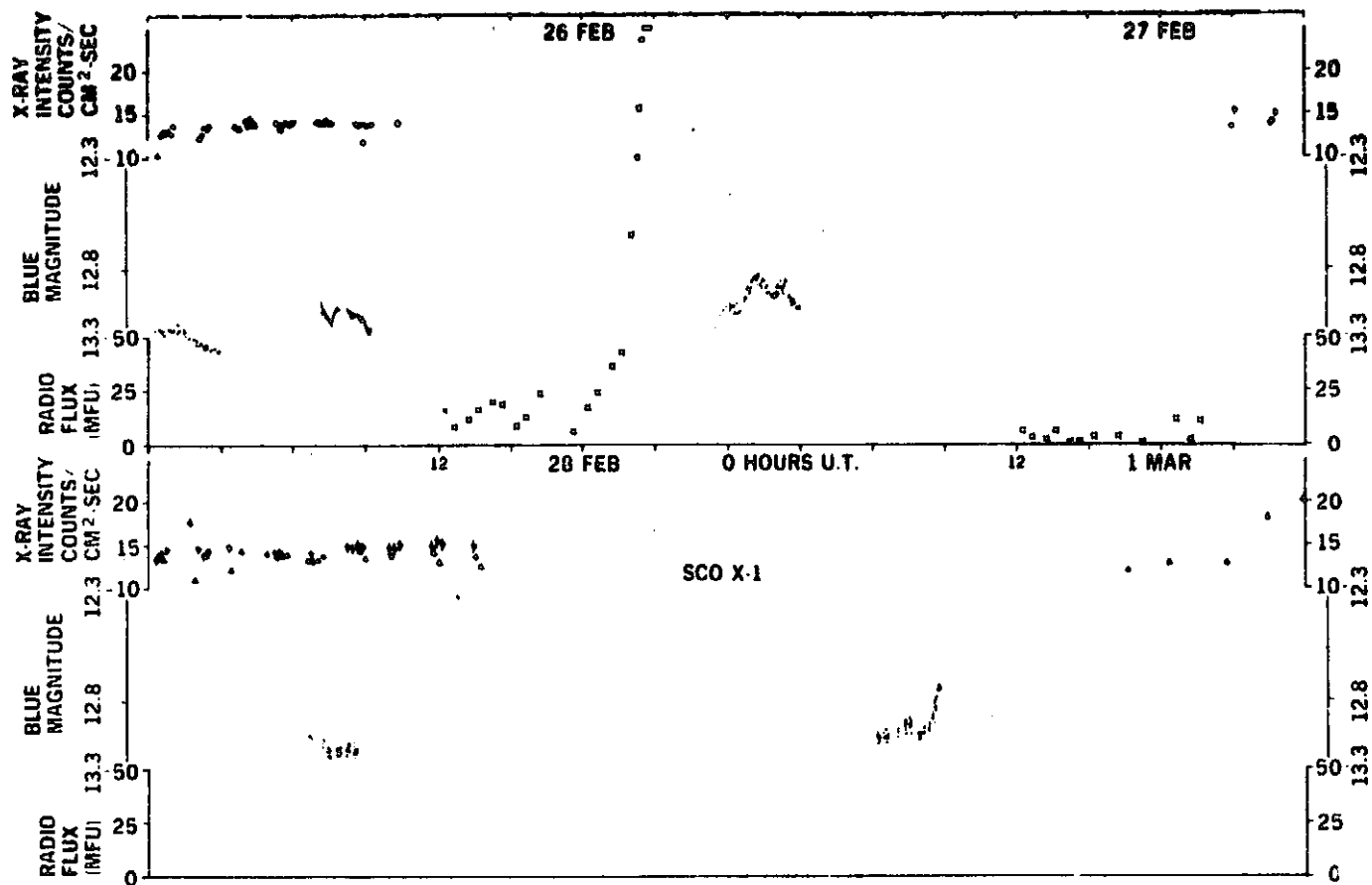


Figure 3-24. Same as Figure 3-23 except for 26 February - 1 March 1971.

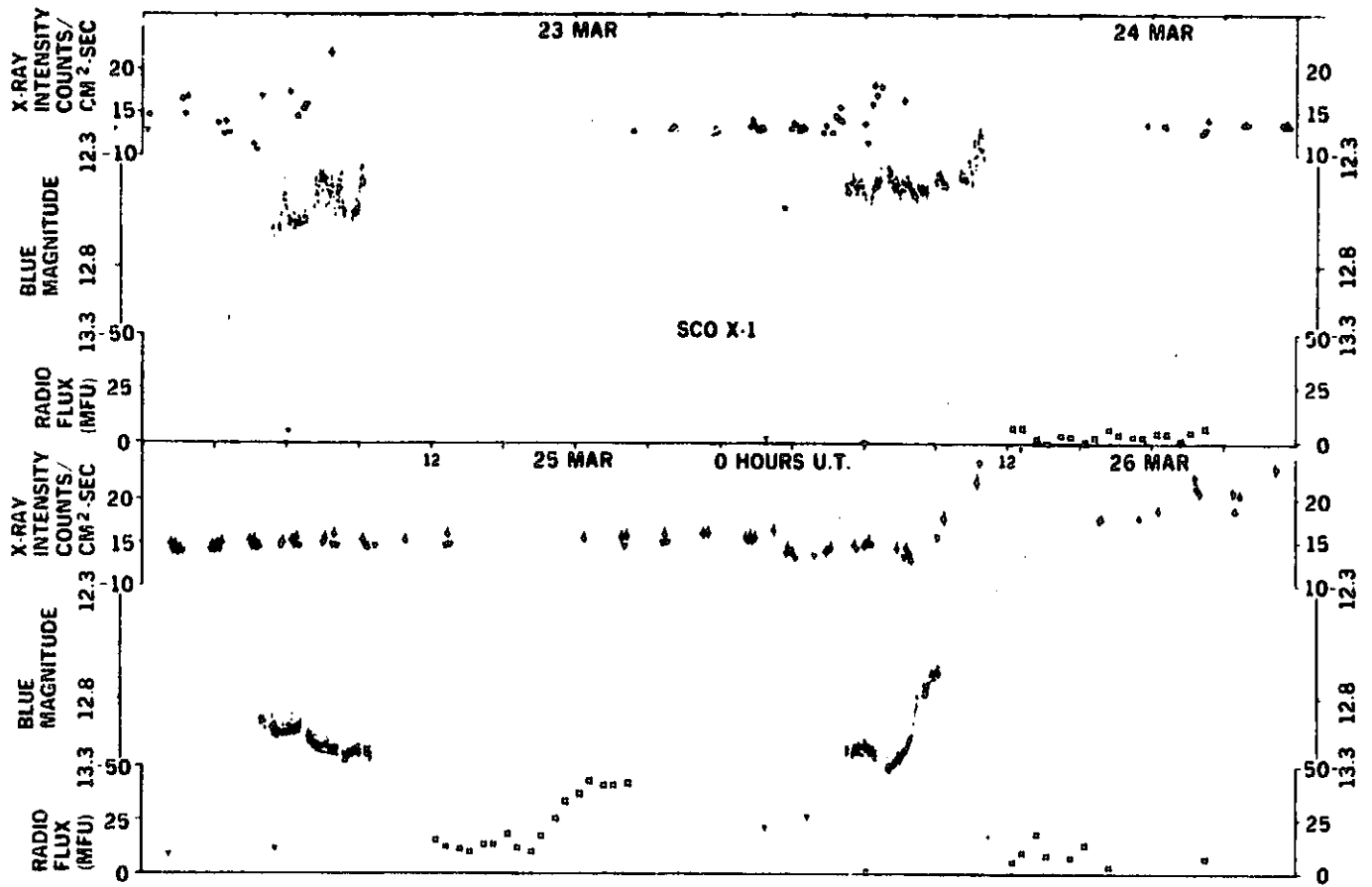


Figure 3-25. Same as Figure 3-23 except for 23-26 March 1971.

March 25, the X-ray intensity is very quiet and the optical is fainter than 13th magnitude. What would be helpful in attempting to understand how the source quieted down would have been more complete coverage on March 24 and 25.

Late on March 25, the radio data show a flare to about 500 milli-flux units; the X-ray source remains low and quiet during this time, although there is a 6 hour gap in the data during the actual radio increase. On March 26 some 15 hours after the radio flare, the optical brightness increases steeply, by several tenths of a magnitude in about an hour. About 1 hour after the optical increase began, the X-ray intensity increases substantially and a bright, variable X-ray state follows. A few scattered radio points suggest that the radio flare may have disappeared some 2 to 4 hours before the optical increase.

In Figure 3-26 we pick up the optical data showing the source still bright and highly variable on March 27 and 28 with a large decrease early on March 29. The X-ray points are also bright and variable on March 27 and most of March 28, and are definitely faint and relatively quiet on March 29. The March 28 data suggest that the X-ray decrease may have preceded the optical decrease by as many as 6 to 8 hours. The X-ray and optical data remain low and quiet on March 29 and 30, with the radio data showing another flare, beginning between 21 and 24 hours on March 29. The previous data from March 25 and 26 suggest that we either look for an optical and X-ray brightening some 15 hours after the start of the radio activity or some 2 to 4 hours after the radio activity ends. Unfortunately, there are no X-ray data after 9 hours later on March 30 nor any optical data at all on March 30, although optical data later on March 31 show the source faint. Thus, no conclusions can be drawn concerning repeated relationships between the radio and the optical and X-ray data.

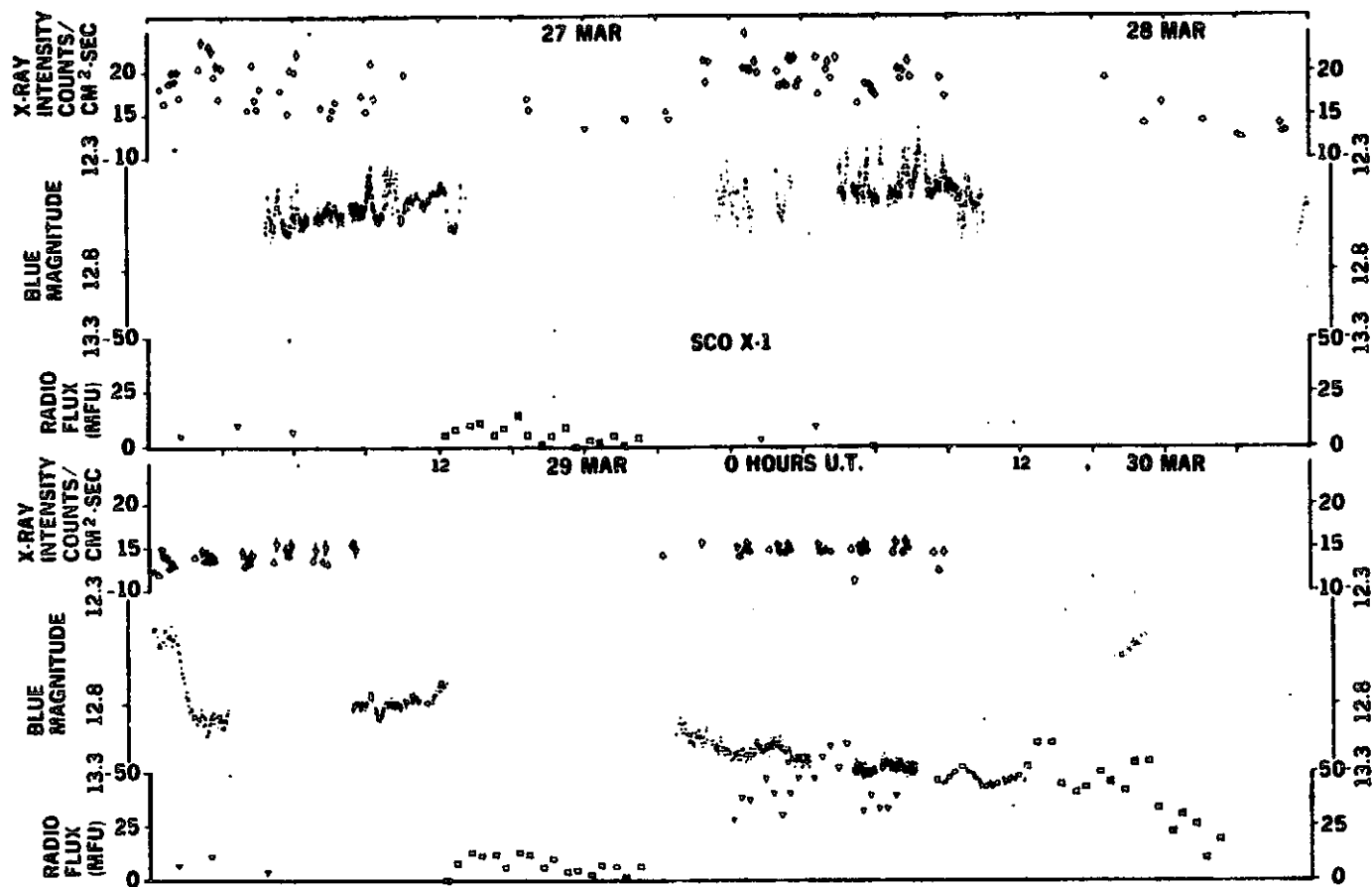


Figure 3-26. Same as Figure 3-23 except for 27-30 March 1971.



Figure 3-27 shows a blue-magnitude occurrence histogram for March 23-28 suggesting two states for Sco X-1, with most of its time spent either bright or faint with little time in the middle. In Figure 3-28 we see the X-ray intensity vs. blue-magnitude for these days. This figure shows the correlation between the X-ray and optical. When the optical source is faint the 2-6 keV X-ray intensity is low and varying only slightly. When the blue-magnitude passes 12.6, the X-ray intensity is greater by up to a factor of 2 and much more variable. This is also related to observations by Hiltner and Mook (1970) that Sco X-1 only flares in the optical when it is brighter than this same 12.6 magnitude. Figure 3-29 is 2 days of these same data where we show the X-ray temperature vs. the 2-6 keV intensity and find the source cooler when it is weaker and hotter and more variable when it is more intense. A better approach would have been to plot temperature versus emission measure here, since the 2-6 keV intensity is of course greatly affected by the exponential temperature factor.

An effort of this type was undertaken by Kitamura et al. (1971) with rocket data and optical observations which suggested a size of  $10^8$  to  $10^9$  cm and a density of  $10^{15-16}/\text{cm}^3$  for the X-ray emitting region. These conclusions were based on the observation that the emission measure decreased as the source became hotter. The UHURU and MIT OSO-7 results suggest that this is not the case, but rather the emission measure increases as Sco X-1 becomes hotter. It may be that different laws govern this relationship depending on whether the source is in the bright flaring state or in the quiet, faint state. Present models suggest the radio emission occurs relatively far out from the X-ray emitting region, with the optical emission coming from a region also outside of but much closer to the X-ray emitting region, resulting in the correlation between the optical and X-ray emission.

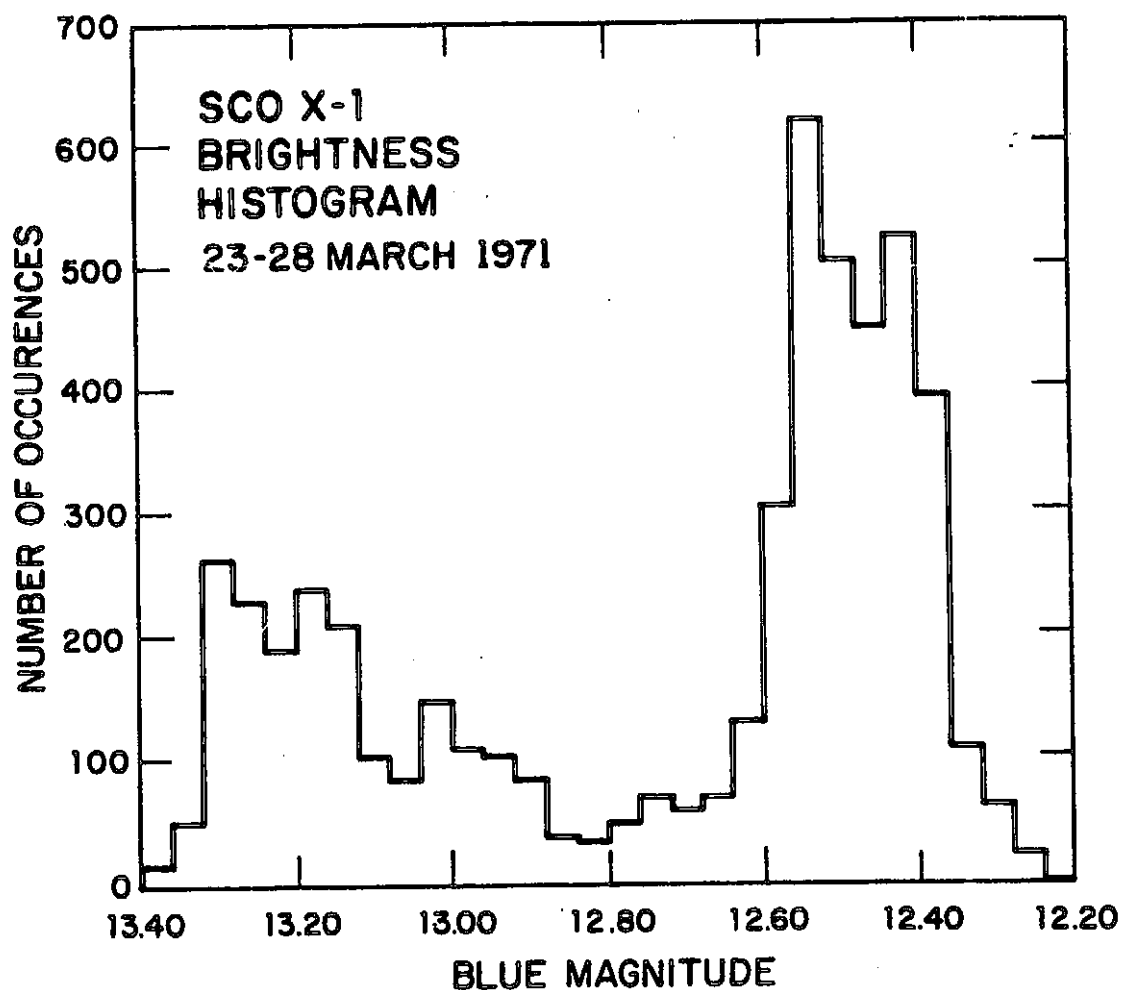


Figure 3-27. Sco X-1 brightness histogram 23 - 28 March 1971. The number of occurrences of each blue magnitude is plotted vs. blue magnitude. The data indicate the clustering around 13.2 magnitude and 12.5 magnitude as discussed in the text.

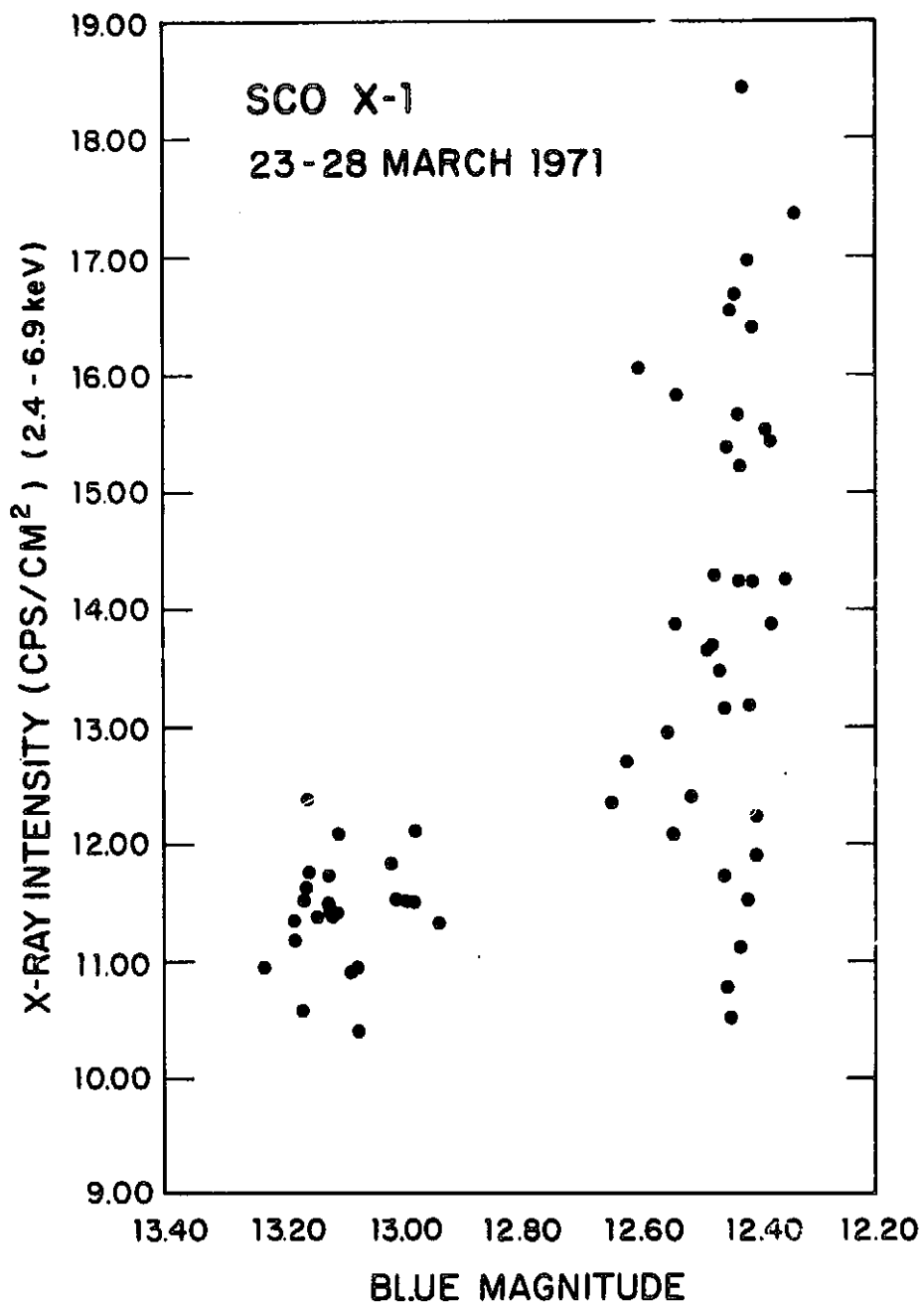


Figure 3-28. Simultaneous X-ray-optical variability of Sco X-1. Each point represents a single, simultaneous measurement of the X-ray and optical intensity of Sco X-1. Note the relatively quiet, faint state and the highly variable, bright state.

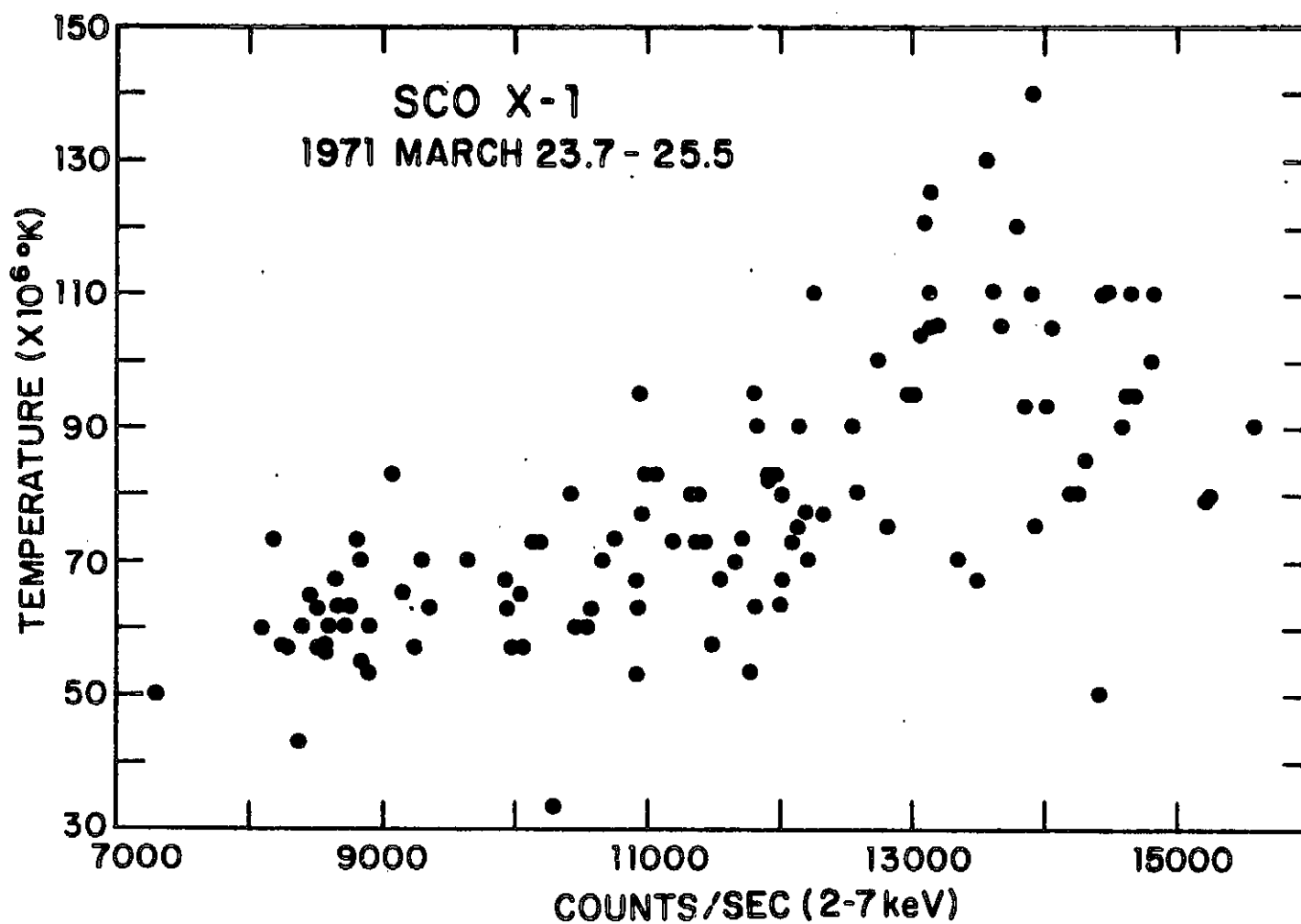


Figure 3-29. Temperature versus X-ray intensity for Sco X-1. Each point represents a single temperature and X-ray intensity observation. We see that as the source intensity increases the temperature increases and is more variable.

## REFERENCES

1. Becklin, E.E., Hawkins, F.J., Mason, K.O., Matthews, K., Neugebauer, G., Sanford, P.W., and Wynn-Williams, C.G., 1973, preprint.
2. Bolton, C.T., 1972a, *Nature*, 235, 271.
3. Bolton, C.T., 1972b, *Nature Phys. Sci.*, 240, 124.
4. Braes, L. and Miley, G.K., 1971, *Nature*, 232, 246.
5. Bregman, J., Butler, D., Kemper, E., Koski, A., Kraft, R.P., and Stone, R.P.S., 1973, preprint.
6. Canizares, C.R., McClintock, J.E., Clark, G.W., Lewin, W.H.G., Schnopper, H.W., and Sprott, G.F., 1973, *Nature Phys. Sci.*, 241, 26.
7. Cherepashchuk, A.M., Lyutiy, V.M., and Sunyaev, R.A., 1973, *Astron. Zhur.*, 50, 3.
8. Faulkner, J., 1973, Tucson Workshop on Compact X-Ray Sources.
9. Gregory, P.C., Kronberg, P.P., Seaquist, E.R. Hughes, V.A., Woodsworth, A., Viner, M.R., and Retallack, D., 1972, *Nature Phys. Sci.*, 239, 440.
10. Gursky, H., 1973, Private Communication.
11. Hiltner, W.A. and Mook, D.W., 1970, *Ann. Rev. Astr. and Ap.*, 8, 139.
12. Hjellming, R.M., 1973, *Astrophys. J. (Letters)*, 182, L29.
13. Hjellming, R.M. and Wade, C.M., 1971, *Astrophys. J. (Letters)*, 168, L21.
14. Holt, S., Boldt, E., Schwartz, D., Serlemitsos, P., and Bleach, R., 1971, *Astrophys. J. (Letters)*, 166, L65.
15. Kitamura, T., Matsuoka, M., Miyamoto, S., Nakagawa, M., Oda, M., Ogawara, Y., Takagishi, K., Rao, U.R., Chitnis, E.V., Jayanthi, U.B., Prakasa-Rao, A.S., and Bhandari, S.M., 1971, *Astrophys and Space Science*, 12, 378.

## REFERENCES

16. Margon, B., Bowyer, S., and Stone, R., 1973, *Astrophys. J.* (Letters), to be published.
17. Mauder, H., 1973, *Astron. and Astrophys.*, to be published.
18. Parsignault, D.R., Gursky, H., Kellogg, E.M., Matilsky, T., Murray, S., Schreier, E., Tananbaum, H., Giacconi, R., and Brinkman, A.C., 1972, *Nature*, 239, 123.

### 3.9 Cyg X-2

Cyg X-2 is believed to be similar to Sco X-1 except there is not nearly so much information available concerning it. Its intensity is only about 1/40 of Sco X-1. The optical identification was proposed by Giacconi (1967), based on the discovery of a star with characteristics similar to that of Sco X-1 within the area of uncertainty of the X-ray source. The position of Cyg X-2 has been considerably refined since then (S. Murray) as is shown in Figure 3-30. However, simultaneous X-ray-optical correlations have not been reported; thus the identification cannot be regarded as being positively established.

In both optical and X-ray, variations in intensity of order a factor two are observed on a time scale of a day or less; however, the two states characteristic of Sco X-1 are not yet reported from Cyg X-2. The X-ray spectrum is best fit by an exponential with  $T \approx 4 \times 10^7$  K, somewhat lower than that of Sco X-1.

The optical Cyg X-2 is actually very dissimilar from Sco X-1 although they share certain common features. The spectral lines show large changes in radial velocity which were thought to be evidence of binary motion; however, Kraft and Demoulin (1967) showed that these variations, which are of the order of several hundred Km/sec were not periodic. Furthermore, they found that the bulk of the optical emission could be accounted for by the presence of a G-type subdwarf star based on the absorption-line spectrum. With this information the distance is estimated to be 500 - 700 pc.

Based on this distance, the X-ray luminosity is of order  $10^{36}$  erg/sec, the optical luminosity is lower by a factor of 100 and is dominated by the G-type star. The optical emission from the X-ray

\*From H. Gursky, *Les Astres Occlus*, Les Houches 1972, p. 295, Ed. DeWitt and DeWitt, reproduced by permission of Gordon and Breach Science Publishers.

region could be, as in Sco X-1 about  $10^{-3}$  of X-ray emission.

Several other X-ray sources have properties, in terms of the spectrum and variabilities of the X-ray intensity, similar to Sco X-1 and Cyg X-2; however, there has been no other identification of a similar optical object. If, however, the ratio  $L_x/L_{opt} = 10^3$  then this is not so surprising. Sco X-1 and Cyg X-2 are not only bright in X-rays but located at high galactic latitude out of regions of high optical obscuration. The visible emission from a source  $10^{-2}$  of Sco X-1 located in the galactic plane would appear of 17 m if its optical emission were  $10^{-3}$  of its X-ray emission. Allowing for several magnitudes of obscuration, such a star would be hopelessly difficult to find.

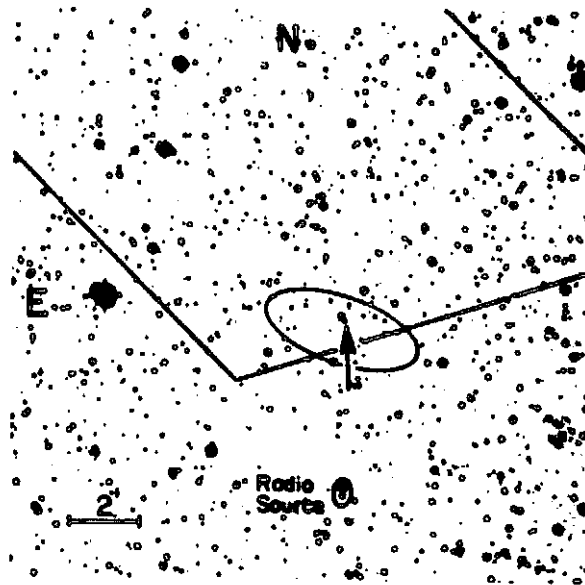


Figure 3-30. X-ray position of Cygnus X-2. The position from the 2 UHURU catalog is the small ellipse and the arrow points to the blue star believed to be the optical counter part. The large diamond (partially cutoff) is the 1967 position.



## REFERENCES

1. R. Giacconi, P. Gorenstein, H. Gursky, P.D. Usher, J.R. Waters, A. Sandage, P. Osmer, and J. V. Peach, Ap. J. (Letters) 148, L119, 1967.
2. S. Murray, Private Communication.
3. R. Kraft and M. Demoulin, Ap. J. (Letters) 150, L183, 1967.

## 4.0 EXTRAGALACTIC X-RAY ASTRONOMY \*

### 4.1 Introduction

The UHURU satellite, launched in December 1970, has had a great impact on extragalactic X-ray astronomy. Before data from this satellite became available, there were only a few extragalactic X-ray sources known. Sources near M87 (1,2) and 3C273 (3) and NGC1275 (4) had been observed definitely, and ones near NGC5128 (3), the Coma Cluster (5) and the Large Magellanic Cloud (6), had been reported using sounding rocket data. The first fairly complete sky survey with UHURU has revealed more than 40 X-ray sources off the galactic plane by 20 degrees or more. Figure 4-1 shows the locations in galactic coordinates of the sources (7), and it shows some shaded areas we have not yet surveyed. At least fifteen of the high latitude sources are already identified with unusual galaxies, or with clusters of galaxies. We believe that most of the remaining unidentified high latitude sources will turn out to be extragalactic.

As was expected, ordinary galaxies are detected as X-ray sources at comparable luminosity to our own galaxy. We also confirm that unusual active galaxies have enhanced X-ray luminosity. The most exciting discovery we have made is that sources in clusters of galaxies are very luminous and are extended, with sizes as large as a few megaparsecs. We also find that the luminosity function of high latitude sources is consistent with a uniform volume distribution as expected for distant extragalactic sources. Also, that the diffuse background might be the superposition of many distant discrete sources.

### 4.2 Identified Sources

Figure 4-2 shows the identified extragalactic sources by class with their distances, ranging from 50 kpc for the Magellanic Clouds to 600 Mpc for the most distant objects. The top of each shaded area represents the distance of the nearest member of each class. The nearest ordinary galaxies are the Magellanic Clouds, located at the top of the shaded area for the class of ordinary galaxies. The Small Cloud is dominated by emission from a single binary X-ray star (8,9).

From "UHURU Results on Extragalactic X-ray Sources", E. Kellogg, 1973 IAU Sym. 55-X-and Gamma-Ray Astronomy, p. 171, D. Reidel Publishing Co.

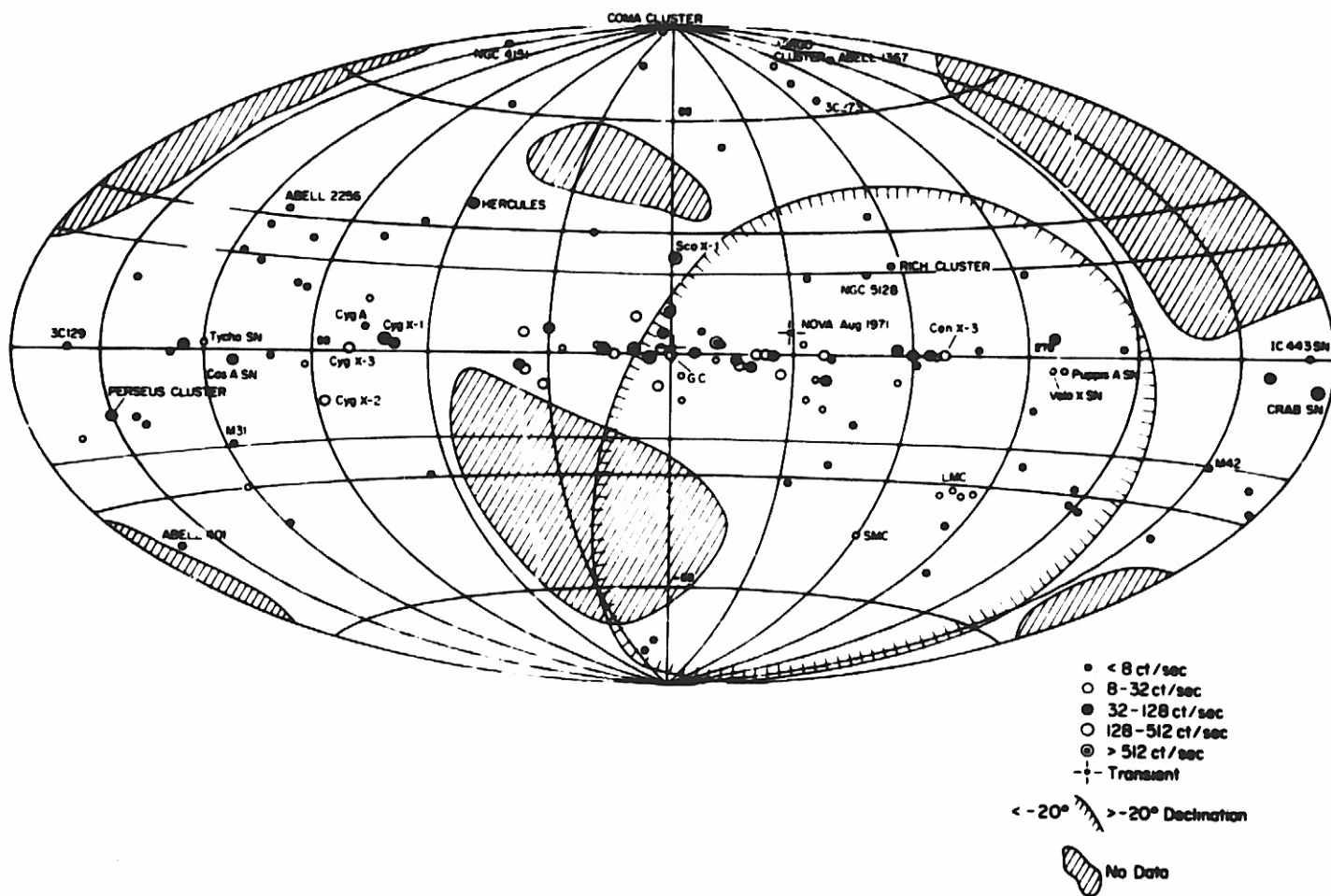


Figure 4-1. The X-ray sources in the UHURU Catalog (7), plotted in galactic coordinates.

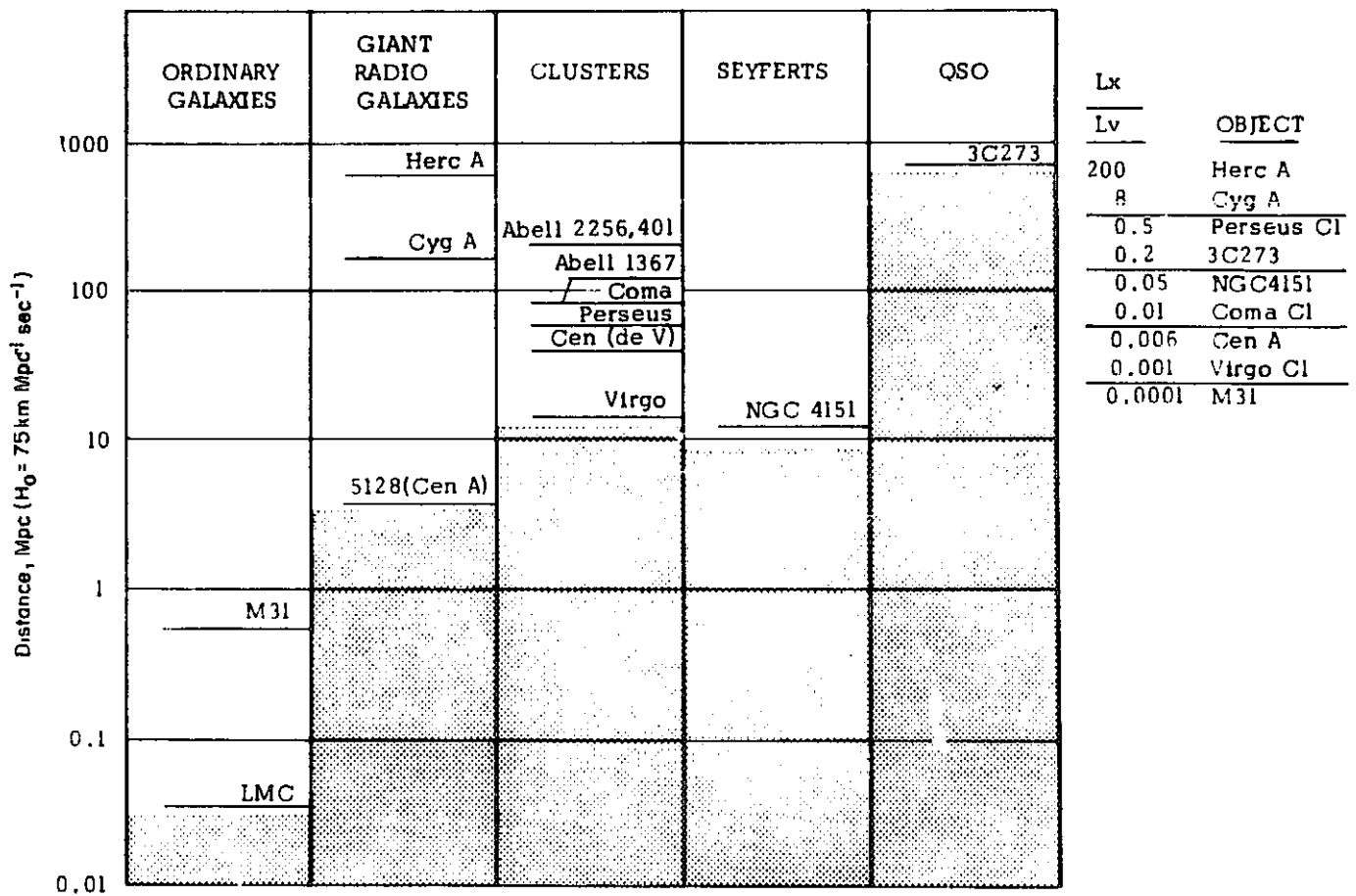


Figure 4-2. Identified extragalactic X-ray sources. The top of the shaded region for each class indicates the distance of the nearest known member of that class. The Seyfert galaxies are the only group where the nearest member, NGC4051, is not detected, but a more distant member is detected. The table at the right lists the ratio of X-ray to optical luminosity for representative identified sources.

The emission from the Large Cloud is due to four discrete sources (7). The ratio of X-ray to optical luminosity for ordinary galaxies is  $10^{-4}$  or less, as listed in the table at the right. We have detected the nearest giant radio galaxy, Cen A (10, 11), located at the top of the shaded area for radio galaxies, and two much more luminous distant radio galaxies, Cyg A (7) and Herc A. Figure 4-3 shows our best estimates of the locations for Cyg A and Herc A. The updated Herc A location contains more recent data than that included in the UHURU Catalog (7). The X-ray to visible ratios have a large range from  $6 \times 10^{-3}$  for Cen A to about 200 for Herc A. However, the X-ray to radio luminosity ratio does not vary so widely for these galaxies. We have detected the nearest great cluster in Virgo, and several more distant rich clusters. Luminosity ratios range from  $10^{-3}$  for Virgo to about one in Perseus. We see only one Seyfert galaxy, NGC4151. The top of the shaded area is at the distance of NGC4051, the nearest Seyfert, which is not a source. NGC4051 and NGC1068 are less than 1/3 as luminous as 4151. We also see the nearest QSO, 3C273. If these classifications are physically meaningful, we'd expect each class to have a typical luminosity; then the nearest ones would be detectable first. It appears that only the ordinary galaxies are well behaved in that sense, and possibly QSOs. The other classes show a wide range of luminosities. The enhanced X-ray to visible luminosity ratios for radio galaxies, clusters, the Seyfert and the QSO suggest that the X rays in these objects are not produced in stars as they are in our own galaxy, but by some other mechanism.

The second major finding from UHURU is that sources in clusters are very luminous and extended. We have now identified about 8 sources associated with clusters. In Figure 4-4 we see four such sources from the great clusters in Virgo, Cen, Perseus and Coma. The Virgo source is centered on M87, the active giant elliptical galaxy (12). The bands are the source centers obtained from 5 different UHURU scans. They intersect at M87. The inset shows the error box obtained by combining the 5 scans. M87 is within 3' of the centroid of the extended X-ray source. Its size is shown by the circle. The true shape of

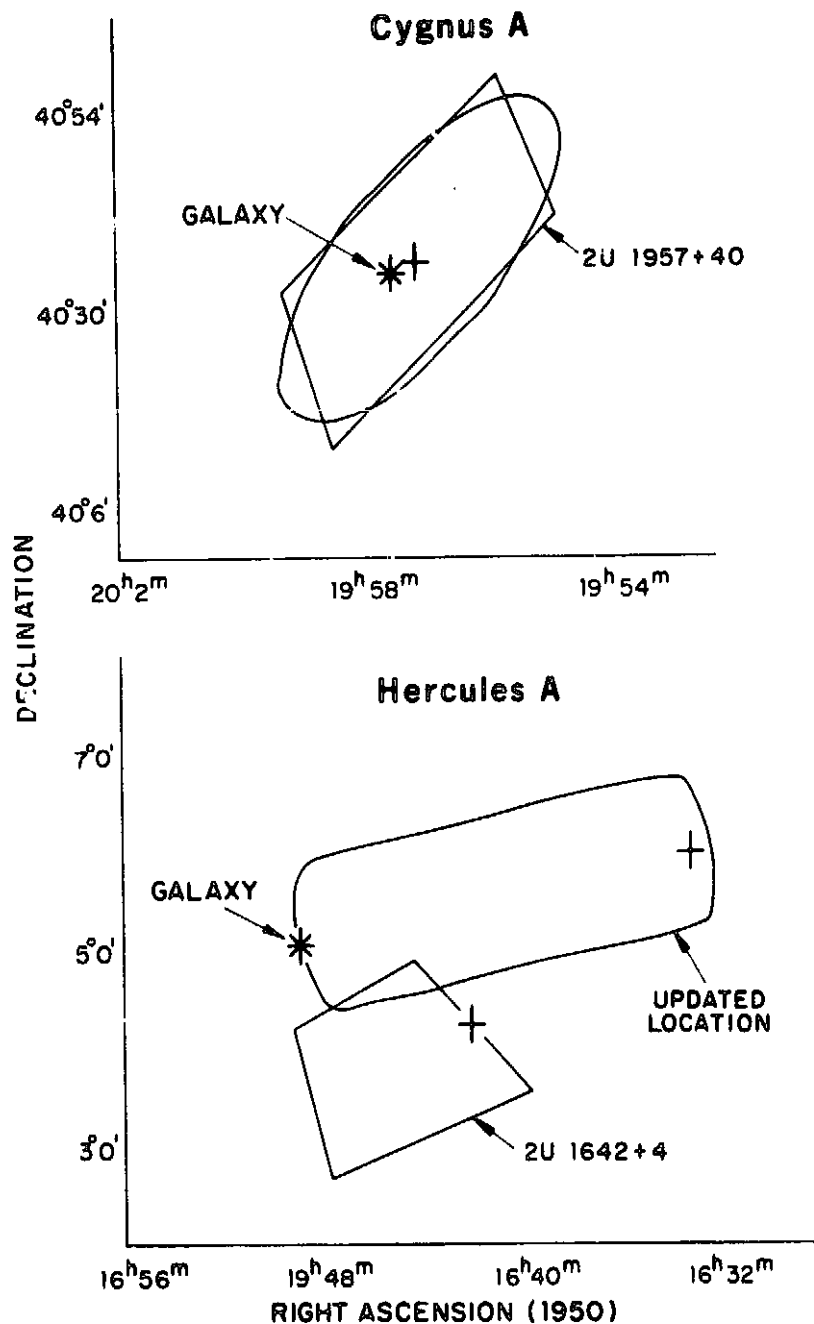
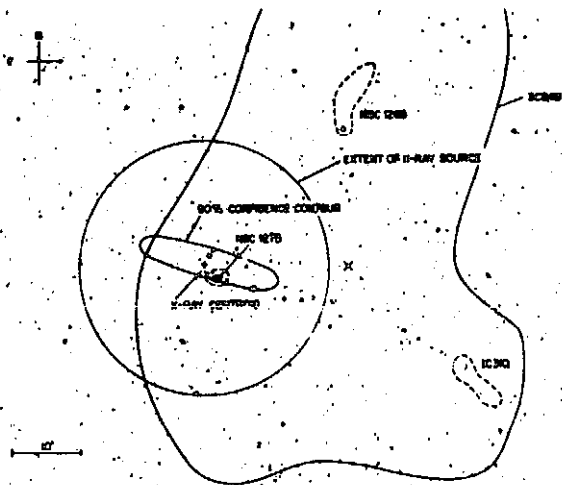
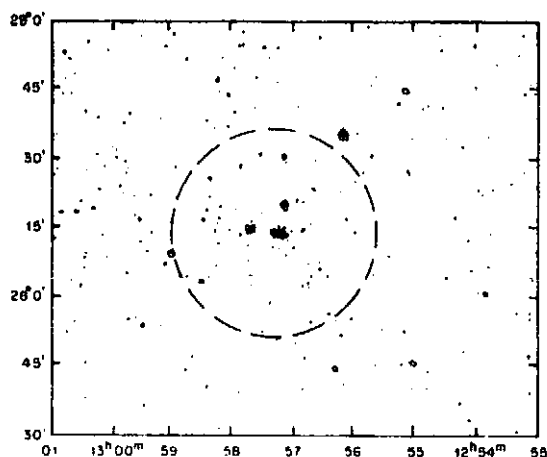


Figure 4-3. Locations of two UHURU sources identified with distant radio galaxies. For Cygnus A, the quadrilateral is the error box listed in the UHURU Catalog (7). The ellipse is a more exact location contour from which the UHURU error box was obtained. The peak of the location probability distribution is shown by a vertical cross. For Hercules A, new data obtained since the UHURU catalog was generated were added to obtain the updated locations.

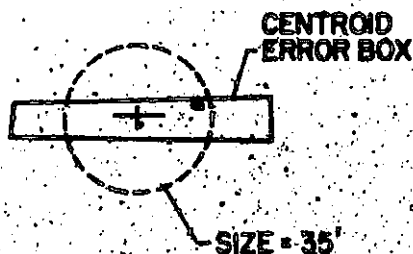
## PERSEUS CLUSTER



## COMA CLUSTER



## CEN CLUSTER



## VIRGO CLUSTER

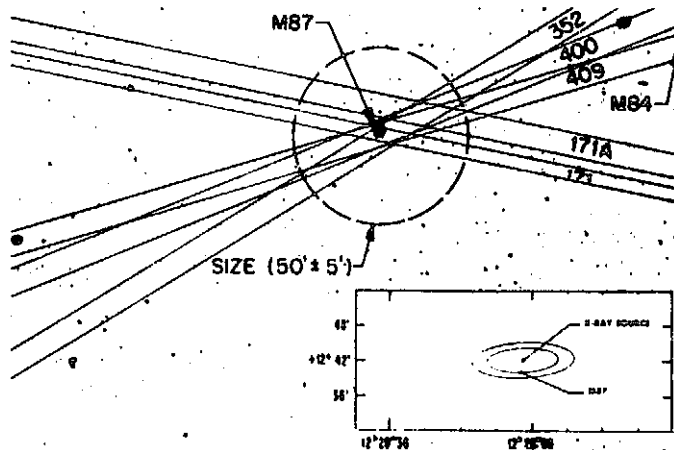


Figure 4-4. X-ray sources in clusters of galaxies: These are the four strongest cluster sources. In each case, we indicate the extent of the source by the simplest figure, a circle, since we have no information on the details of the shape.

The Virgo picture also shows the one-directional locations for the centroid of the extended source obtained from five scans, labelled by the orbit number pertaining to each scan. The inset is the two-dimensional error box obtained by combining the five one-directional locations. The inner contour corresponds to 68% confidence and the outer corresponds to 90% confidence. The Centaurus source, 2U1247-41 contains NGC4696 within its centroid error box. The Perseus source contains NGC1275, the exploding Seyfert galaxy, within the centroid error box. In Coma, both the giant elliptical NGC4874 and the kinematic center of the cluster lie within the error box.

each of these four extended sources is probably not circular, but we cannot tell from our data, so we represent the source shape in the simplest way possible, a circle, whose description requires only a single parameter, its diameter.

The Cen cluster is about 3 times further away than Virgo, and the source is weaker. We have just developed a new technique for measuring the size of weaker sources, and we find it to be extended. The giant elliptical galaxy NGC4696 is located in the error box for the centroid of the extended X-ray source. The size is again shown by a circle, 35' in diameter. The Perseus cluster source is centered very close to NGC1275, a violently active Seyfert galaxy (13). The source in Coma may be centered on either the giant elliptical galaxy NGC4874, or on the kinematic center of the cluster which is very close to 4874 (13).

We have tried to measure the angular extent of nine sources located in clusters (see (14) for the list of cluster sources). Five of these are definitely extended, as summarized in Figure 4-5; the other four were too weak to measure sizes on. They are Abell 401, Abell 1367, 3C129, and one Zwicky cluster, and ZW 0444.7+0828. The last two sources listed are identified with individual galaxies not located in clusters, and are found not to be extended. Abell 2256 is the most distant extended source we have yet detected and the most luminous. These data show that the clusters have a large range of sizes and luminosities. In fact, there appears to be some correlation between the X-ray luminosity of a cluster and its velocity dispersion, as shown in Figure 4-6. This effect was noticed by Solinger and Tucker (15). The observed luminosities are consistent with a fourth power dependence on  $\Delta V$ . If this type of correlation holds up under future observations, we must interpret that there is a connection between X-ray emission and cluster dynamics involving the presence of some fraction of the virial mass in intergalactic gas, and that thermal bremsstrahlung is the X-ray emission mechanism. This would be the first unambiguous observation of intergalactic gas, whose presence has been suspected in the past, but not confirmed.



	SIZE		<u>Lx</u>
	<u>angular</u>	<u>kpc</u>	<u>( erg/sec )</u>
ABELL 2256	35' $\pm$ 15'	2800	5 X 10 <sup>44</sup>
PERSEUS - NGC 1275	35' $\pm$ 3'	740	3 X 10 <sup>44</sup>
COMA	36' $\pm$ 4'	1050	2 X 10 <sup>44</sup>
CEN - NGC 4696	37' $\pm$ 8'	500	2 X 10 <sup>43</sup>
VIRGO - M87	50' $\pm$ 5'	200	7 X 10 <sup>42</sup>
NGC 4151	$\leq$ 15'	$\leq$ 60	1 X 10 <sup>42</sup>
NGC 5128	$\leq$ 10'	$\leq$ 20	6 X 10 <sup>41</sup>

Figure 4-5. Sizes and X-ray luminosities of extragalactic X-ray sources. Five extended cluster sources and two compact sources not in clusters are listed. The cluster sources are much more luminous than the compact sources.

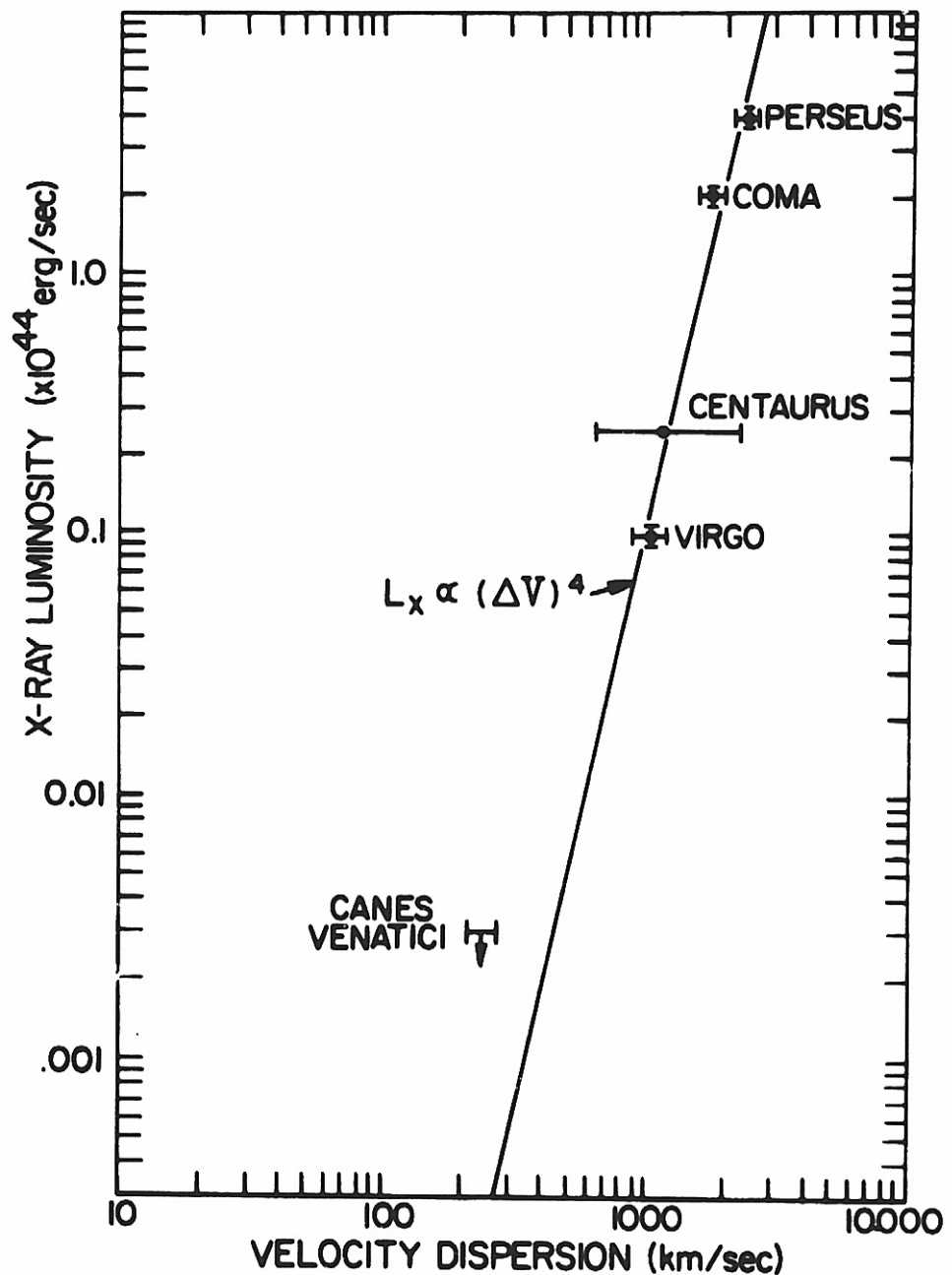


Figure 4-6. Luminosity versus velocity dispersion for X-ray sources in clusters. The curve is arbitrarily normalized. For the three clusters with well determined velocity dispersions, the correlation between  $\Delta V$  and  $L_x$  is undeniable. More detailed analysis may prove that the data fit a curve slightly different from the  $(\Delta V)^4$  curve shown, however.

Some new UHURU observations of the spectra of extragalactic sources are shown in Figure 4-7. The ordinates are logarithmic and represent relative counting rates. The abscissae represent photon energy. In the upper right corner, is the spectrum of the Crab Nebula, which we use as a standard. We assumed interstellar absorption corresponding to  $(1.6 \pm 0.16) \times 10^{21}$  H atoms/cm<sup>2</sup> as observed in radio, which corresponds to  $E_a = 0.45 \pm 0.02$  keV. The spectral index was allowed to vary, with the best fit value being  $0.99 \pm 0.05$ . The histogram for the Crab represents both the observed count rate distribution in the UHURU pulse height analyzer and the calculated fit, because the statistical errors are very small. The middle column shows the count rate distributions from cluster sources as histograms with 1 sigma error bars. The circles are the computed fits. Perseus - NGC1275 is similar to the Crab which has a power law index of 1. M87 has a steep spectrum with a power law index close to two. The spectrum of the Coma cluster fits better to isothermal bremsstrahlung than a power law;  $kT$  is  $6.0 \pm 0.3$  keV. The Cen cluster and Abell 2256 and 401 are similar to Coma and NGC1275. We see no definite low energy cutoff in any cluster source.

The left column shows data from individual galaxies and 3C273. They all have a cutoff. The top spectrum is from the source at the nucleus of our own galaxy, GCX (16). The suggestion is that we are seeing X rays from the nuclei of these other galaxies as well. Since we see no cutoffs in the cluster sources, we are led to believe that the X-ray emission mechanism is different for clusters than for individual galaxies. In particular, it appears that the cluster sources are truly diffuse, and not just a collection of active galaxies.

As an example of how we can use these observed cutoffs, consider 3C273. We find a cutoff of 2.6 keV. This is probably not due to intergalactic material since such material at the critical density would not have the heavy element abundance required to give that much absorption; also it must be very hot if present, so it would be ionized and absorb still less. The absorption is most likely at the source, and corresponds to  $5 \times 10^{22}$  atoms/cm<sup>2</sup> assuming normal galactic abundance ratios in 3C273.

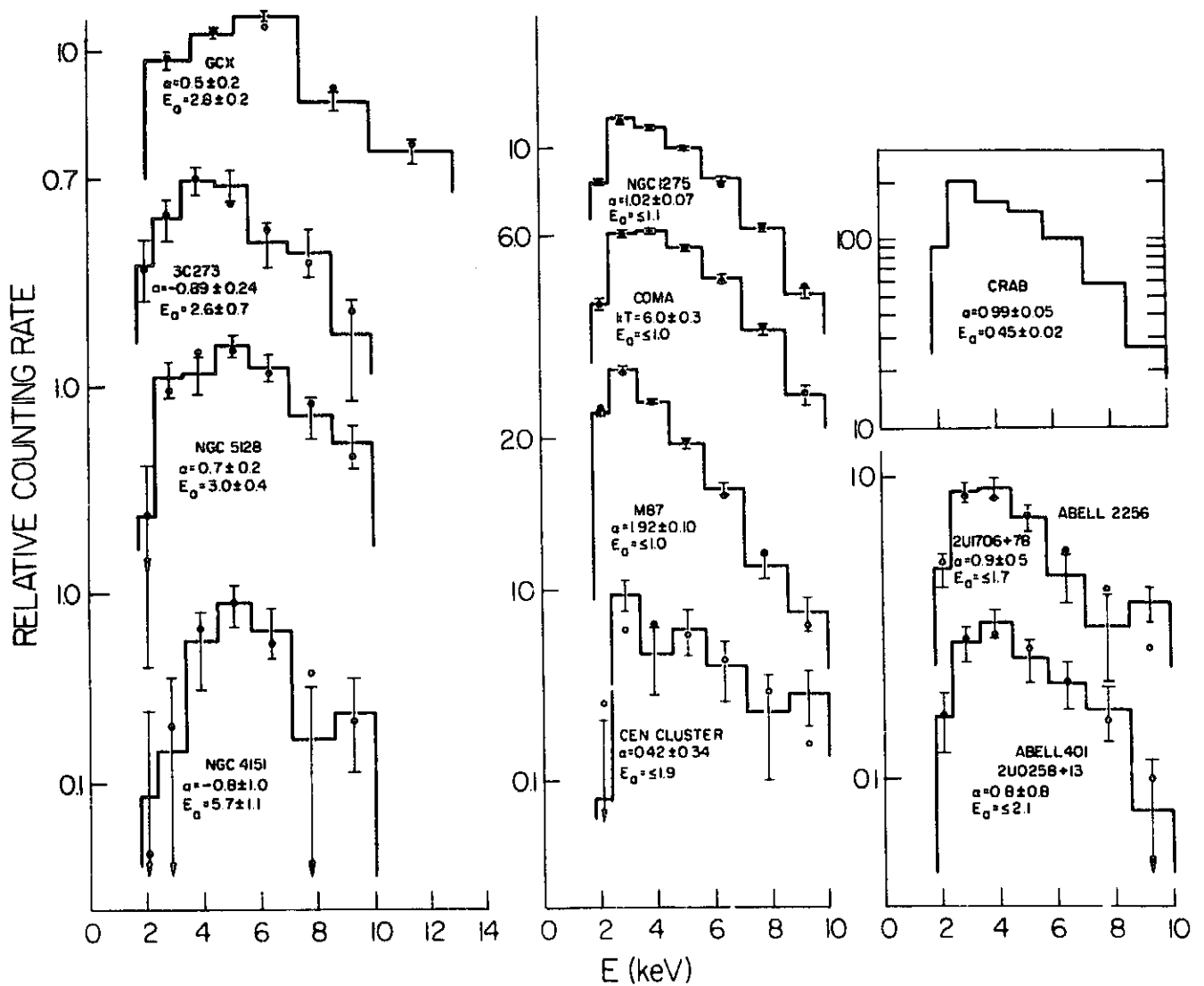


Figure 4-7. Spectra of extragalactic sources. Counting rates versus energy are plotted as histograms with one sigma error bars. The closed circles are the predicted count rates assuming model spectra as inputs and computing the count rate after accounting for counter efficiency, pulse height resolution and fluorescence escape effects. The slope is given as  $\alpha$  for the energy index of a fit to a power law, or  $kT$  for an exponential.  $E_0$  is the low energy cutoff in keV, assuming photoelectric absorption. The four spectra in the left column show a drastic turnover at low energies. The spectra in the center column and the two lower ones in the right are from sources located in clusters, and show no cutoff. The spectrum of the Crab Nebula is shown at the top of the right column for comparison.

If we assume that the X rays and the point radio source 3C273B are coming from the nucleus of a galaxy, then the lack of a radio cutoff down to  $\approx 80$  MHz means that the cloud of material surrounding the source has a radius  $> 30$  kpc along the line of sight, assuming a temperature of  $10^4$  degrees. This is consistent with 3C273 being at cosmological distance.

Figure 4-8 shows NGC5128 or Cen A. This is a giant radio galaxy with two lobes several degrees in size. There are also two inner lobes just 7' apart centered on the optical galaxy, and a compact radio source (17) and red and IR hot spots (18,19) which are at the center. We have found that the X rays are coming from a source  $\leq 10'$  in size whose location is centered on the optical galaxy. Our upper limit on X rays from the outer lobes sets an upper limit on the temperature of the universal blackbody radiation of  $5.1^\circ\text{K}$ , assuming a magnetic field strength of  $4 \times 10^{-6}$  gauss in the lobes which corresponds to equipartition between magnetic and electron energy density. Or, if we fix the blackbody radiation at  $2.7^\circ\text{K}$ , we obtain a lower limit of  $1 \times 10^{-6}$  gauss in the giant lobes of Cen A (11). The X-ray source is probably coming from the nucleus of NGC5128, since we see it strongly cut off. This must be the center of the high energy activity which has produced the lobes in the past, but has been obscured from us by the great amount of dust in NGC5182.

The unidentified high latitude sources are listed in Figure 4-9. The first group are located near 3C or MSH radio sources. The second group are not associated with strong radio sources. The six coincidences between X-ray sources and strong radio sources are somewhat higher than would be expected on a chance basis and may be due to a real physical association. Among the others there are probably many chance coincidences, such as the three sources near undistinguished NGC or IC galaxies.

The latitude distribution of these sources is shown in Figure 4-10. This has been corrected for nonuniform sky coverage. The horizontal line is the mean for all latitudes above  $20^\circ$  and the dashed lines are  $\pm 1$  sigma. The apparent excess in the  $20$  to  $43^\circ$  zone is not statistically significant, being only 1.4 sigma. Therefore, to the best of our knowledge, they are distributed uniformly on the sky.

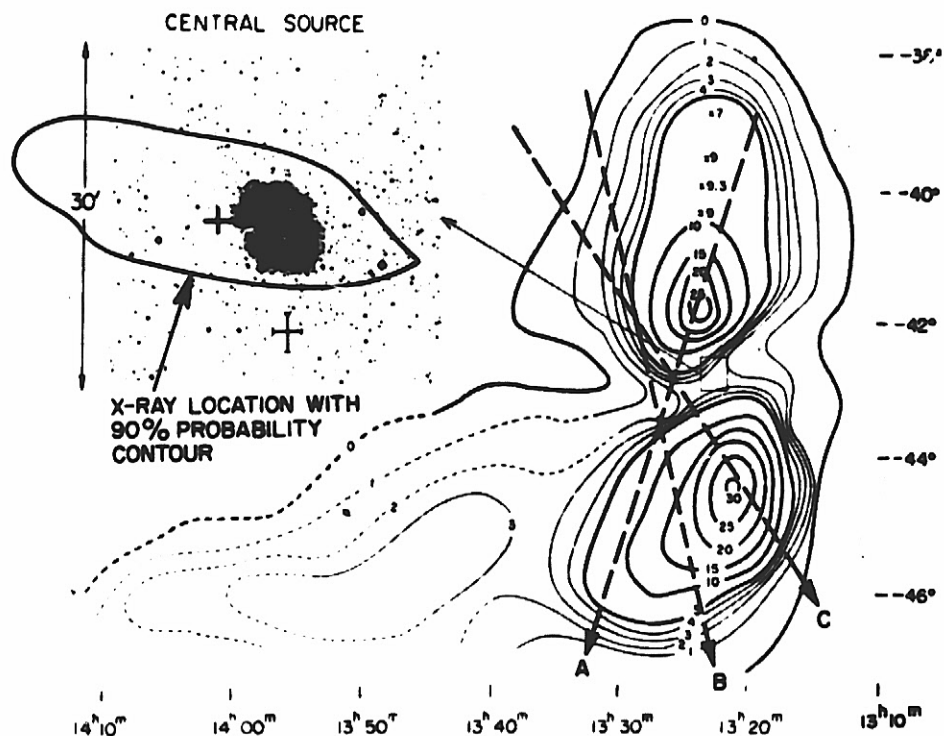


Figure 4-8. Centaurus A. The optical galaxy NGC5128 is located within the X-ray source error box. The size of the source is less than  $10'$ . This still allows the X-ray emission to be coming from the inner radio lobes shown in the inset, or from the optical galaxy. The nucleus of the optical galaxy is the most likely location of the source, since it is so strongly cut off at low X-ray energies, due to absorption.

1. NEAR STRONG RADIO SOURCES ( $\geq 30$  F.U.)

<u>2U</u>	<u>RADIO</u>
0410 + 10	3C113 (WEAK)
0515 - 34	MSH 05 - 310
0525 - 38	MSH 05 - 36
0426 - 63	MSH 04 - 64
1253 - 28	MSH 12 - 212
2128 + 81	3C435.1

2. UNCERTAIN I.D.

<u>2U</u>	<u>CANDIDATE</u>
0043 + 32	ZW 0041.1 + 3235 OR OB + 368
0426 - 10	(SOUTH)
0440 + 7	CLUSTER?
0544 - 39	(SOUTH)
0628 - 54	(SOUTH)
1231 + 7	IC 3576?
1420 - 02	NGC 5604
1443 + 43	CLUSTER?
1808 + 50	ABELL 2298?
1843 + 67	CLUSTER?
1849 - 77	(SOUTH)
1954 - 68	(SOUTH)
2134 + 11	CLUSTER?
2346 - 32	NGC 7793?
2358 - 29	(SOUTH)

Figure 4-9. Unidentified high latitude X-ray sources ( $|b| > 20^\circ$ ).

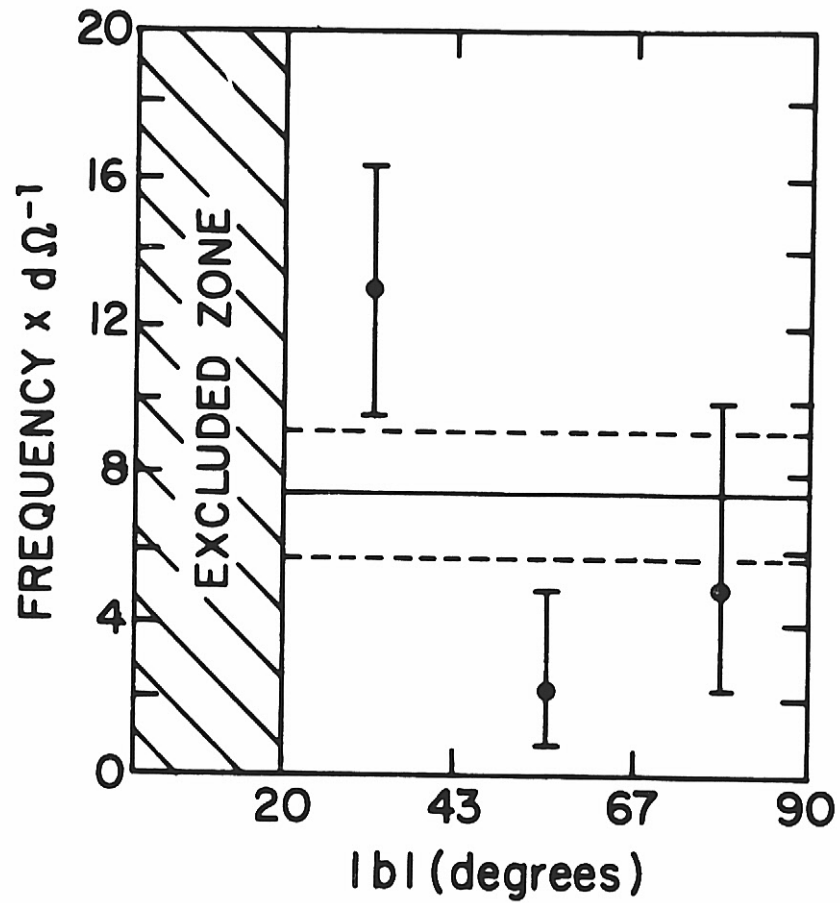


Figure 4-10. Galactic latitude distribution of unidentified X-ray sources. This is a plot of the distribution of the high latitude sources listed in Figure 9, with galactic latitude. Corrections have been made for the solid angle, sky coverage in each zone and sensitivity versus source strength. The solid horizontal line is the mean, and the dashed lines are one sigma errors in the mean.



Suppose these sources were very close to us, within the disk of our galaxy. Then we would have observed the integrated effect of other sources similar to them but further away as a galactic ridge of X-ray intensity. Such a strong ridge has not been seen. Therefore, we believe these unidentified sources are a new class of distant extragalactic object.

Figure 4-11 shows the luminosity function of high and low latitude sources (20). The low latitude sources were discussed by Tananbaum (9). The high latitude sources agree well with a 1.5 power law expected for a uniform volume distribution, with constant space density and luminosity.

Does the luminosity function continue to weaker sources than we have yet observed? Figure 4-12 shows the fluctuations in the background counting rate obtained as differences in adjacent  $5^\circ$  regions in the sky. (21). The curve is that expected from counting statistics. The excesses at 1.6 to 2.4 counts/sec are most likely due to sources below our present threshold of detectability. The estimated number at this intensity level fits well on the log N log S curve, which predicts that we will observe about 300 high latitude sources down to 1 count/sec with UHURU eventually.

With this positive indication that still weaker sources than we have yet observed exist, we can integrate the contributions of the various types of sources to the X-ray background. Figure 4-13 shows the estimated contributions from identified classes of X-ray sources. About equal contributions are obtained from Seyferts and clusters. We assume that one third of all Seyferts are X-ray sources, based on our results for NGC4151, 4051 and 1068. The contribution from Seyferts could be much less than we have calculated if the fraction of Seyferts which are strong X-ray sources like NGC4151 is much less than 1/3.

We could approach the problem differently by integrating the log N log S curve out to a faint source limit of  $5 \times 10^{-3}$  c/sec to explain the background. If we assume that this intensity cutoff corresponds to the edge of the observable

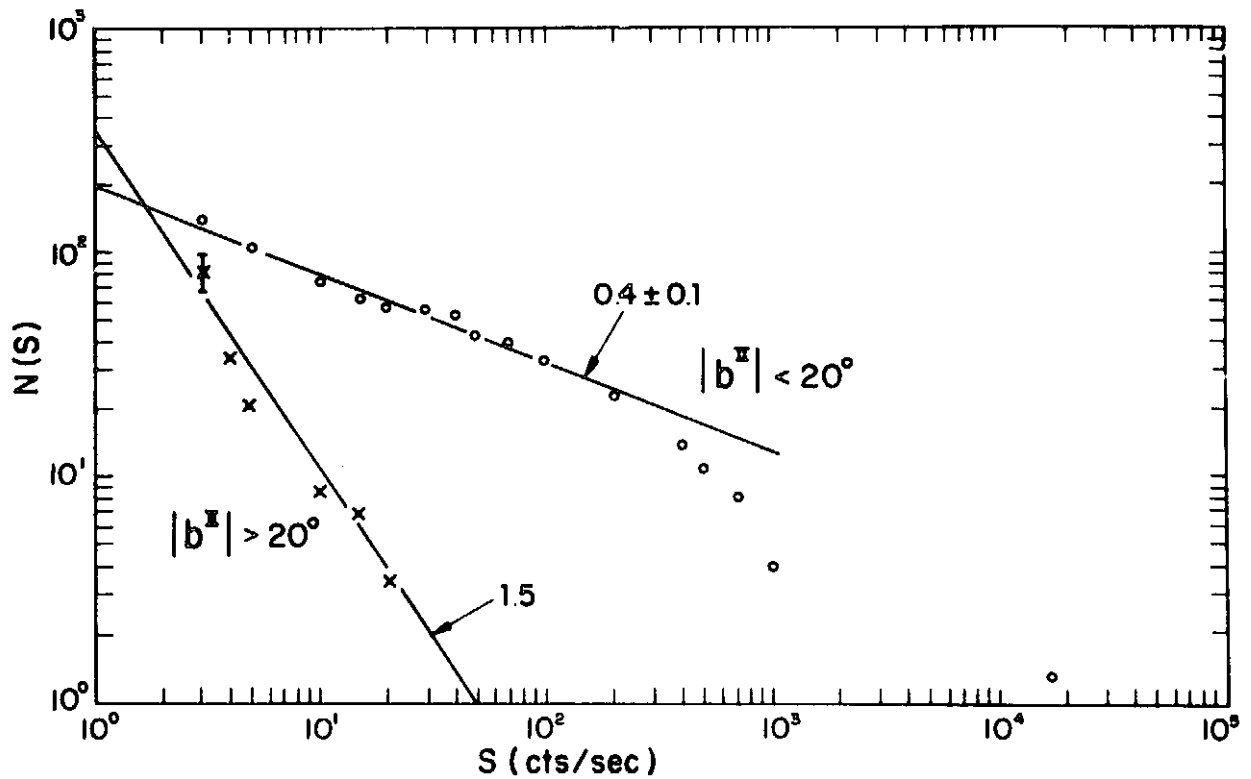


Figure 4-11. Integral distribution of number of sources versus strength,  $S$ . The sources used are those given in the UHURU Catalog (7); the numbers given have been corrected to complete sky coverage and to 100% source detection efficiency down to the limit of 3 counts  $\text{sec}^{-1}$ . The high latitude sources are consistent with a distribution of constant luminosity sources distributed uniformly throughout space, giving a distribution with a slope of 1.5 as shown by the solid curve drawn through the X's.

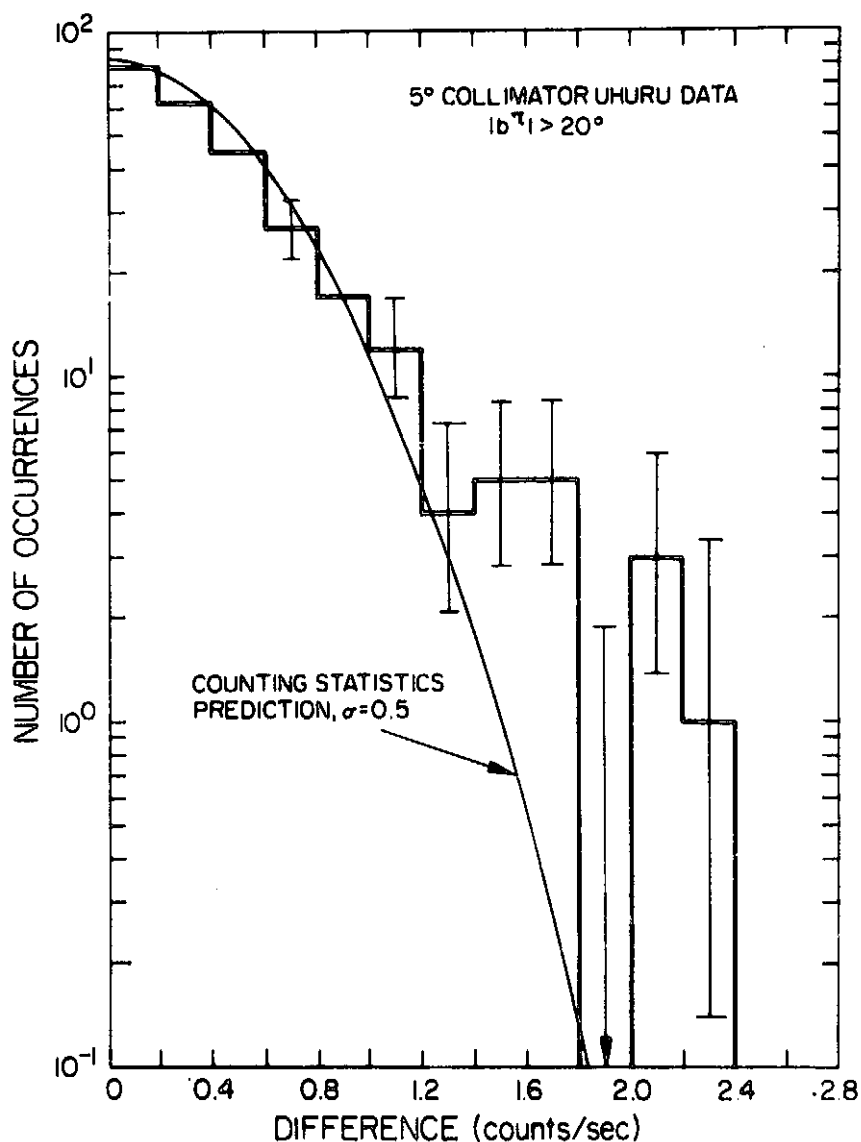


Figure 4-12. Point-to-Point Count Rate Differences. Data from each great circle scan at high latitude are analyzed for fluctuations by taking the difference in absolute magnitude of count rate between adjacent  $5^\circ$  bins. The frequency distribution of these differences is shown here. If the differences were due only to counting statistics, we would expect the solid gaussian curve. We observe excesses at about 1.6 counts/sec and 2.2 counts/sec. These are undoubtedly due to weak sources just below the UHURU threshold of detectability.

<u>TYPE</u>	<u>Lx</u> <u>erg/sec</u>	<u><math>\rho</math> (Mpc<sup>-3</sup>)</u>	<u>df</u> <u>erg/cm sec ster</u>
NORMAL GALAXIES	$2 \times 10^{39}$	.03	$.24 \times 10^{-8}$
RADIO GALAXIES	$6 \times 10^{41}$	$3 \times 10^{-5}$	$.07 \times 10^{-8}$
SEYFERTS	$10^{42}$	$3 \times 10^{-4}$	$1.2 \times 10^{-8}$
QSOS	$3 \times 10^{45}$	$10^{-8}$	$.08 \times 10^{-8}$
CLUSTERS	$2 \times 10^{44}$	$10^{-6}$	$.8 \times 10^{-8}$

$$\text{TOTAL} = 2.4 \times 10^{-8}$$

$$\text{OBSERVED} = 3 \times 10^{-8} \text{ ergs/cm}^2 \text{ sec ster}$$

Figure 4-13. Contributions to the diffuse X-ray background (2-6 keV).  
The two types of source which could contribute significantly to the background are Seyferts and clusters.

universe, we have a distance scale for the twenty or so weak sources already detected at about 3c/sec. They are about 150 Mpc away, perhaps not close enough to have been noticed in earlier surveys in optical and radio. It seems that a large fraction of the all-sky X-ray background is certainly contributed by distant rich clusters of galaxies and possibly Seyferts. The rest may be contributed by the unidentified class of sources extrapolated to great distances.

It is to be expected that further study of the powerful extended X-ray sources in clusters of galaxies will tell us much about the evolution of clusters and perhaps about cosmological phenomena. Based on the results presented here, one may speculate that the Virgo and Perseus clusters are similar in that they contain an active galaxy on which an extended X-ray source is centered; the source has a power law spectrum. Also, these two clusters are irregular. In Coma, we do not see such a prominent active galaxy. The source may be centered on the kinematic center of the cluster, and seems to show a spectrum closer to that of isothermal bremsstrahlung at a temperature corresponding to the RMS velocity of galaxies in the cluster. Also, the cluster has a more symmetrical appearance, and is believed by many to be bound. If the X-ray emission from these clusters is due to hot gas, we may be seeing the active galaxies in Virgo and Perseus heating up the gas contemporaneously, whereas in Coma we see the thermalized remnant of a heating process which ended more than  $10^9$  years ago.

The rich clusters, being very luminous and of great size, will be observable with finite angular size out to distances where redshift effects dominate. At 3200 Mpc, with  $Z=1.4$ , sources like the Coma cluster will have an angular size of one arc minute and should be observable with large orbiting telescopes of the near future. We may even be able to detect clusters out to  $Z=3$ , and learn about evolution of clusters in the early stages of the formation of the universe.

## REFERENCES

- 1 Byram, E. T., Chubb, T. A. and Friedman, H.: 1966, Science **152**, 66.
- 2 Bradt, H., Mayer, W., Naranan, S., Rappaport, S. and Spada, G.: 1967, Astrophys J (Letters) **150**, L199.
- 3 Bowyer, C., Lampton, M., Mack, J. and deMendonca, F.: 1970, Astrophys. J. (Letters) **161**, L1.
- 4 Fritz, G., Davidsen, A., Meekins, J. and Friedman, H.: 1971, Astrophys. J. (Letters) **164**, L81.
- 5 Meekins, J., Gilbert, F., Chubb, T., Friedman, H. and Henry, R.: 1971, Nature **231**, 107.
- 6 Mark, H., Price, R., Rodrigues, R., Seward, F., Swift, C.: 1969, Astrophys. J. (Letters) **155**, L143.
- 7 Giacconi, R., Murray, S., Gursky, H., Kellogg, E., Schreier, E. and Tananbaum, H.: 1972, Astrophys. J., to be published.
- 8 Leong, C., Kellogg, E., Gursky, H., Tananbaum, H. and Giacconi, R.: 1971, Astrophys J. (Letters) **170**, L67.
- 9 Tananbaum, H. IAU Symposium, May 12, 1972, Madrid
- 10 Kellogg, E., Gursky, H., Leong, C., Schreier, E., Tananbaum, H. and Giacconi, R.: 1971, Astrophys. J. (Letters) **165**, L49.
- 11 Tananbaum, H., Kellogg, E., Gursky, H. and Giacconi, R., to be published.
- 12 Kellogg, E., Gursky, H., Tananbaum, H., Giacconi, R. and Pounds, K.: 1972, Astrophys. J. (Letters) to be published.
- 13 Forman, W., Kellogg, E., Gursky, H., Tananbaum, H. and Giacconi, R., to be published,
- 14 Gursky, H., Solinger, A., Kellogg, E., Murray, S., Tananbaum, H., Giacconi, R. and Cavaliere, A.: 1972, Astrophys. J. (Letters) **173**, L99.
- 15 Solinger, A. and Tucker, W., to be published.
- 16 Kellogg, E., Gursky, H., Murray, S., Tananbaum, H. and Giacconi, R.: 1971, Astrophys. J. (Letters) **169**, L99
- 17 Wade, C., Hjellming, R., Kellermann, K. and Wardle, J.: 1971, Astrophys. J. (Letters) **170**, L11.
- 18 Kunkel, W. and Bradt, H.: 1971, Astrophys. J. (Letters) **170**, L7.

- 19 Becklin, E., Frogel, J., Kleinmann, D., Neugebauer, G., Ney, E. and Strecker, D.: 1971, Astrophys. J. (Letters) 170, L15.
- 20 Matilsky, T. et al., to be published.
- 21 Gursky, H. et al., to be published.

## 5.0 NEW TECHNOLOGY

No new technology was developed under this data analysis contract.



## 6.0 BIBLIOGRAPHY

A complete list of all the publications of results presented under this data analysis contract.

1. R. Giacconi, E. Kellogg, P. Gorenstein, H. Gursky and H. Tananbaum. An X-ray Scan of the Galactic Plane from UHURU. 1971: Ap. J. 165, L27.
2. H. Tananbaum, E. Kellogg, H. Gursky, S. Murray, E. Schreier and R. Giacconi. Measurement of the Location of the X-ray Sources Cygnus X-1 and Cygnus X-2 From UHURU. 1971: Ap. J. 165, L37.
3. H. Gursky, E. Kellogg, C. Leong, H. Tananbaum and R. Giacconi. Detection of X-rays from the Seyfert Galaxies, NGC 1275 and NGC 4151 by the UHURU Satellite. 1971: Ap. J. 165, L43.
4. E. Kellogg, H. Gursky, C. Leong, E. Schreier, H. Tananbaum, and R. Giacconi. X-ray Observations of the Virgo Cluster, NGC 5128 and 3C273 from the UHURU Satellite. 1971: Ap. J. 165, L49.
5. M. Oda, P. Gorenstein, H. Gursky, E. Kellogg, E. Schreier, H. Tananbaum and R. Giacconi. X-ray Pulsations from Cygnus X-1 Observed From UHURU. 1971: Ap. J. 166, L1.
6. R. Giacconi, H. Gursky, E. Kellogg, E. Schreier and H. Tananbaum. Discovery of Periodic X-ray Pulsations in Cen X-3 From UHURU. Ap. J. 167, L67.
7. H. Gursky, E. Kellogg, S. Murray, C. Leong, H. Tananbaum and R. Giacconi. A Strong X-ray Source in the Coma Cluster Observed by UHURU. 1971: Ap. J. 167, L81.
8. H. Tananbaum, H. Gursky, E. Kellogg, and R. Giacconi. X-ray Observations of GX 17 + 2 From UHURU. 1971: Ap. J. 168, L25.
9. E. Schreier, H. Gursky, E. Kellogg, H. Tananbaum and R. Giacconi. Further Observations of the Pulsating X-ray Source Cygnus X-1 From UHURU. 1971: Ap. J. 170, L21.
10. E. Kellogg, H. Gursky, S. Murray, H. Tananbaum and R. Giacconi. X-ray Sources Near the Galactic Center Observed by UHURU. 1971: Ap. J. 169, L99.
11. C. Leong, E. Kellogg, H. Gursky, and R. Giacconi. X-ray Emission from the Magellanic Clouds Observed by UHURU. 1971: Ap. J. 170, L67.

12. E. Kellogg. Variable X-ray Sources Observed by UHURU. Presented at the International Astronomical Union Colloquium No. 15 "New Directions and New Frontiers in Variable Star Research" Bamberg, Germany 1971
13. W. Forman, E. Kellogg, H. Gursky, H. Tananbaum and R. Giacconi. Observations of the Extended X-ray Source in the Perseus and Coma Clusters From UHURU. 1972: Ap. J. 178 309.
14. A.B. Sollinger and W. H. Tucker. Relationship Between X-ray Luminosity and Velocity Dispersion in Clusters of Galaxies. 1972: Ap. J. 175, L107.
15. H. Gursky. Advanced X-ray Observations. Publications of the Astronomical Society of the Pacific, 84, No. 479, Feb. 1972 99.
16. H. Tananbaum. UHURU Results on Galactic X-ray Sources. IAU Symposium No. 55, "X- and Gamma - Ray Astronomy," Madrid (ed. Bradt and Giacconi) D. Reidel Publ., Dordrecht p.9
17. E. Kellogg. UHURU Results on Extragalactic X-ray Sources. IAU Symposium No. 55, X- and Gamma- Ray Astronomy, Madrid (ed. Bradt and Giacconi) D. Reidel Publ., Dordrecht p. 171
18. H. Tananbaum, H. Gursky, E. Kellogg, R. Giacconi and C. Jones. Observation of a Correlated X-ray-Radio Transition in Cygnus X-1. 1972: Ap. J. 177, L5
19. E. Schreier, R. Giacconi, H. Gursky, E. Kellogg, and H. Tananbaum. Discovery of the Binary Nature of SMC X-1 From UHURU. 1972: Ap. J. 178, L71
20. H. Gursky. Observations of Galactic X-ray Sources. Les Astres Occlus, Les Houches 1972, Gordon & Breach (ed. DeWitt and DeWitt). p295
21. D. Parsignault, H. Gursky, E. Kellogg, T. Matilsky, S. Murray, E. Schreier, R. Giacconi, and A.C. Brinkman. Observations of Cygnus X-3 by UHURU. 1972: Nature Phys. Sci., 239, 123
22. E. Kellogg, H. Gursky, H. Tananbaum and R. Giacconi. The Extended X-ray Source at M87. 1972: Ap. J. 174, L65.

23. T.A. Matlsky, R. Giacconi, H. Gursky, E. M. Kellogg and H. Tananbaum. A New Transient Source Observed by UHURU. 1972: Ap. J. 174, L53.
24. H. Tananbaum, H. Gursky, E. Kellogg, R. Levinson, E. Schreier and R. Giacconi. Discovery of a Periodic Pulsating Binary X-ray Source in Hercules from UHURU. 1972: Ap. J. 174, L143.
25. H. Gursky, A. Solinger, E. Kellogg, S. Murray, H. Tananbaum, R. Giacconi and A. Cavaliere. X-ray Emission from Rich Clusters of Galaxies. 1972 Ap. J. 173, L99.
26. R. Giacconi, S. Murray, H. Gursky, E. Kellogg, E. Schreier and H. Tananbaum. The UHURU Catalog of X-ray Sources. 1972: Ap. J. 178, 281
27. E. Schreier, R. Levinson, H. Gursky, E. Kellogg, H. Tananbaum and R. Giacconi. Evidence For the Binary Nature of Cen X-3 From UHURU X-ray Observations. 1972: Ap. J. 172, L79.
28. G.R. Blumenthal and A. Cavaliere, W.K. Rose and W. Tucker. A Model For the Centaurus X-3 Phenomenon. 1972: Ap. J. 173, 213.
29. G.R. Blumenthal and W. H. Tucker. A Mechanism For the X-ray Pulsations in Cyg X-1. 1972: Nature 235, 97
30. H. Gursky, The Association of X-ray Sources with Bright Stars. 1972: Ap. J. 175, L41.
31. E. Kellogg, S. Murray, R. Giacconi, and H. Gursky. Clusters of Galaxies with a Wide Range of X-ray Luminosities. 1973: Ap. J. 185, L13.
32. C. Jones, W. Forman, H. Tananbaum, E. Schreier, H. Gursky, E. Kellogg, and R. Giacconi. Evidence for the Binary Nature of 2U 1700-37. 1973: Ap. J. 181, L43.
33. W. Forman, C. Jones, H. Tananbaum, H. Gursky, E. Kellogg, and R. Giacconi. UHURU Observations of the Binary X-ray Source 2U 0900-40. 1973: Ap. J. 182, L103.
34. A.C. Brinkman, D. Parsignault, E. Schreier, H. Gursky, E. Kellogg, and R. Giacconi. Correlation Analysis of X-ray Emission for Cygnus X-1. 1974: Ap. J. 188, 604

35. W. Tucker, E. Kellogg, H. Gursky, R. Giacconi, and H. Tananbaum. X-ray Observations of NGC5128 (Centaurus A) From UHURU. 1973: Ap. J. 180, 715.
36. T. Matlsky, H. Gursky, E. Kellogg, H. Tananbaum, S. Murray and R. Giacconi. The Number Intensity Distribution of X-ray Sources Observed by UHURU. 1973: Ap. J. 181, 753.
37. E. Kellogg, H. Tananbaum, F.R. Harnden, Jr., H. Gursky, R. Giacconi, and J. Grindlay, The X-ray Structure of the Vela X Region Observed from UHURU. 1973: Ap. J. 183, 935.
38. R. Giacconi, H. Gursky, E. Kellogg, R. Levinson, E. Schreier, and H. Tananbaum. Further X-ray Observations of Hercules X-1 from UHURU. 1973: Ap. J. 184, 227.
39. R. Giacconi, Binary X-ray Sources, International Astronomical Union #64 on Gravitational Radiation and Gravitational Collapse, September 5-8, 1973: Warsaw, Poland.
40. R. Giacconi. The UHURU Satellite. For Publication in BRITANNICA YEARBOOK OF SCIENCE AND THE FUTURE, 1973.
41. J. Bahcall and E. Kellogg, Radio Stars and X-ray Sources. 1973 Nature. Physical Sci. 244, 135.
42. S. Lea, J. Silk, E. Kellogg, and S. Murray. Thermal-Bremsstrahlung Interpretation of Cluster X-ray Sources. 1973: Ap. J. 184, L105.
43. R. Giacconi, X-ray Astronomy, THE PHYSICS TEACHER, Vol. 11, No. 3 March 1973, p. 135.
44. R. Giacconi, Progress in X-ray Astronomy, PHYSICS TODAY, Vol. 26, No. 5 May 1973, p. 38.
45. R. Giacconi, Observational Results on Compact Galactic X-ray Sources, 16th International Solvay Congress on Physics, September 24-28, 1973, Brussels, Belgium.
46. A. Cavaliere, A. Friedland, H. Gursky, and G. Spada. Description of Small-Scale Fluctuations in the Diffuse X-ray Background. 1973: Ap. J. 182, 405.
47. P.L. Coleman, A.N. Bunner, W.L. Kraushaar, D. McCammon, F.O. Williamson, E. Kellogg and D. Koch, X-ray Spectrum of the Tycho Supernova. Ap. J. 185, L121.

48. R. Giacconi, S. Murray, H. Gursky, E. Kellogg, E. Schreier, T. Matilsky, D. Koch and H. Tananbaum, The Third UHURU Catalog of X-ray Sources, 1974 February Supplement Series Ap. J. 237, Vol. 27, 37
49. S.S. Holt, E.A. Boldt, P.J. Serlemitsos, S.S. Murray, R. Giacconi, E. M. Kellogg, and T.A. Matilsky. On the Nature of the Unidentified High Latitude UHURU Sources, 1973: Ap. J. 188, L97.
50. D. Schwartz. Geomagnetic Background Events Observed by UHURU. Proceedings of Conference on Particle Contamination of Low Energy X-ray Astronomy Experiments, April 1974. NASA, Washington
51. C. Jones, R. Giacconi, W. Forman, and H. Tananbaum, Observations of Circinus X-1 from UHURU, 1974 Ap. J. 191, L71.
52. C. Jones, R. Giacconi, W. Forman, and H. Tananbaum, UHURU Observations of Short-Time Scale Variations of the Crab. 1974; Ap. J. 193, L67.
53. E. Kellogg and S. Murray. Studies of Cluster X-ray Sources: Size Measurements, 1974 Ap. J 193, I57.
54. E. Kellogg and J.R. Baldwin, and D. Koch. Studies of Cluster X-ray Sources: Energy Spectra for the Perseus, Virgo, and Coma Clusters. Center for Astrophysics; - 1974 submitted for publication to Ap. J.
55. David Koch, H. Gursky, H. Tananbaum, and E. Kellogg, Gamma Ray Bursts Seen by UHURU. 1973 Proc. of conf. on Transient Cosmic Gamma and X-ray Sources. Los Alamos LA-5505-c (ed. Ian Strong)

APPENDIX: THE UHURU CATALOG OF X-RAY SOURCES \*

\*Reproduced by permission of University of Chicago Press  
Ap. J. Suppl. 237, 1974, 27, 37.

# THE ASTROPHYSICAL JOURNAL

*Supplement Series*

S U P P L E M E N T N U M B E R 2 3 7

VOLUME 27 · PAGES 37-64 · 1974 · FEBRUARY

*The Third Uhuru Catalog of X-Ray Sources*

BY R. GIACCONI, S. MURRAY, H. GURSKY, E. KELLOGG, E. SCHREIER,  
T. MATILSKY, D. KOCH, AND H. TANANBAUM



PUBLISHED BY THE UNIVERSITY OF CHICAGO PRESS FOR  
THE AMERICAN ASTRONOMICAL SOCIETY

APJSA2 27 (237) 37-64 (1974)



\$3.00

# THE ASTROPHYSICAL JOURNAL

## *Supplement Series*

PUBLISHED BY THE UNIVERSITY OF CHICAGO PRESS FOR  
THE AMERICAN ASTRONOMICAL SOCIETY

HELMUT A. ABT, *Managing Editor*  
*Kitt Peak National Observatory*

DIMITRI MIHALAS, *Associate Managing Editor*  
*High Altitude Observatory*

### EDITORIAL BOARD

PETER A. STRITTMATTER (1974-78)  
*Steward Observatory*

SIDNEY VAN DEN BERGH (1972-76)  
*David Dunlap Observatory*

GEORGE B. FIELD (1973-77)  
*Harvard University*

ALAN H. BARRETT (1971-75)  
*Massachusetts Institute of Technology*

HERBERT FRIEDMAN (1970-74)  
*U.S. Naval Research Laboratory*

*Production Manager:* ELMARS BILSENS

*Manuscript Editor:* JEANNE HOPKINS

★ ★ ★

*The Astrophysical Journal Supplement Series* is published irregularly for the American Astronomical Society by The University of Chicago Press, 5801 Ellis Avenue, Chicago, Illinois 60637. The Supplements are paged consecutively and are collected into volumes containing about 500 pages.

The subscription rates per volume are: \$16.00, domestic; \$17.00, all other countries. The price of single copies varies and is announced as each Supplement is issued. Subscription rate for the microfiche edition is \$16.00 per volume in any part of the world. Combined subscriptions to both paper and microfiche editions are \$28.80 per volume, U.S.A.; and \$29.80 per volume, all other countries.

The Supplements are intended to provide a medium for the publication of extensive investigations, such as wavelength lists of stars of special interest, photometric data, results of numerical integrations pertaining to stellar interiors, model stellar atmosphere calculations, and original memoirs. Normally, each Supplement will consist of a single paper, although on occasion a Supplement might include several related papers submitted together.

Claims for missing numbers should be made within the month following the month of publication. The publishers expect to supply missing numbers free only when losses have been sustained in transit and when the reserve stock will permit.

Business correspondence should be addressed to The Astrophysical Journal Supplement Series, The University of Chicago Press, Chicago, Illinois 60637.

Manuscripts should be sent to Helmut A. Abt, Managing Editor, Kitt Peak National Observatory, Box 4130, Tucson, Arizona 85717 (602 327-5511).

One copy of the corrected galley proof should be returned as soon as possible to the Production Manager, THE ASTROPHYSICAL JOURNAL, The University of Chicago Press, 5801 Ellis Avenue, Chicago, Illinois 60637. Authors should take notice that the manuscript will *not* be sent with the proof; and reprint orders must accompany galleys.

Page charges: Page charges for the Supplement Series of THE ASTROPHYSICAL JOURNAL are \$50.00 per page, \$15.00 per plano page, \$35.00 per combination plano/text page, and \$50.00 per insert page; partial pages are counted as full pages. Additional charges will be made for excessive corrections in proof.

Subscriptions are payable in advance. Please make all remittances payable to THE ASTROPHYSICAL JOURNAL SUPPLEMENT SERIES, The University of Chicago Press, in United States currency or its equivalent by postal or express money orders, bank drafts, or UNESCO book coupons.

## THE THIRD *UHURU* CATALOG OF X-RAY SOURCES

R. GIACCONI,\* S. MURRAY,\* H. GURSKY,\* E. KELLOGG,\* E. SCHREIER,\*  
T. MATILSKY, D. KOCH, AND H. TANANBAUM\*

American Science & Engineering, Inc., Cambridge, Massachusetts 02139

Received 1973 August 27

### ABSTRACT

A new edition of the catalog of X-ray sources observed with *Uhuru* is presented. About 125 days of data have been analyzed for the 3U catalog, yielding a total of 161 X-ray sources. The distribution of sources is similar to that obtained for earlier editions of this catalog. Location error regions for many of the sources previously listed in the 2U catalog have been significantly reduced in size.

*Subject heading:* X-ray sources

### I. INTRODUCTION

With the continued analysis of data received from the *Uhuru* satellite, we have expanded the 2U catalog (Giacconi *et al.* 1972) to include results from the nighttime portions of 125 days of observations. This represents the major portion of the data from *Uhuru* for which high-precision aspect data are available. Sky coverage is nearly complete to a sensitivity of about 10 counts  $s^{-1}$ .

### II. DATA ANALYSIS

The data analysis procedures are the same as those used in the previous catalog (2U). The updated all-sky map of automatically obtained lines of positions is given in figure 1. There are 1878 lines of position which have been obtained from the analysis of 125 days of data. In addition, we have determined the actual nighttime sky coverage to a sensitivity of  $\sim 10$  counts  $s^{-1}$ , and this is shown in figure 2.

The requirements for source existence are those used in the 2U catalog which we summarize as follows:

a) *Two-way intersections.*—We require each line to have less than a 10 percent chance of being spurious which results in requiring  $\geq 3.4\sigma$  observations in side 1 ( $0.5^\circ \times 5^\circ$ ) and  $\geq 2.4\sigma$  observations in side 2 ( $5^\circ \times 5^\circ$ ).

b) *Three-way intersections.*—We require that either the three lines all yield consistent source intensity and that there be no more than a 1 percent chance of the intersection being due to chance, or for variable sources that at least one line have less than a 1 percent chance of being spurious.

c) *Multiple intersections.*—For more than three-way intersections no further conditions are imposed.

The source locations are calculated with the same algorithms which were first used for the 2U catalog. We use a probability calculation which is equivalent to a maximum-likelihood analysis. The basic assumption is that for each source the lines of position are uniquely assignable to that source and are the only

data used in obtaining the location and error region. For complex regions with high source density, there is not necessarily a unique interpretation; in such instances we have chosen a model which requires the smallest number of sources consistent with the data.

### III. COMPARISONS WITH THE 2U CATALOG

The 3U catalog is an extension of the results contained in the earlier 2U edition of the *Uhuru* catalog of X-ray sources. Of the 125 2U sources, all but one, 2U 0240+44, are contained in the current catalog. (This source has been found to be due to a spurious line of position.) In table 1 we present an abridged listing of the 3U catalog giving source name, location, error-box area, intensity, and reference to the 2U listing.

With the inclusion of additional data beyond that used for compiling the 2U catalog we have reanalyzed regions of high source density (complex regions), and in these regions there have been significant revisions of source locations. In table 2 complex regions at high galactic latitudes are specifically noted and the 2U and 3U sources are listed. It is not always possible to make a unique one-to-one correspondence between 2U and 3U sources in these regions. For many of the 2U sources, additional data have yielded improved source location precision. There are also a few sources for which larger uncertainties are now given. This is due to reanalysis of the original source-location data. In some extreme cases, updated positions for 2U sources are outside the original error regions. However, the number of such instances is within the expected 10 percent based on the catalog criteria. In table 3 these differences are summarized by listing those 2U sources for which there is a significantly revised location and error-box region.

### IV. THE CATALOG

The data presented in the 3U catalog are contained in table 4 and are in essentially the same format as the 2U catalog. We have updated the comments; counterpart listings for each source reflect the new location and error boxes. For new sources, standard lists of

\* Present address: Center for Astrophysics, Cambridge, Massachusetts 02138.

NORTH



FIG. 1.—The 1878 lines of position which result from the computer scan of superposed data are plotted on an equal-area projection of the sky in galactic coordinates. The line widths are  $\pm 1 \sigma$  as determined by the minimum  $\chi^2$  fits to the superposed data.

ORIGINAL PAGE IS  
OF POOR QUALITY

TABLE 1

SOURCE NAME (1)	LOCATION OF A.4.115501 (2A)	MAXIMUM PROBABILITY DEC.119501 (2B)	DENSITY b (2C)	AREA OF ERROR BOX (3)	INTENSITY AVG/MAX (4A)	RANGE (4B)	PREVIOUS NAME (5)
3U0001-31	0 1 11	-31 3 0	17.852	-78.958	5.100	3.220.4	2U2358-29
3U0002-05	0 12 35	-5 16 29	99.991	-66.239	0.230	4.920.0	
3U0021-42	0 21 47	+42 0 0	117.616	-20.316	15.000	1.92.30	2U0022+42
3U0027+63	0 22 38	+63 54 0	120.105	1.448	0.007	9.520.50	2U0022+63
3U0326-09	0 26 0	-9 42 0	104.878	-71.488	1.200	4.321.1	
3U0327+24	0 32 47	+24 12 0	118.295	-38.252	18.000	6.821.4	2U0333+24
3U0327+32	0 42 50	+32 46 48	121.508	-29.802	0.140	7.020.5	2U0343+32
3U0344-79	1 55 26	-79 41 13	302.635	-37.708	0.180	2.220.6	
3U0057-23	0 57 41	-23 55 29	152.908	-86.010	1.200	7.120.4	
3U0115-73	1 15 19	-73 41 41	300.455	-43.575	0.001		29 2U0115-73
3U0115+3	1 15 28	+63 31 36	125.943	1.111	0.004	70	7 2U0116+63
3U0134-01	1 34 11	-1 20 23	144.415	-61.397	0.200	6.221.7	
3U0132-47	1 43 16	+61 19 47	129.464	-0.599	0.027	7.220.5	2U0143+61
3U0151+32	1 51 21	+36 45 0	136.664	-24.193	0.940	2.420.4	
3U0227+43	2 27 11	+63 42 0	141.156	-15.420	13.000	4.220.6	2U0227+43
3U0254+13	2 54 35	+13 15 0	163.882	-39.220	0.220	3.420.3	2U0258+13
3U0254+60	2 58 35	+60 43 11	134.202	1.994	0.230	2.920.2	
3U0312-47	3 12 33	-47 18 3	259.398	-57.236	2.000	3.220.8	
3U0345+3	3 15 15	+3 11 11	142.834	-4.219	0.130	2.420.8	
3U0316+41	3 16 34	+41 21 10	150.573	-13.234	0.012	4.740.0.6	2U0316+41
3U0311+55	3 18 11	+55 0 0	143.267	-1.434	0.980	4.720.7	
3U0324-52	3 24 0	-52 28 47	264.447	-51.327	18.000	1.720.4	2U0328-52
3U0352+10	3 52 21	+10 54 15	161.091	-17.113	0.006	20.220.5	2U0352+30
3U0401-54	4 0 21	-50 0 0	273.611	-44.533	9.000	1.820.6	
3U0405+10	4 0 11	+10 2 24	141.723	-79.570	0.570	3.420.4	2U0413+10
3U0426-53	4 26 47	-63 33 0	274.794	-39.937	0.870	7.620.4	2U0426-63
3U0431+37	4 30 47	+37 14 23	164.350	-7.028	1.900	6.720.9	
3U0441-10	4 41 35	-10 0 0	205.880	-34.977	4.400	3.020.1	2U0446-10
3U0440+06	4 40 2	+6 59 24	190.264	-74.452	0.500	5.620.0	2U0440+07
3U0446+44	4 46 38	+44 57 35	160.527	0.314	0.053	6.220.5	2U0447+44
3U0447+66	4 40 31	+66 50 24	143.621	14.431	3.270	5.122.3	2U0449+66
3U0510-44	5 10 18	-44 39 15	257.725	-35.972	18.000	2.320.5	2U0544-39
3U0521-72	5 21 35	-72 1 11	281.101	-37.665	0.014	14.921.0	2U0521-72
3U0527-05	5 27 35	-5 51 0	233.787	-23.735	1.400	4.220.5	2U0525-06
3U0531-37	5 30 11	-17 7 0	241.633	-11.019	1.600	2.520.1	2U0515-34
3U0531+21	5 31 27	+21 59 41	134.533	-5.790	0.003	947210	2U0531+22
3U0532-66	5 32 15	-66 37 11	276.696	-32.555	0.190	9.422.1	2U0532-66
3U0537-64	5 37 21	-64 4 47	273.517	-32.707	0.014	29.721.0	2U0539-64
3U0541-65	5 40 57	-65 48 0	290.232	-31.438	0.022	19.321.3	2U0540-69
3U0545-32	5 45 26	-32 12 11	231.242	-26.433	1.800	3.220.4	2U0525-33
3U0614+04	6 14 14	+9 10 11	231.849	-3.337	0.035	60	6 2U0613+09
3U0627+23	6 20 23	+23 24 0	134.014	4.646	6.100	5.020.5	2U0601+21
3U0624-55	6 24 0	-55 4 47	263.366	-25.677	0.250	1.220.4	2U0628-54
3U0657-45	6 57 35	-35 6 0	265.684	-13.731	2.200	1.220.4	
3U0709-45	7 5 35	-45 9 0	265.680	-19.935	1.000	1.221.4	
3U0750-49	7 50 21	-49 27 0	263.250	-11.355	0.790	9.422.1	
3U0757-26	7 57 48	-26 24 3	244.124	1.750	0.900	1.020.5	2U0757-26
3U0806-53	8 4 47	-53 3 0	267.577	-11.213	1.000	3.620.5	2U0757-53
3U0821-42	8 21 35	-42 39 35	263.373	-3.169	0.022	7.920.6	2U0821-42
3U0833-45	8 33 35	-45 3 0	263.634	-2.921	0.052	7.121.7	2U0832-45
3U0900-40	9 0 15	-40 21 35	263.365	3.933	0.001	100	10 2U0900-40
3U0901-05	9 1 35	-5 24 0	239.461	23.916	2.600	4.420.8	
3U0917+53	9 17 44	+63 27 0	150.905	40.657	0.190	4.020.5	
3U0918-55	9 18 45	-55 0 47	275.352	-3.977	0.016	6.320.3	
3U0919+71	9 19 35	+71 15 35	147.467	39.248	5.300	4.020.5	
3U0940-10	9 40 14	-10 45 0	267.895	17.319	0.130	5.620.4	2U1005-32
3U1022-55	10 22 24	-55 29 23	281.737	1.430	0.081	10.420.7	2U1022-55
3U1044-33	10 44 0	-30 24 0	273.125	24.947	11.000	2.220.9	
3U1055+59	11 9 31	+59 42 0	141.652	51.447	0.300	2.420.4	
3U1111-60	11 11 55	-60 19 4	293.367	7.351	0.001	160	220 2U1119-60
3U1134-61	11 14 24	-61 36 3	294.256	-0.269	0.031	8.720.9	2U1134-61
3U1144+15	11 44 5	+19 43 11	245.361	73.270	0.130	1.620.3	2U1144+19
3U1144-74	11 44 47	-74 49 47	298.745	-12.761	0.150	4.320.8	
3U1145+11	11 45 31	+11 53 24	295.597	-0.204	0.020	72	9 2U1146-61
3U1227+34	12 7 53	+39 46 11	155.142	74.961	0.130	5.020.8	2U1207+39
3U1217-46	12 17 21	-46 38 24	298.875	-2.149	0.020	6.020.6	2U1211-64
3U1227+62	12 27 53	+62 33 36	309.106	-0.171	0.004	32	1 2U1223-62
3U1224+02	12 24 55	+2 19 35	239.039	60.257	0.140	4.220.4	2U1224+02
3U1228+12	12 23 4	+12 42 0	233.555	74.507	0.021	21.720.3	2U1228+12
3U1231+07	12 31 35	+7 8 23	250.693	69.324	1.250	6.721.4	2U1231+07
3U1237-07	12 37 45	-7 12 0	298.100	55.293	2.800	1.320.4	
3U1247-41	12 47 19	-41 2 23	302.657	21.599	0.051	6.220.3	2U1247-41
3U1252-28	12 52 28	-28 57 15	331.914	33.614	0.130	4.420.3	2U1253-28
3U1254+09	12 54 21	+69 1 11	301.481	-6.675	0.001	25.520.6	2U1254+09
3U1257+28	12 57 28	+28 11 23	56.334	87.964	0.011	14.820.3	2U1257+28
3U1258+61	12 58 2	+61 20 9	334.095	1.245	0.002	47	5 2U1258-61
3U1320-61	13 20 41	-61 43 29	306.745	0.645	0.140	5.221.4	

ORIGINAL PAGE IS  
OF POOR QUALITY

TABLE 1—Continued

(1)	(2A)	(2B)	(2C)	(2D)	(3)	(4A)	(4B)	(5)
301322-42	13 22 11	-42 47 23	339,448	19,395	0.013	8,020.3		201322-42
301344-24	13 44 11	+24 27 0	24,081	76,156	12.000	3,920.9		201344-24
301410-03	14 10 15	- 3 1 15	319,173	53,732	0.140	3,520.5		201420-02
301439-19	14 39 2	-39 1 48	325,271	18,777	4.000	3,320.4		201440-39
301443-43	14 43 2	+43 2 23	74,660	62,164	0.150	3,020.7		201443-43
301510-54	15 10 7	-59 0 0	320,313	-1,214	0.014	6,420.6		201509-58
301516-56	15 16 43	-56 59 2	322,111	0,766	0.001	720	220	201516-56
301538-52	15 38 14	-52 10 47	327,353	2,238	0.010	11,320.7		201538-52
301543-62	15 43 0	-62 24 36	121,703	-6,793	0.003	36	3	201542-62
301543-47	15 43 53	-47 33 36	339,927	5,367	0.001	2900	2100	201543-47
301544-75	15 44 0	-75 45 3	313,239	-16,749	0.075	3,120.3		201544-75
301551-15	15 51 15	+15 54 0	27,505	46,299	15.000	2,120.5		
301555-27	15 55 29	+27 12 0	41,919	49,874	0.340	5,120.7		
301556-60	15 56 54	-60 37 47	324,137	-5,967	0.010	17,020.9		201556-60
301617-15	16 17 6	-15 32 13	359,387	23,767	0.007	17,030.7	2.5	201617-15
301621-05	16 21 11	+ 5 24 0	19,745	34,661	12.000	2,520.4		201621-05
301624-19	16 24 19	-49 5 24	334,915	-3,267	0.002	50	5	201624-19
301626-47	16 26 41	-47 21 43	321,745	-13,357	0.008	10,220.4		201626-47
301631-47	16 30 17	-47 16 22	336,001	0,232	0.001	150	3	201631-47
301632-64	16 32 47	-64 8 24	324,632	-11,379	0.180	11,721.1		201632-64
301636-53	16 36 56	-53 39 3	332,915	-4,311	0.001	2613		201637-53
301631-60	16 39 21	+60 17 55	63,660	41,339	5.300	4,020.6		
301642-45	16 42 6	-45 31 29	349,374	-7,375	0.001	391	3	201641-45
301645-21	16 45 14	+21 32 23	42,563	36,439	1.100	5,121.4		
301641-15	16 41 11	+15 36 7	59,258	38,120	0.740	100	26	201705-34
301649-43	16 49 57	-43 43 37	319,925	-4,322	0.001	344	3	
301700-37	17 0 26	-37 40 11	347,745	2,193	0.009	107	23	201700-37
301702-36	17 2 15	-16 21 35	349,091	2,756	0.001	715	2	201702-36
301712-42	17 2 14	-42 59 47	343,337	-1,772	0.016	34,027.6		201704-42
301716-32	17 4 31	-32 4 45	352,763	4,963	0.358	14,021.2		201701-31
301716-34	17 5 22	-44 3 0	343,322	-2,353	0.001	283	3	201716-34
301721-32	17 6 21	+32 6 0	54,644	36,738	9.800	4,120.6		
301726-73	17 6 47	+73 32 23	110,823	11,810	0.054	3,227.1		201726-73
301730-23	17 6 20	+23 21 35	7,534	5,240	0.007	39	5	201735-22
301714-31	17 14 55	-31 14 0	343,207	-0,942	0.003	11,622.7		201718-39
301727-21	17 27 21	-21 42 0	344,235	7,139	0.000	45	13	201726-33
301723-24	17 24 49	-24 43 1	1,914	4,917	0.003	60,322.4		201728-24
301724-16	17 24 49	-16 56 52	4,493	9,327	0.001	260	1.7	201728-16
301735-44	17 35 11	-44 25 12	336,044	-0,774	0.007	21026		201735-44
301735-28	17 35 22	-28 27 0	355,573	1,556	0.040	565	213	201735-28
301736-43	17 36 23	+43 3 0	64,326	31,031	1.830	10,827.4		201735-43
301734-29	17 34 35	-29 7 47	359,951	-0,327	0.092	4025		201734-29
301744-26	17 44 44	-26 33 53	2,272	0,470	0.001	467	3	201744-26
301746-37	17 46 47	-37 7 35	351,134	-4,949	0.014	30,721.8		
301759-33	17 59 31	-33 43 0	357,240	-4,337	0.014	47	3	201757-33
301758-25	17 58 7	-25 4 47	5,046	-1,332	0.001	1127	2	201757-25
301754-22	17 54 44	-22 32 13	3,071	1,147	0.001	595	2	201754-22
301800-50	18 0 24	+50 14 47	78,193	26,951	0.390	5,120.3		201800-50
301811-17	18 11 42	-17 11 6	13,515	0,132	0.001	130	1	201811-17
301817-12	18 17 4	-12 6 35	18,007	2,447	0.037	17,121.2		201813-12
301813-14	18 13 9	-14 4 35	15,424	1,230	0.001	588	1.5	201813-14
301823-13	18 23 25	-13 23 23	2,785	-7,437	0.001	293	1.5	201820-13
301827-14	18 27 14	-17 11 23	356,787	-11,240	0.023	16,921.4		201822-14
301827-20	18 27 51	- 0 2 0	29,951	5,762	0.009	10,621.7		201822-20
301825-41	18 25 13	+41 18 0	113,193	27,943	0.690	2,720.3		201828-41
301837-02	18 37 0	-23 13 11	10,476	-6,349	0.046	4,920.9		
301837-05	18 37 9	- 5 19 0	26,357	1,243	0.190	9,121.0		201833-05
301837-14	18 37 19	+ 4 59 24	36,049	4,891	0.001	270	2	201836-05
301841-67	18 41 26	+67 33 0	97,883	24,434	2.100	3,520.4		201841-67
301845-77	18 45 3	-77 6 0	317,455	-26,453	0.150	1,323.5		201849-77
301901-13	19 1 10	+ 3 1 11	37,141	-1,470	0.034	37	4	201907-02
301906-67	19 6 47	+67 0 0	97,823	23,561	1.100	521		201912-67
301906-09	19 6 23	+ 9 41 11	43,621	0,649	0.220	7,621.4		
301906-70	19 6 7	+ 7 31 11	35,666	-4,072	0.007	199	3	201908-00
301912-07	19 12 35	+ 7 42 0	42,553	-1,649	0.770	21,521.0		
301915-05	19 15 35	- 5 15 47	31,342	-8,321	0.120	23	57	201912-05
301927-44	19 27 40	+44 28 43	75,509	13,010	0.200	6,320.6		201926-43
301931-31	19 31 55	+31 56 23	64,390	1,835	0.013	63	5	201934-31
301936-45	19 36 0	+45 3 0	97,817	17,996	2.800	4,720.4		202006-59
301936-35	19 36 27	+35 3 36	71,314	3,084	0.001	1175	5	201936-35
301957-11	19 57 47	+11 36 0	51,301	-9,265	0.047	17,420.9		
301957-40	19 57 11	+40 36 0	76,139	5,845	0.230	5,621.6		201957-40
301957-42	19 57 35	-42 0 0	125,853	-31,669	0.870	2,920.4		201954-68
302030-40	20 30 34	+40 47 5	79,836	0,710	0.001	194	23	202030-40
302041-75	20 41 45	+75 25 12	109,361	19,857	1.210	3,420.7		202041-75
302052-47	20 52 23	+47 55 12	87,849	7,090	3.100	6,220.5		
302128-81	21 28 47	+81 36 0	116,171	21,838	1.100	1,520.3		202128-81
302129-47	21 29 57	+47 1 48	91,996	-1,106	0.027	11,620.5		202130-47
302131-11	21 31 11	+11 49 11	65,547	-2,078	1.400	4,120.4		202131-11
302147-18	21 47 35	+35 5 13	87,322	-11,316	0.001	540	22.5	202142-18
302204-54	22 4 35	+54 29 23	101,024	-1,137	0.100	4,020.8		202208-54
302233-59	22 33 0	+59 33 0	106,532	1,359	2.800	4,720.4		
302321-58	23 21 12	+58 33 28	111,750	-2,116	0.001	93,421.0		202321-58
302344-25	23 44 7	+25 30 0	105,990	-34,020	7.000	7,021.2		

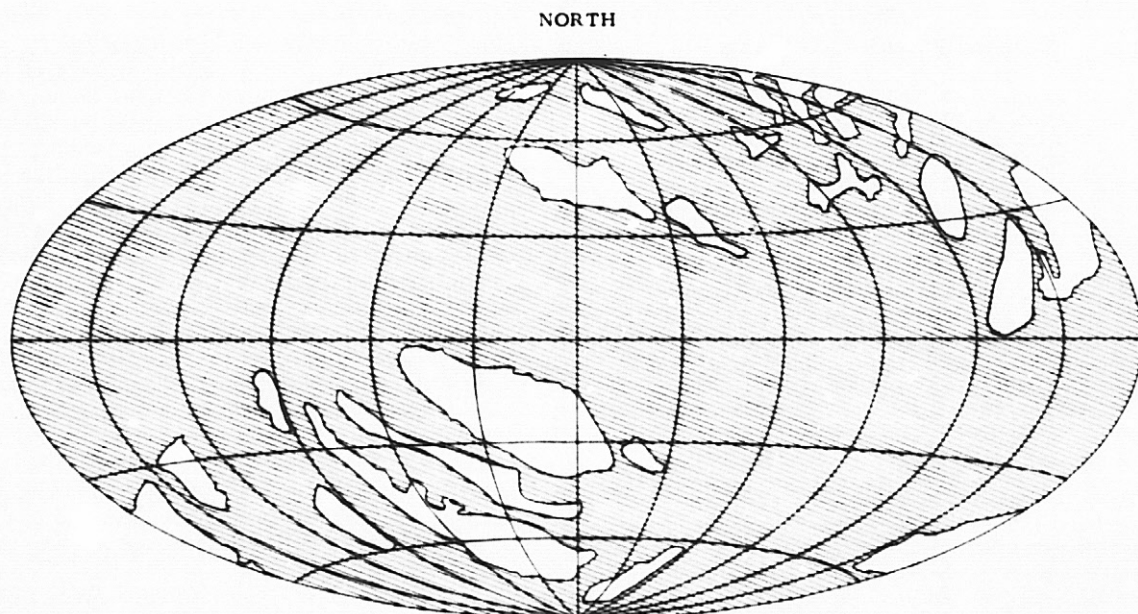


FIG. 2.—The hatched area indicates the portion of the sky scanned by the spacecraft *Uhuru* to a sensitivity of 10 counts  $s^{-1}$  or better. The blank areas have not been scanned. Due to the triangular response of the collimator, blank regions within  $5^\circ$  of the borders may have been scanned to a sensitivity of greater than 10 counts  $s^{-1}$ .

TABLE 2  
COMPLEX REGIONS

Region	2U Sources	3U Sources
1.....	0515-34 ... 0510-44 0525-38 ... 0530-37 0544-39 ... 0545-32	
2.....	0757-53 ... 0705-55 0750-49 0804-53	
3.....	1843+67 ... 1843+67 2006+59 ... 1904+67 2012+62 ... 1956+65 2041+75 ... 2041+75	
4.....	2346-32 ... 0001-32 2358-29	

interesting objects have been checked for positional coincidence. As a result of our experience with the 2U catalog, we have deleted references to the Zwicky catalogs of galaxies and clusters of galaxies. This is due to the difficulty we have found in defining uniform objective criteria for having possible counterparts from these catalogs. For X-ray sources which have been studied in more detail, we have added an annotation (table 5) following table 4 which summarizes the observational results.

The catalog lists 161 sources giving locations with 90 percent confidence error boxes, 2-6 keV intensities, and comments on peculiar properties, previous X-ray observations, and possible counterparts. In figure 3 a map of the source locations in galactic coordinates is shown.

TABLE 3A  
SOURCES WHICH HAVE SMALLER  
ERROR-BOX AREAS

i) By a Factor 10 or greater:	
3U 0946-30	3U 1735-44
3U 1258-61	3U 1837+04
3U 1641-45	3U 1901+03
3U 1700-37	3U 2131+11
ii) By a Factor 5 to 10:	
3U 0614+09	3U 1728-24
3U 0900-40	3U 1736+43
3U 1118-60	3U 1744-26
3U 1223-62	3U 1755-33
3U 1322-42	3U 1812-12
3U 1516-56	3U 1822-37
3U 1630-47	3U 1822-00
3U 1636-53	3U 1915-05
3U 1702-36	3U 1953+31
3U 1704-32	3U 2321+58
3U 1709-23	
iii) By a Factor 2 to 5:	
3U 0022+63	3U 1556-60
3U 0352+30	3U 1624-49
3U 0405+10	3U 1705-44
3U 0446+44	3U 1706+78
3U 0527-05	3U 1727-33
3U 0624-55	3U 1728-16
3U 1022-55	3U 1757-25
3U 1210-64	3U 1809+50
3U 1224+02	3U 1811-17
3U 1247-41	3U 1813-14
3U 1252-28	3U 1820-30
3U 1254-69	3U 1832-05
3U 1410-03	3U 1908+00
3U 1510-59	3U 1921+43
3U 1538-52	3U 2030+40
3U 1543-62	

TABLE 3B  
SOURCES WHICH HAVE LARGER  
ERROR-BOX AREAS

3U 0426-10 ( $\times 3$ )	3U 1439-39 ( $\times 8$ )
3U 0449-66 ( $\times 2$ )	3U 1623+05 ( $\times 4$ )
3U 1145-61 ( $\times 4$ )	3U 1632-64 ( $\times 3$ )
3U 1231+07 ( $\times 2$ )	

TABLE 3C  
SOURCES FOR WHICH THE LOCATION  
HAS CHANGED SIGNIFICANTLY

3U 0115-63	3U 1702-42
3U 0254-13	3U 1709-23
3U 0620-23	3U 1714-39
3U 0946-30	3U 1735-44
3U 1145-61	3U 1837+04
3U 1410-03	

The sources which comprise this catalog are listed in table 4 with the following information:

a) The source designation is given as the right ascension and declination (1950 epoch) of the location of the maximum of the joint probability distribution truncated to minutes of right ascension and degrees of declination. The error-box corners at the 90 percent confidence level as discussed in the 2U catalog and the error-box area are also listed as is the most probable source location. Locations are given in equatorial coordinates in both time and arc and decimal degree notation. In addition, the most probable location is also given in galactic coordinates.

b) For each source an intensity is listed which is the count rate measured with *Uhuru* from 2 to 6 keV

corrected for elevation in the collimator fields of view. For sources which are not observed to vary, the intensity given is the weighted average of individual sightings. For variable sources, we list the maximum observed intensity and the range of variability. In the case of nonvarying sources, the uncertainty in intensity is also given. This value is derived from the individual uncertainties in each sighting as determined from the minimum  $\chi^2$  fit of the collimator response to the data. These uncertainties approximately reflect the statistical significance of the sources.

c) In addition to statistical uncertainties, the source intensities given in this catalog are subject to systematic uncertainties due to the elevation corrections which depend on source location. In general, sources with poor location precision are subject to large systematic uncertainties in intensity. Unless otherwise indicated by an asterisk, the intensities listed are corrected for elevation using the most probable source location. Sources with identified counterparts have intensities corrected for the known location of the counterpart.

d) The listed intensities are in terms of *Uhuru* count rates from 2 to 6 keV. For typical spectral shapes and using an effective area for the *Uhuru* detectors of 840  $\text{cm}^2$  the conversion of these intensities to energy flux is  $1.7 \times 10^{-11} \text{ ergs cm}^{-2} \text{ s}^{-1}$  per count  $\text{s}^{-1}$ . As discussed in the 2U catalog, we expect no more than a  $\pm 30$  percent uncertainty in this value due to the spectral shape, and an additional  $\pm 10$  percent uncertainty which is due to uncertainties in the detector effective area.

e) The comments given for the sources consist of general remarks which point out peculiar X-ray properties, such as spectrum or time scales of

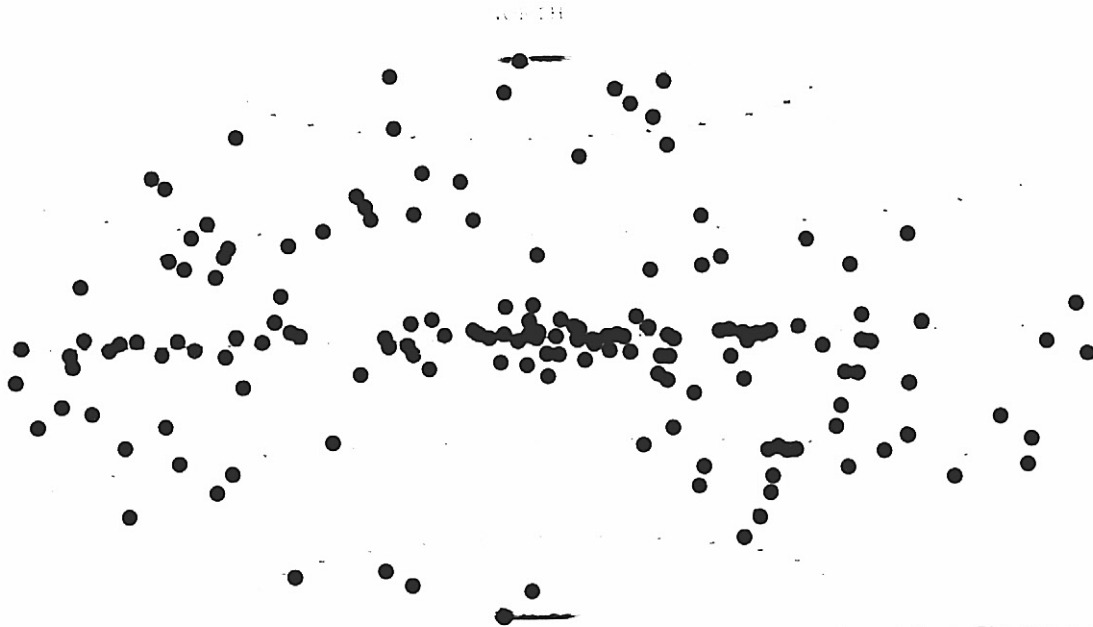


FIG. 3.—The 161 sources seen by *Uhuru*. The locations are determined from the lines of position of fig. 1. The map is an equal-area projection in galactic coordinates.



TABLE 4A

SOURCE NAME (1)	LOCATION OF MAXIMUM PROBABILITY DENSITY ALPHA (1950) DELTA (1950) (2A)	MAXIMUM PROBABILITY DENSITY D (2B)	ERROR REGION FOR 90 PERCENT CONFIDENCE				AREA SQ. DEG (3E)	INTENSITY AVERAGE OR MAXIMUM (4A)	MAX. OBS. OR MIN. OBS. (4B)	COMMENTS GENERAL REMARKS COUNTERPARTS (5A) PREVIOUS K-RAY (5B)	
			1 ALPHA DELTA (3A)	2 ALPHA DELTA (3B)	3 ALPHA DELTA (3C)	4 ALPHA DELTA (3D)					
3U0001-31	0 11 12 -31 3 0 0.30 -31.05	10.85 -78.96	0 11 12 -30 27 0 2.80 -30.45	23 51 24 -30 27 0 357.85 -30.45	23 51 24 -31 39 0 357.85 -31.65	0 11 12 -31 39 0 2.80 -31.65	5.1000	3.7±0.4			2U2346-32 & 2U2358-29
3U0012-05	0 12 36 -5 16 30 3.150 -5.275	99.99 -66.24	0 12 17 -5 6 36 3.07 -5.11	0 9 36 -5 40 12 2.40 -5.67	0 10 29 -5 46 12 2.62 -5.77	0 13 0 -5 25 48 3.25 -5.43	0.2300	4.9±2.0			
3U0021+42	0 21 48 42 0 0 5.45 42.00	117.62 -20.32	1 9 3 42 57 0 17.25 42.95	0 20 55 42 57 0 5.23 42.95	1 9 0 41 12 0 17.25 41.20	0 20 55 41 12 0 5.23 41.20	15.0000	1.9±.30		M31	2U0022+42
3U0022+63	0 22 38 63 54 0 5.66 63.93	120.11 1.45	0 23 22 63 55 48 5.84 63.93	0 22 29 63 55 48 5.62 63.93	0 21 55 63 51 36 5.48 63.86	0 22 48 63 51 36 5.70 63.86	0.0068	9.5±0.50		TYCHO'S SNR = 3010	CEP XR-1 (1) TYCHO (2) CEP 1 (3) 2U0022+63
3U0026-09	0 26 0 -9 42 0 6.5 -9.7	104.88 -71.49	0 38 24 9 24 0 9.2 -9.4	0 14 0 -9 48 0 3.5 -9.8	0 14 0 -13 0 0 3.5 -10.0	0 38 0 -9 36 0 9.5 -9.6	1.2000	4.3±1.1		NGC195 ?	
3U0032+24	0 32 48 24 12 0 8.20 24.20	118.29 -38.25	1 11 12 24 0 0 17.8 24.00	0 31 36 25 12 0 7.9 25.20	0 28 0 23 12 0 7.0 23.20	1 10 48 22 18 0 17.7 22.30	18.0000	6.8±1.4		STAR: 34C AND ? PKS0335+23 (050) ? ARP 282 ? NGC160,169 ? IC1559 ?	2U0033+24
3U0042+32	0 42 50 32 46 48 10.71 32.78	121.51 -29.80	0 45 55 33 3 36 11.48 33.06	0 40 0 32 36 0 10.00 32.60	0 40 7 32 30 0 10.03 32.50	0 46 0 32 57 0 11.50 32.95	0.1400	7.0±0.5			2U0043+32
3U0055-79	0 55 27 -79 41 13 13.862 -79.687	302.64 -37.71	1 0 36 -79 30 0 15.15 -79.50	0 50 12 -79 30 0 12.55 -79.50	0 50 12 -79 53 24 12.55 -79.89	1 0 36 -79 53 24 15.15 -79.89	0.1800	2.2±0.6			

REFERENCES TO TABLE 4A.—(1) Oda and Matsuoka 1970; (2) Kellogg 1970; (3) Seward 1970; (4) Leong *et al.* 1971; (5) Kellogg *et al.* 1973a; (6) Fritz *et al.* 1971; (7) Giacconi *et al.* 1971; (8) Gursky *et al.* 1971a; (9) Lewin *et al.* 1971a; (10) Ricker *et al.* 1973; (11) Kellogg *et al.* 1971a; (12) Margon *et al.* 1972; (13) Gursky *et al.* 1971b; (14) Schreier *et al.* 1971; (15) Hunter and Lu 1969; (16) Bradt *et al.* 1971; (17) Markert *et al.* 1973; (18) Kellogg *et al.* 1971b; (19) Lewin *et al.* 1971b; (20) Hawkins *et al.* 1973.



TABLE 4A—Continued

(1)	(2A)	(2B)	(3A)	(3B)	(3C)	(3D)	(3E)	(4A)	(4B)	(5A)	(5B)
BU0057-73	0 57 42 -73 55 30 14 47 5 71.52	152.91 -86.31	0 58 0 -23 45 0 14 50 -23.75	0 40 36 -24 42 0 10.15 -24.70	0 40 36 -24 42 0 10.15 -24.95	0 58 24 -24 6 0 14.60 -24.10	1.2037 2.110.4				
BU0115-73	1 15 19 -73 48 42 10.85 71.69	400.45 -43.58	1 15 31 -73 40 48 10.08 -73.680	1 14 24 -73 41 6 10.60 -73.680	1 15 14 -73 43 12 10.81 -73.720	1 16 29 -73 43 12 10.12 -73.720	0.0033	28	29	STAN: SANDULFAR 160 AT Q: 16 15m 448.3 8-73° 42' 53" 6	SMC K-1 (4) + 200115-73
BU0115-63	1 15 29 63 31 36 18.87 64.50	225.94 1.11	1 15 43 63 37 12 18.93 63.67	1 15 2 63 31 48 18.76 63.53	1 15 14 63 30 0 18.81 63.50	1 15 55 63 35 24 18.98 63.54	0.0044	70	7		200115-63
BU0130-01	1 38 12 -1 20 24 74.55 -1.36	149.41 -61.40	1 37 22 -1 10 12 74.14 -1.17	1 36 10 -1 40 12 24.04 -1.67	1 36 41 -1 47 24 24.17 -1.79	1 39 0 -1 29 24 24.75 -1.49	0.2300	6.741.7			
BU0143-61	1 43 17 61 19 48 25.82 61.33	129.46 -0.59	1 43 58 61 24 0 25.99 61.40	1 42 29 61 24 0 25.62 61.40	1 42 29 61 15 0 25.62 61.25	1 43 58 61 15 0 25.99 61.25	0.0266	7.240.5			
BU0151-36	1 51 24 36 45 0 27.05 36.75	116.66 -24.19	1 54 0 37 34 12 28.5 37.57	1 46 24 36 4 12 26.6 36.07	1 49 12 35 57 0 27.3 35.95	1 56 0 37 21 0 29 37.35	0.9400	2.440.4		CLUSTER: ADULT 242 7 (5) PAKISTAN 7 7	200143-61
BU0227-63	2 27 12 43 42 0 36.8 41.7	141.16 -15.42	3 2 24 43 24 0 45.6 43.4	2 12 24 44 42 0 33.1 44.7	2 11 36 43 18 0 32.9 43.3	3 0 0 42 0 0 45.0 42.0	13.0000	4.240.6		1066 7	200227-63
BU0254-13	2 54 36 13 15 0 41.65 13.25	163.84 -39.21	2 55 31 13 28 48 43.88 13.48	2 52 36 13 16 48 43.15 13.28	2 53 31 13 2 24 43.38 13.04	2 56 34 13 15 0 44.14 13.25	0.2200	3.440.1		CLUSTER: ADULT 401 (5)	200254-13

ORIGINAL PAGE  
OF POOR QUALITY

TABLE 4A—Continued

(1)	(2A)	(2B)	(3A)	(3B)	(3C)	(3D)	(3E)	(4A)	(4B)	(5A)	(5B)
3U0298+00	2 58 36 60 43 12 44.65 6C.72	138.20 1.99	2 57 48 60 58 12 44.65 60.97	2 54 0 61 0 0 43.50 61.00	2 59 36 60 27 0 44.90 60.45	3 3 12 60 27 0 45.80 60.45	0.2300	2.940.7			
3U0302+47	3 2 34 -47 18 0 45.64 -47.3	250.40 -57.24	3 15 36 -65 51 0 48.9 -45.85	2 49 36 -68 10 12 42.4 -48.17	2 52 24 -68 24 0 43.1 -48.72	3 12 24 -66 43 12 40.1 -48.72	2.0000	3.180.8			
3U0305+53	3 5 55 53 1 12 46.40 53.07	142.83 -4.24	3 6 14 53 13 48 46.50 53.23	3 3 40 52 59 24 45.95 52.99	3 5 11 52 49 12 46.30 52.32	3 0 0 53 3 36 47.00 53.06	0.1300	2.840.8	STAR: 23 7 PER 7		
3U0316+41	3 16 35 41 21 11 49.465 41.953	150.58 -13.23	3 17 0 41 25 59 49.252 41.433	3 16 3 41 19 12 49.011 41.370	3 16 8 41 15 54 49.034 41.265	3 17 6 41 22 30 49.277 41.375	0.0123	47.440.6	PERSEUS CLUSTER: ABELL 426 PER K-1 161 + 200316+41		
3U0318+55	3 18 12 55 4 0 49.55 55.15	143.27 -1.48	3 19 12 56 6 0 49.80 56.10	3 13 43 54 25 48 48.43 54.43	3 17 7 54 15 0 49.28 54.25	3 22 48 55 55 12 50.70 55.92	0.9800	4.940.7			
3U0328+57	3 28 0 -52 28 48 52.00 -52.48	264.45 -51.33	3 42 0 -50 24 0 55.5 -50.4	3 12 0 -50 24 0 48.0 -50.4	3 12 0 -54 24 0 48.0 -54.4	3 42 0 -54 24 0 55.5 -54.4	10.0000	1.740.4	IC 1933, 1954 7		
3U0352+30	3 52 27 30 54 36 50.09 30.91	163.09 -17.17	3 52 48 30 57 36 50.20 30.96	3 51 55 30 53 24 57.98 30.89	3 51 53 30 51 36 57.97 30.86	3 52 58 30 56 24 58.24 30.94	0.0062	20.720.5	STAR: A PER 7 AT G = 30 52m 158.2 B = +13° 54' 01"	200324+52	
3U0400+59	4 0 24 -59 0 0 40.1 -59.	270.61 -44.53	4 10 24 -55 18 0 62.6 -55.3	3 44 48 -60 54 0 56.2 -60.9	3 57 36 -61 36 0 59.4 -61.6	4 16 0 -56 42 0 64. -56.7	9.0000	3.230.6	NGC 1533, 1536, 1543 7 NGC 1546, 1549, 1553 7 IC 2038 7	200352+30	

ORIGINAL PAGE IS  
OF POOR QUALITY

TABLE 4A—Continued

(1)	(2A)	(2B)	(3A)	(3B)	(3C)	(3D)	(3E)	(4A)	(4B)	(5A)	(5B)
3U0405+10	4 5 12 10 2 24 61.30 10.06	181.72 -29.52	4 10 24 10 24 0 62.60 10.40	3 59 24 9 50 24 94.85 9.84	4 0 0 9 41 24 60.00 9.69	4 11 12 10 14 24 62.80 10.24	0.5200	3.440.4	CLUSTER: ABFIL 478 7		
3U0426-03	4 26 48 -63.33 0 66.70 -61.55	274.79 -39.94	4 30 24 -61 48 36 62.60 -61.81	4 21 31 -64 57 0 65.38 -64.95	4 23 51 -65 3 0 65.97 -65.05	4 32 7 -62 7 12 68.03 -62.12	0.8700	2.620.4		2U0413+10	
3U0430+17	4 30 48 37 14 24 67.7 37.24	164.35 -7.03	4 38 48 37 21 36 69.7 37.36	4 20 48 37 38 24 65.7 37.64	4 16 24 37 15 0 66.1 37.25	4 38 48 36 51 0 69.7 36.85	1.9000	6.020.9		2U0426-03	
3U0431-10	4 31 36 -10 0 0 67.90 -10.03	205.88 -34.98	4 39 36 -8 42 0 68.9 -8.7	4 22 24 -10 30 0 65.6 -10.5	4 24 0 -11 30 0 65.0 -11.5	4 40 48 9 30 0 70.2 -9.5	4.4300	3.020.3		2U0426-10	
3U0440+06	4 40 2 6 59 24 70.01 6.99	190.27 -24.46	4 42 55 7 38 24 70.73 7.64	4 36 43 6 38 24 69.18 6.64	4 37 12 6 24 36 69.30 6.41	4 43 36 7 24 36 70.90 7.41	0.5500	5.620.9		2U0440+07	
3U0446+44	4 46 38 44 57 36 71.66 44.96	160.53 0.31	4 47 36 45 7 48 71.90 45.13	4 45 31 44 52 48 71.38 44.88	4 45 50 44 45 48 71.46 44.78	4 48 0 45 1 48 72.00 45.03	0.0534	6.220.5	3C129 (CLUSTER 7 151) 3C129.1		
3U0449+66	4 49 31 66 50 24 72.38 66.84	143.62 14.43	4 52 12 67 9 0 73.05 67.15	4 45 36 66 48 0 71.40 66.80	4 45 55 66 28 48 71.48 66.48	4 54 48 66 54 36 73.70 66.91	0.2700	8.122.3		2U0449+64	
3U0510-44	5 10 38 -44 39 36 77.56 -44.66	250.03 -35.89	5 18 0 -40 42 0 79.5 -40.7	4 54 48 -46 30 0 75.7 -46.5	5 2 48 -48 42 0 75.7 -48.7	5 26 48 -43 0 0 91.7 -43.0	0.0330	2.020.5	PIC A = MS105-42.05-431 7		2U0510-39

ORIGINAL PAGE  
OF FOUR QUALITY

TABLE 4A-- Continued

(11)	(12A)	(12B)	(13A)	(13B)	(13C)	(13D)	(13E)	(14A)	(14B)	(15A)	(15B)
3U0521-72	5 21 36 -72 1 12 80.40 -72.02	283.10 -32.66	5 21 41 -71 56 24 80.42 -71.94	5 20 14 -72 3 0 80.06 -72.05	5 21 14 -72 6 0 80.06 -72.10	5 22 30 -72 0 36 80.06 -72.01	0.0144	14.921.0		IN LMC	LMC X-2 (4)  2U0521-72
3U0527-05	5 27 36 -5 51 0 81.90 -5.85	208.79 -20.73	5 43 12 -3 57 0 85.0 -3.95	5 27 12 -5 42 0 81.8 -5.70	5 27 12 -6 6 0 81.8 -6.10	5 43 12 -4 15 0 85.8 -4.25	1.4000	4.240.5		M42 = ORION NEBULA	2U0525-06
3U0530-37	5 30 19 -37 0 0 82.58 -37.00	241.63 -31.04	5 37 12 -37 6 0 84.3 -37.1	5 25 36 -36 24 0 81.4 -36.4	5 23 12 -36 54 0 80.8 -36.9	5 35 12 -37 42 0 83.8 -37.7	1.6000	2.590.3			2U0515-34
3U0531+21	5 31 27 21 59 42 82.864 21.995	184.54 -5.79	5 31 33 22 1 16 82.886 27.021	5 31 15 21 59 6 82.814 21.985	5 31 25 21 57 56 82.856 21.965	5 31 42 22 0 4 82.926 22.001	0.0027	947421.0		C4 OB NEBULA PULSAR: NPO531 AT Q = 5N 31m 31s B = 21° 58' 55"	TAU X-1 (11) CR88 (2) TAU 1 (13) + 2U0531+22
3U0532-66	5 32 19 -66 37 12 83.08 -66.62	276.60 -32.55	5 34 48 -66 16 12 83.70 -66.27	5 32 0 -66 14 24 83.00 -66.24	5 30 24 -66 57 0 82.60 -66.95	5 32 48 -66 59 24 83.20 -66.99	0.1900	9.422.1		IN LMC	LMC X-6 (4)  2U0532-66
3U0539-64	5 39 22 -64 4 48 84.84 -64.08	273.54 -32.31	5 39 41 -64 1 12 84.92 -64.02	5 30 14 -64 6 36 84.56 -64.11	5 39 2 -64 9 0 84.76 -64.15	5 40 24 -64 3 36 85.10 -64.06	0.0136	70.741.0		IN LMC	LMC X-3 (4)  2U0539-64
3U0540-69	5 40 58 -69 48 0 85.24 -69.83	280.23 -31.64	5 41 46 -69 42 36 85.44 -69.71	5 40 19 -69 42 36 85.08 -69.71	5 40 19 -69 53 24 85.08 -69.69	5 41 46 -69 53 24 85.44 -69.89	0.0224	19.321.3		IN LMC	LMC X-1 (4)  2U0540-69
3U0545-37	5 45 26 -32 12 0 86.36 -32.23	237.24 -26.80	5 54 0 -31 24 0 86.5 -31.4	5 35 36 -32 36 0 83.9 -32.6	5 36 48 -33 0 0 84.2 -33.0	5 55 36 -31 47 0 86.9 -31.7	1.6000	3.220.4			2U0525-38

ORIGINAL PAGE IS  
OF POOR QUALITY

TABLE 4A—Continued

(1)	(2A)	(2B)	(3A)	(3B)	(3C)	(3D)	(3E)	(4A)	(4B)	(5A)	(5B)
3U0614+09	6 14 14 9 10 12 91.56 9.17	200.37 -32.39	6 14 26 9 12 16 91.61 9.21	5 13 58 9 10 48 91.49 9.18	9 14 0 9 8 24 91.50 9.14	6 14 29 9 10 12 91.67 9.17	0.0053	60	6		2U0613+09
3U0620+23	6 20 24 23 24 0 95.17 21.60	189.71 4.67	6 30 24 23 6 0 91.6 21.1	6 25 12 24 30 0 96.3 24.5	6 9 36 23 36 0 92.4 23.6	6 14 48 22 12 0 91.7 22.2	0.1303	5.010.5		IF 443 (SAR) = 3C157 PUL SAR: PSR3611+22 7	2U0601+21
3U0624+55	6 24 0 -55 4 48 96.00 -55.08	263.86 -25.64	6 26 54 -54 28 48 96.73 -54.48	6 22 53 -55 0 36 95.72 -55.01	6 24 36 -55 13 12 96.15 -55.22	6 24 36 -54 40 48 97.15 -54.68	J.2500	3.410.4			2U0628+54
3U0657+15	6 57 16 -15 6 0 104.4 -35.1	245.64 -13.73	7 2 24 -34 25 12 105.6 -34.47	6 46 24 -35 25 12 101.6 -35.47	6 54 24 -35 39 0 103.6 -35.65	7 8 0 -34 48 0 102.0 -34.9	2.2000	3.010.9			
3U0705+55	7 5 16 -55 9 0 106.4 -55.15	265.68 -19.93	7 12 48 -55 18 0 108.7 -55.3	6 58 0 -55 0 0 105.0 -54.6	6 58 0 -55 0 0 104.5 -55.0	7 11 12 -55 48 0 107.8 -55.9	1.0003	3 2+0.4			
3U0750+49	7 50 24 -49 27 0 117.6 -49.45	263.25 -11.56	7 56 0 -48 30 0 119.0 -48.5	7 43 12 -50 18 3 115.8 -50.3	7 44 48 -50 30 0 116.2 -50.5	7 57 36 -48 16 0 119.4 -48.6	J.1900	9.452.3	STAR: V PUP 7		
3U0757+26	7 57 48 -26 24 0 119.45 -26.4	244.12 1.75	8 3 12 -25 30 0 120.8 -25.5	7 52 0 -27 0 0 118.0 -27.0	7 53 12 -27 12 0 118.3 -27.2	8 4 24 -25 42 0 121.1 -25.7	0.9303	3.010.5			2U0757+26
3U0804+53	8 4 48 -53 3 0 121.20 -53.05	267.58 -11.21	8 13 12 -53 0 0 123.3 -53.0	7 59 36 -52 36 0 119.9 -52.6	7 56 0 -53 0 0 119.0 -53.0	8 9 36 -53 24 0 122.4 -53.4	1.0000	3.610.5			2U0757+53

ORIGINAL PAGE IS  
OF POOR QUALITY

TABLE 4A—Continued

(1)	(2A)	(2B)	(3A)	(3B)	(3C)	(3D)	(3E)	(4A)	(4B)	(5A)	(5B)
3U0821-42	0 21 3 -42 30 36 125.39 -42.66	260.17 -3.17	8 21 36 -42 31 48 125.40 -42.53	8 20 55 -42 45 36 125.23 -42.76	8 21 26 -47 47 24 125.36 -42.79	0 21 55 -42 36 0 125.48 -42.60	0.0215	7.540.6		PUP A VEL XR-2 (1) ? PUP A (2)	
3U0833-45	8 33 36 -45 3 0 128.40 -45.05	263.58 -2.92	8 34 2 -44 51 36 128.51 -44.86	8 32 31 -45 11 24 128.13 -45.19	8 33 14 -45 14 24 128.31 -45.24	8 34 41 -44 54 0 128.67 -44.90	0.0521	9.121.0		VELA X PULSAR: PSR0833-45 AT Q = 30 33m 38s B = -45° 00' 19"	VEL XR-1 (1) ? VEL XR-2 (1) ? VELA X (2) + 2U0832-45
3U0900-4C	9 0 15 -40 21 36 115.064 -43.360	263.07 3.93	9 0 27 -40 20 46 115.082 -40.346	9 0 10 -40 20 46 115.043 -40.346	9 0 10 -40 22 34 115.043 -40.376	9 0 20 -40 22 34 115.082 -40.376	0.0009	100	10	STAR: HD77581 AT Q = 9h 00m 13s.2 B = -43° 21' 25".2	GX263+3 (2) VEL XR-1 (1) ? VEL 1 (1) + 2U0900-40
3U0901-09	9 1 36 -9 24 0 135.4 -9.4	238.46 23.82	9 12 0 -9 12 0 138.0 -9.2	9 51 12 -9 12 0 132.8 -9.2	9 51 12 -9 42 0 132.8 -9.7	9 12 0 -9 42 0 138.0 -9.7	2.6000	4.450.8		CLUSTER: ABELL 754 (5)	
3U0917+03	9 17 45 63 27 0 139.931 63.45	150.99 40.66	9 20 36 63 36 36 140.15 63.61	9 15 6 63 36 36 138.775 63.61	9 15 6 63 17 30 138.775 63.294	9 20 36 63 17 30 140.150 63.294	0.1900	4.020.5			
3U0918-55	9 18 55 -55 0 58 139.688 -55.016	275.85 -3.88	9 18 55 -54 55 37 139.73 -54.927	9 18 5 -55 1 34 139.52 -55.026	9 18 18 -55 6 7 139.66 -55.102	9 19 24 -55 0 18 139.85 -55.005	0.0161	6.150.1		STAR: # VEL ?	
3U0943+71	9 43 36 71 15 36 145.90 71.26	140.47 39.25	10 21 12 70 36 0 155.3 70.60	9 37 36 72 6 0 144.4 72.10	9 27 36 70 57 0 141.9 70.95	10 37 12 69 0 0 159.3 69.00	5.5000	4.020.5		MO2 ? MERKATYAN 120 ? 4936 ?	
3U0946-10	9 46 14 -30 45 0 146.56 -30.75	262.90 17.32	9 45 26 -30 31 48 146.36 -30.53	9 44 29 -30 39 0 146.12 -30.55	9 47 7 -30 50 48 146.78 -30.98	9 48 2 -30 52 12 147.01 -30.87	0.1500	5.650.4			2U1009-32

ORIGINAL FACTORS  
OF POOR QUALITY

TABLE 4A—Continued

(1)	(2A)	(2B)	(3A)	(3B)	(3C)	(3D)	(3E)	(4A)	(4B)	(5A)	(5B)
3U1022-55	10 22 29 -55 29 24 155.62 -55.490	203.24 1.40	10 21 53 -55 17 10 155.47 -55.286	10 20 53 -55 24 43 155.22 -55.412	10 22 50 -55 41 24 155.76 -55.690	10 24 7 -55 33 50 156.03 -55.564	0.0810	1C.4±0.7			2U1022-55
3U1044-30	10 44 0 -30 24 0 161.0 -30.4	273.43 24.95	10 27 12 -26 24 0 156.8 -26.4	10 25 12 -27 48 0 156.3 -27.8	10 40 48 -31 36 0 160.2 -31.6	10 48 24 -29 6 0 162.1 -29.1	11.0000	2.2±0.8		CLUSTER: ABELL 1060 (5)	
3U1109+59	11 9 31 59 42 0 167.38 59.7	143.89 53.49	11 12 24 60 57 0 168.1 60.95	10 52 48 60 45 0 163.2 60.75	11 5 12 58 27 0 168.3 58.45	11 26 48 58 41 24 171.7 58.69	6.3000	2.4±0.4		AHP 296.299 ? MARKARYAN 169 ? NGC 1470, 3610, 3642 ?	
3U1118-60	11 18 55 -60 19 5 165.730 -60.318	292.07 0.36	11 18 53 -60 17 35 169.722 -60.293	11 18 47 -60 18 32 169.697 -60.309	11 18 58 -60 20 35 169.740 -60.343	11 19 3 -60 19 41 169.764 -60.328	0.0007	16C	27)		CEN X-3 (1,2) ? CEN X-3 (7) CEN 3 (1) ? ↑ 2U1119-60
3U1134-61	11 34 26 -61 36 0 173.61 -61.60	294.26 -0.27	11 35 29 -61 43 12 173.87 -61.77	11 34 48 -61 30 36 173.70 -61.51	11 33 19 -61 32 24 173.33 -61.54	11 34 24 -61 43 12 173.60 -61.72	0.0312	8.1±0.8			2U1134-61
3U1144+19	11 44 5 19 43 12 176.02 19.72	236.86 73.28	11 43 43 19 55 48 175.93 19.73	11 42 34 19 52 12 175.64 19.87	11 44 26 19 30 36 176.11 19.51	11 45 36 19 35 24 176.40 19.59	0.1300	3.6±0.3		CLUSTER: ABELL 1367 (5) 3C 264 = NGC 3962	2U1144+19
3U1144-74	11 44 48 -74 49 48 176.2 -74.83	298.75 -12.76	11 43 36 -74 28 12 175.9 -74.47	11 41 36 -74 48 0 175.4 -74.80	11 46 0 -75 12 36 176.5 -75.21	11 48 0 -74 52 48 177.0 -74.88	0.1500	4.3±0.8			
3U1145-61	11 45 11 -61 53 24 176.38 -61.83	295.60 -0.20	11 46 19 -61 36 36 176.58 -61.61	11 45 53 -61 39 0 176.47 -61.65	11 44 43 -62 12 36 176.18 -62.21	11 45 14 -62 6 0 176.31 -62.10	0.0197	72	5		2U1146-61

ORIGINAL PAGE  
OF POOR QUALITY

TABLE 4A—Continued

(1)	(2A)	(2B)	(3A)	(3B)	(3C)	(3D)	(3E)	(4A)	(4B)	(5A)	(5B)
3U1207+39	12 7 34 39 46 12 181.89 39.77	155.14 76.96	12 9 19 39 50 24 182.33 39.84	12 5 50 39 50 24 181.46 39.84	12 5 50 39 41 24 182.33 39.69	12 9 19 39 41 24 182.33 39.69	0-1000	5.020-8		NGC4151 (8)	
3U1210-64	12 10 22 -64 38 24 182.59 -64.64	298.88 -2.35	12 10 50 -64 33 0 182.71 -64.55	12 9 53 -64 33 0 182.47 -64.74	12 9 53 -64 44 24 182.71 -64.74	12 10 50 -64 44 24 182.71 -64.74	0.0195	6.020-6			2U1207+39
3U1223-62	12 23 50 -62 33 16 185.96 -62.56	300.11 -0.10	12 23 46 -62 28 48 185.94 -62.48	12 23 36 -62 32 24 185.98 -62.54	12 23 55 -62 38 24 185.98 -62.64	12 24 5 -62 35 24 186.02 -62.59	0.0040	37	3	VERY FLAT SPECTRUM GX301+0 (9,10)	2U1223-62
3U1224+02	12 24 55 2 18 16 186.23 2.31	289.04 64.26	12 25 53 2 26 24 186.47 2.44	12 22 43 2 19 12 185.68 2.32	12 24 0 2 11 24 186.00 2.19	12 27 2 2 18 0 186.76 2.30	0.1400	6.220-50		1C273 (1050)	3C273 (11,2,11)
3U1228+12	12 28 5 12 42 0 187.02 12.70	283.56 74.51	12 28 34 12 45 0 187.14 12.75	12 27 36 12 45 0 186.90 12.75	12 27 36 12 39 36 186.90 12.66	12 28 34 12 39 36 187.14 12.66	0.0211	21.720-3		VIRGO CLUSTER M87 = VIR A	VIR XE-1 (11) M87 (2) (11) + 2U1228+12
3U1231+07	12 31 36 7 8 24 187.90 7.15	290.69 69.32	12 24 48 7 54 0 186.2 7.9	12 22 48 7 42 0 185.7 7.7	12 38 48 6 24 0 189.7 6.4	12 38 24 6 42 0 189.6 6.7	1.2000	6.721-4		1C3576 (112)	
3U1237-07	12 37 46 -7 12 0 189.44 -7.2	298.10 55.29	12 45 0 -6 30 0 191.25 -6.5	12 18 48 -8 6 0 186.7 -6.1	12 24 48 -8 12 0 186.2 -8.2	12 45 24 -7 0 0 191.35 -7.	2.8000	1.310-4		NGC4428+4433+4487 ?	
3U1247-61	12 47 19 -41 2 24 191.83 -41.04	302.60 21.56	12 48 41 -40 59 24 192.17 -40.99	12 46 0 -40 59 24 191.50 -40.99	12 46 0 -41 5 24 191.50 -41.09	12 46 41 -41 5 24 192.17 -41.04	0.0506	6.240-3		NGC4496 = PRS1245-41 (5) RICH CLUSTER IN SOUTHERN SKY	2U1247-61

ORIGINAL PAGE IS  
OF POOR QUALITY



TABLE 4A—Continued

(1)	(2A)	(2B)	(3A)	(3B)	(3C)	(3D)	(3E)	(4A)	(4B)	(5A)	(5B)
3U1252-28	12 52 29 -28 57 36 191.17 -28.56	303.91 33.63	12 53 31 -28 50 24 191.38 -28.86	12 49 41 -28 57 36 192.88 -28.96	12 51 31 -29 3 36 191.87 -29.06	12 55 17 -28 57 0 191.87 -28.95	0.1300	4.520.3			2U1253-20
3U1256-69	12 56 22 -69 1 17 191.59 -69.07	303.98 -6.43	12 54 17 -69 0 0 193.57 -69.00	12 54 5 -69 1 12 193.52 -69.02	12 54 26 -69 2 24 193.61 -69.04	12 54 38 -69 1 12 193.66 -69.02	0.0010	25.520.6			2U1256-69
3U1257-28	12 57 29 28 11 24 194.37 28.19	306.33 87.46	12 57 55 28 11 24 194.48 28.19	12 57 2 28 14 24 194.26 28.24	12 56 55 28 11 24 194.23 28.19	12 57 48 28 8 24 194.45 28.14	0.0110	14.820.3		COMA CLUSTER: ABELL 1656 COMA 1-1 (113) + 2U1257-28	
3U1258-61	12 58 3 -61 20 10 194.517 -61.336	306.08 1.74	12 58 5 -61 18 4 194.527 -61.301	12 57 51 61 17 56 194.463 -61.299	12 58 3 -61 22 44 194.517 -61.376	12 58 14 -61 22 34 194.558 -61.376	0.0020	47	5	VERY FLAT SPECTRUM GX304-1 (9.101) 2U1258-61	
3U1270-61	12 70 42 -61 43 33 200.175 -61.725	306.74 0.64	12 70 26 -61 24 0 200.11 -61.40	12 70 36 61 25 48 199.05 -61.43	12 71 0 -62 3 0 200.25 -62.05	12 72 36 61 57 0 200.65 -61.95	0.1400	5.221.6			
3U1327-42	13 22 12 -42 47 24 200.55 -42.79	309.45 19.39	13 22 16 -42 44 24 200.65 -42.74	13 21 50 -42 44 24 200.46 -42.74	13 21 50 -42 49 48 200.46 -42.83	13 22 36 -42 49 48 200.65 -42.83	0.0125	8.020.3		NGC 5128 = CEN 2 NGC 5128 (11) + 2U1327-42	
3U1340-24	13 49 12 24 27 0 207.30 24.45	24.08 76.16	14 0 48 25 45 0 210.2 25.75	13 39 36 25 45 0 204.9 25.75	13 40 24 25 6 0 205.1 23.10	14 0 24 23 6 0 210.1 23.10	12.0000	3.820.9			2U1340-24
3U1410-03	14 10 55 -3 3 16 212.73 -3.06	330.17 53.70	14 10 24 -2 49 48 212.60 -2.83	14 9 29 -3 0 0 212.37 -3.00	14 11 24 -3 16 48 212.85 -3.28	14 12 12 -3 7 48 213.05 -3.13	0.1400	3.520.5		NGC 5506, 5507 ? 2U1420-02	

ORIGINAL PAGE IS  
OF POOR QUALITY

TABLE 4A—Continued

(1)	(2)	(3)	(4)	(5)	(6)	(7)	(8)	(9)	(10)	(11)	(12)	(13)	(14)	(15)
201430-39	14 49 2 -19 1 48 219.76 -39.03	125.27 18.70	16 48 0 -38 28 12 217.6 -38.47	14 30 24 -38 28 12 217.6 -38.47	14 30 0 -19 48 24 217.5 -39.64	14 47 16 -19 38 24 221.9 -39.64	4.0000	3.120.4						201440-39
201443-43	14 43 2 43 2 24 220.76 43.04	74.66 67.16	14 44 26 43 11 24 220.39 43.19	14 41 34 42 54 0 220.39 42.90	14 41 34 42 54 0 220.39 42.90	14 44 26 42 54 0 221.11 42.90	0.1500	3.020.7						201443-43
201510-59	15 10 7 -59 0 0 227.53 -59.03	320.11 -1.21	15 10 46 -58 58 48 227.69 -58.98	15 9 36 -58 55 48 227.40 -58.93	15 9 36 -59 1 48 227.39 -59.03	15 10 36 -59 4 12 227.65 -59.07	0.0194	6.440.6						201509-58
201516-56	15 16 44 -56 59 2 229.187 -56.994	326.11 0.05	15 16 40 -56 58 23 229.168 -56.973	15 16 38 -56 58 59 229.160 -56.983	15 16 46 -56 59 38 229.193 -56.994	15 16 50 -56 59 2 229.209 -56.984	0.0002	720	220					201516-56
201538-52	15 38 14 -52 10 48 234.56 -52.18	327.40 2.24	15 38 46 -52 10 48 234.69 -52.18	15 37 55 -52 7 48 234.48 -52.13	15 37 41 -52 11 24 234.42 -52.19	15 38 34 -52 14 24 234.64 -52.24	0.0096	11.120.7						201536-52
201543-62	15 43 0 -62 24 36 235.75 -62.41	321.71 -0.29	15 43 31 -62 24 0 235.88 -62.40	15 42 43 -62 26 0 235.68 -62.40	15 42 26 -62 25 48 235.61 -62.43	15 43 17 -62 25 48 235.87 -62.43	0.0029	36	3					201542-62
201543-67	15 43 50 -47 33 36 235.96 -47.56	330.93 5.36	15 43 55 -47 34 48 235.98 -47.58	15 43 41 -47 31 41 235.92 -47.53	15 43 48 -47 32 24 235.95 -47.54	15 44 2 -47 35 24 236.01 -47.59	0.0006	2000	2100					201543-67
201544-75	15 44 0 -75 45 0 236.00 -75.75	313.24 -16.75	15 47 16 -75 37 48 236.70 -75.63	15 42 48 -75 38 88 235.70 -75.63	15 40 12 -75 52 12 235.05 -75.87	15 45 36 -75 52 12 236.40 -75.87	0.0753	3.150.3						201544-75

ORIGINAL PAGE 1,  
OF POOR QUALITY

TABLE 4A--Continued

(1)	(2A)	(2B)	(3A)	(3B)	(3C)	(3D)	(3E)	(4A)	(4B)	(5A)	(5B)
3U1551-15	15 51 36 15 54 0 232.9 15.9	27.50 46.30	16 6 0 19 0 0 241.5 19.0	15 40 48 15 6 0 239.2 15.1	15 45 12 13 24 0 236.3 13.4	16 10 24 16 54 0 242.6 16.9	15.0000	2.1x0.5		HERCULES CLUSTER: ABELL 2147-2151-2152 (5) ARP 71-122-172-272-324 ? HARKNAN 298-299-300 ?	
3U1555-27	15 55 29 27 12 0 233.872 27.20	43.92 48.82	15 58 0 27 32 24 239.5 27.54	15 52 38 27 6 36 238.16 27.11	15 52 48 26 51 0 238.20 26.85	15 58 19 27 16 48 239.58 27.28	0.3400	5.1x0.7		STAR: 13 e CRB ?	
3U1556-60	15 56 54 -60 37 68 239.227 -60.63	324.13 -5.97	15 57 38 -60 36 0 239.407 -60.60	15 56 12 -60 36 0 239.052 -60.60	15 56 12 -60 39 36 239.052 -60.66	15 57 38 -60 39 36 239.407 -60.66	0.0105	17.0x0.9		NOR XR-2 (1,2) ? NOR 2 (3) ?	
3U1617-15	16 17 7 -15 32 13 244.278 -15.537	359.09 23.77	16 17 4 -15 30 47 244.266 -15.513	16 16 55 -15 31 48 244.231 -15.530	16 17 7 -15 33 36 244.280 -15.560	16 17 18 -15 32 35 244.325 -15.543	0.0021	17.0000	2.5	STAR: SCO X-1 AT G = 16h 17m 04s.3 B = -15° 31' 13"	2U1556-60 SCO X-1 (1,2) SCO 1 (3) + 2U1617-15
3U1623-05	16 23 12 5 24 0 245.80 5.4	19.74 34.84	16 8 19 7 24 3 242.08 7.4	16 8 7 5 48 0 242.03 5.8	16 38 7 3 24 0 249.53 3.4	16 38 43 4 54 0 249.68 4.9	12.0000	2.6x0.4			
3U1626-49	16 24 19 -49 5 24 246.08 -49.09	334.92 -0.27	16 24 7 -49 3 36 246.03 -49.06	16 24 7 -49 4 48 246.03 -49.08	16 24 29 -49 7 48 246.17 -49.13	16 24 34 -49 6 0 246.14 -49.10	0.0020	50	5	NOR XR-1 (1,2) ? NOR 1 (3) ?	2U1626-49
3U1626-67	16 26 41 -67 21 43 246.672 -67.362	321.75 -13.06	16 27 1 -67 18 25 246.755 -67.307	16 25 53 -67 22 5 246.670 -67.168	16 26 22 -67 25 54 246.590 -67.415	16 27 30 -67 21 18 246.875 -67.355	0.0080	10.2x0.4			
3U1630-47	16 30 11 -47 16 23 247.944 -47.273	336.90 0.28	16 30 2 -47 14 53 247.510 -47.248	16 30 1 -47 15 50 247.505 -47.264	16 30 20 -47 18 7 247.585 -47.302	16 30 20 -47 16 52 247.585 -47.281	0.0311	150	3	NOR XR-1 (1,2) ? NOR 1 (3) ?	2U1630-47

ORIGINAL PAGE  
OF POOR QUALITY

TABLE 4A—Continued

(1)	(2A)	(2B)	(3A)	(3B)	(3C)	(3D)	(3E)	(4A)	(4B)	(5A)	(5B)
3U1632-64	16 32 48 -64 8 24 248.20 -64.14	374.63 -11.3F	16 13 29 -63 39 36 248.37 -63.66	16 30 50 -64 19 12 247.71 -64.12	16 32 7 -64 38 24 248.03 -64.64	16 36 46 -63 58 48 248.69 -63.78	0.1830	11.021.1			2U1639-62
3U1636-53	16 36 54 -53 38 6 249.226 -53.651	332.91 -6.81	16 36 54 -53 38 28 249.225 -53.641	16 36 46 -53 38 38 249.183 -53.644	16 36 54 -53 39 47 249.225 -53.663	16 37 4 -53 39 32 249.260 -53.659	0.3005	261.3			2U1637-53
3U1639+40	16 39 22 40 13 55 249.84 40.232	63.86 41.34	16 46 24 41 12 0 251.0 41.20	16 32 0 41 12 0 248.0 41.20	16 32 0 39 16 48 248.0 39.28	16 46 24 19 16 48 251.6 19.28	2.3000	4.020.6		CLUSTER: ABELL 2197 ? (5) 3C345 1050: OPTICAL VAR. BY 2 <sup>m</sup> (15) ?	
3U1642-45	16 42 6 -45 31 30 250.526 -45.525	339.58 -0.08	16 42 4 -45 30 32 250.515 -45.509	16 41 56 -45 30 54 250.465 -45.515	16 42 9 -45 32 31 250.536 -45.542	16 42 17 -45 42 13 250.570 -45.537	0.0008	381	3	GX340+0 (16) ARA 1 (3) ? (L3.GX340-2) (1) ?	2U1641-45
3U1645+21	16 45 14 21 32 24 251.31 21.54	40.56 36.41	16 13 19 22 31 48 248.33 22.53	16 32 31 22 16 12 248.13 22.27	16 52 31 21 3 0 253.13 21.05	16 53 19 21 9 0 253.33 21.15	1.1000	6.111.8			
3U1653+35	16 53 12 35 16 0 253.30 35.6	58.26 38.12	17 6 14 34 58 12 256.56 34.97	16 48 19 35 58 12 252.08 35.97	16 46 46 35 51 0 251.69 35.85	17 4 38 34 51 36 256.16 34.86	0.7400	100	26	STAR: MZ HER AT α = 16 <sup>h</sup> 56 <sup>m</sup> 02 <sup>s</sup> δ = +35° 25' 03"	2U1705+34
3U1658-48	16 58 58 -48 43 37 256.74 -48.727	338.93 -4.32	16 59 10 -48 43 1 256.69 -48.717	16 58 46 -48 43 1 256.69 -48.717	16 58 46 -48 44 17 256.69 -48.738	16 59 10 -48 44 17 256.79 -48.738	0.0013	344	3	GX339-4 (17)	
3U1700-37	17 0 26 -37 46 12 255.110 -37.77	347.75 2.19	17 0 51 -37 48 0 255.213 -37.80	17 0 51 -37 46 24 255.213 -37.74	17 0 6 -37 44 24 255.025 -37.74	17 0 6 -37 48 0 255.025 -37.80	0.0089	102	23	STAR: HD153919 AT α = 17 <sup>h</sup> 00 <sup>m</sup> 32 <sup>s</sup> .7 δ = -37° 46' 27"	2U1700-37

ORIGINAL PHOTO  
OF POOR QUALITY

TABLE 4A—Continued

(1)	(2A)	(2B)	(3A)	(3B)	(3C)	(3D)	(3E)	(4A)	(5A)	(5B)
3U1702-36	17 2 19 -36 21 36 255.58 -36.36	349.59 2.76	17 2 14 -36 20 24 255.56 -35.34	17 2 10 -36 21 0 255.54 -36.35	17 2 24 -36 22 12 255.60 -36.37	17 2 29 -36 21 36 255.62 -36.36	0.0008	715		GX49+2 (2) 15CO XR-2+L6,GK-10.71 (1,2) SCO 2 (3) 2U1702-36
3U1702-42	17 2 19 -42 58.48 255.58 -42.98	343.84 -1.27	17 2 55 -42 57 36 255.73 -42.96	17 1 58 -42 55 48 255.49 -42.93	17 1 46 -43 0 36 255.44 -43.01	17 2 41 -43 3 0 255.67 -43.05	0.0160	34.027.6		ARA XR-1 (1) ? GX-16.1 (2) ? 2U1704-42
3U1704-32	17 4 31 -32 6 36 256.13 -32.11	352.76 4.96	17 3 34 -31 55 12 255.89 -31.92	17 3 5 -31 57 36 255.77 -31.96	17 5 14 -32 17 24 256.31 -32.29	17 5 58 -32 16 12 256.49 -32.27	0.0577	14.021.2		LB (1) ? 2U1701-31
3U1705-44	17 5 24 -44 5 0 256.349 -44.05	343.32 -2.36	17 5 17 -44 1 48 256.319 -44.03	17 5 15 -44 2 24 256.313 -44.06	17 5 29 -44 4 12 256.373 -44.07	17 5 31 -44 3 0 256.380 -44.05	0.0008	280		2U1705-44
3U1706+32	17 6 24 32 6 0 256.6 32.1	54.64 34.76	16 57 12 34 12 0 253.3 34.2	16 56 42 32 26 0 253.7 32.4	17 19 12 29 54 0 259.8 29.9	17 22 24 31 12 0 260.6 31.2	9.8000	4.110.6		
3U1706+70	17 6 48 78 32 24 256.70 78.56	110.82 31.81	17 5 48 78 44 24 256.45 78.74	17 4 19 78 30 0 256.08 78.50	17 7 40 79 19 12 256.95 78.32	17 9 7 78 34 12 257.28 78.57	0.0536	3.240.3	CLUSTER: ABELL 2256 (5)	2U1706+70
3U1709-23	17 9 26 -23 21 36 257.36 -23.36	0.53 9.24	17 9 48 -23 22 48 257.45 -23.38	17 9 22 -23 19 12 257.34 -23.32	17 9 2 -23 21 36 257.26 -23.36	17 9 31 -23 24 36 257.38 -23.41	0.0076	39		OPH XR-2 (1) BPH 2 (3) 2U1705-22
3U1710-39	17 14 55 -39 10 0 250.73 -39.30	348.21 -0.99	17 15 55 -39 10 48 250.98 -39.18	17 13 55 -39 12 0 250.48 -39.20	17 13 55 -39 25 12 250.48 -39.42	17 15 55 -39 23 24 250.98 -39.39	0.0832	11.642.2		(SCO XR-2+L6,GK-10.71 (1) ? (SCO XR-51 (1) ? (SCO 2,SCO 5) (3) ? 2U1710-39

ORIGINAL PAGE IS  
OF POOR QUALITY

TABLE 4A—Continued

(1)	(2)	(3)	(4)	(5)	(6)	(7)	(8)	(9)	(10)	(11)	(12)	(13)	(14)	(15)	(16)
3U1727-33	17 27 22 -33 42 0 261.86 -33.70	354.24 0.13	17 27 53 -33 44 26 261.97 -33.74	17 26 58 -33 37 12 261.70 -33.62	17 26 40 -33 30 26 261.93 -33.76	17 27 43 -33 45 36 261.93 -33.76	0.0078	65	10						GR354-0 (16) IM4,GR354-53 (1) GR-5.6 (1,2) 2U1726-
3U1728-24	17 28 50 -26 49 1 262.207 -26.717	1.91 4.82	17 29 1 -26 41 53 262.255 -24.698	17 28 41 -26 41 53 262.172 -24.698	17 28 38 -24 43 59 262.158 -24.733	17 28 59 -24 43 59 262.248 -24.733	0.0027	60.342.4							GR144 (10,19) SGR 6 (3) 7 CX2+5 (20) 2U1728-24
3U1728-16	17 28 50 -16 50 53 262.208 -16.948	8.49 9.03	17 28 48 -16 56 10 262.202 -16.936	17 28 44 -16 56 38 262.195 -16.944	17 28 52 -16 57 36 262.216 -16.960	17 28 56 -16 57 36 262.234 -16.952	0.0005	260	1.7						GR49+9 (1,2) NPH 3 (3) 2U1728-16
3U1735-44	17 35 12 -44 25 12 263.80 -44.42	346.04 -0.97	17 35 5 -44 26 0 263.77 -44.40	17 34 55 -44 25 12 263.73 -44.42	17 35 17 -44 26 24 263.82 -44.44	17 35 26 -44 25 12 263.86 -44.42	0.0019	210.6							2U1658-46
3U1735-70	17 35 24 -28 27 0 263.85 -28.45	359.57 1.56	17 35 36 -28 18 0 263.90 -28.30	17 34 48 -28 27 0 263.70 -28.45	17 35 12 -28 36 0 263.80 -28.60	17 36 0 -28 27 0 264.00 -28.45	0.0396	565	210						2U1735-28 +
3U1736-43	17 36 74 43 3 0 264.10 43.05	68.83 31.08	17 41 24 44 8 24 265.35 44.14	17 37 50 42 10 48 261.96 42.18	17 30 53 41 51 36 262.72 41.86	17 44 12 43 49 48 266.04 43.83	1.8000	10.827.4							GLIMULAR CLUSTER: M92 = GC0341 ? 2U1735-43
3U1743-79	17 43 36 -29 7 48 265.5 -29.13	359.95 -0.33	17 45 12 -29 6 0 266.3 -29.1	17 43 12 -29 6 0 265.8 -29.0	17 42 24 -29 6 0 265.6 -29.1	17 43 36 -29 18 0 265.9 -29.3	0.0917	40.5							GR54-4551 ? ISNR1742-20, SNR1741-74 ? SGR 1 (3) 7 (11,13,14) (1) 7 2U1743-29 +
3U1744-26	17 44 44 -26 33 43 266.185 -26.567	2.27 0.80	17 44 42 -26 32 53 266.176 -26.548	17 44 38 -26 33 29 266.157 -26.558	17 44 46 -26 34 36 266.193 -26.576	17 44 51 -26 33 58 266.214 -26.566	0.0007	460							GR3+16GR+2.6+114, SGR 44-1 (1) GR3+1 (1,10) SGR 6 (3) 2U1744-26

ORIGINAL PAGE IS  
OF POOR QUALITY

TABLE 4A--Continued

(1)	(2A)	(2B)	(3A)	(3B)	(3C)	(3D)	(3E)	(4A)	(4B)	(5A)	(5B)
3U1746-37	17 46 48 -37 0 36 266.7 -37.01	353.55 -4.99	17 47 48 -36 56 49 266.95 -36.947	17 47 0 -36 56 49 266.95 -36.947	17 45 55 -37 3 54 266.48 -37.065	17 46 41 -37 3 54 266.67 -37.065	0.0184	30.781-8		GLOBAL CLUSTER: NGC6441 ?	
3U1755-33	17 55 34 -33 48 0 268.69 -33.80	357.24 -6.91	17 55 19 -33 43 48 268.03 -33.73	17 54 58 -33 46 12 268.16 -33.77	17 55 48 -33 52 12 268.95 -33.87	17 56 10 -33 49 48 269.04 -33.83	0.0144	47	3	GX-2.5 (1,2) SCO XR-6 (1)	
3U1758-25	17 58 7 -25 4 40 269.53 -25.08	5.08 -8.03	17 58 7 -25 4 12 269.53 -25.07	17 58 0 -25 4 48 269.50 -25.08	17 58 7 -25 6 0 269.53 -25.10	17 58 14 -25 5 24 269.56 -25.09	0.0008	1127	2	GX5-1.0 (GX+5.2, L27, SGR XR-3) (1) GX5-1 (2,10) SGR 5 (3)	2U1757-33
3U1758-2C	17 58 34 -20 32 13 269.643 -20.537	9.07 1.15	17 58 34 -20 31 37 269.640 -20.527	17 58 29 -20 32 6 269.623 -20.535	17 58 35 -20 32 49 269.646 -20.547	17 58 39 -20 32 20 269.664 -20.539	0.0004	595	2	GX9+1.0 (GX+9.1, L18, L19, M3) (1) SGR 3 (3) G9+1 (2)	
3U1809+50	18 9 24 50 19 48 277.35 50.33	78.18 26.85	18 5 22 50 49 12 271.34 50.82	18 4 19 50 37 12 271.08 50.62	18 13 31 50 52 48 273.38 49.88	18 14 34 50 2 24 273.64 50.04	0.3900	5,110.3			2U1808+50
3U1811-17	18 11 42 -17 11 6 272.927 -17.185	13.52 0.08	18 11 42 -17 10 26 272.925 -17.174	18 11 36 -17 10 52 272.902 -17.181	18 11 43 -17 11 38 272.928 -17.194	18 11 48 -17 11 17 272.952 -17.188	0.0005	380	3	GX13.5+5.120, SGR XR-2 (1) GX13+1 (1,2) SGR 2 (3)	
3U1812-12	18 12 5 -12 6 36 273.02 -12.11	18.01 2.45	18 11 38 -11 59 24 272.91 -11.99	18 11 17 -12 3 0 272.82 -12.05	18 12 31 -12 14 24 273.13 -12.24	18 12 55 -12 10 12 273.23 -12.17	0.0372	12,111.2		SFR XR-2 (1) ?	
3U1813-14	18 13 10 -14 3 36 273.29 -14.06	16.42 1.28	18 13 17 -14 3 36 273.32 -14.06	18 13 7 -14 2 24 273.28 -14.04	18 13 2 -14 3 36 273.26 -14.06	18 13 14 -14 3 36 273.31 -14.07	0.0009	583	1-5	GX17+2.0 (GX+16.7) (1,2) L21, SFR XR-2 (1) ? SGR 2 (3) + 2U1813-14	

ORIGINAL PAGE 1.  
OF POOR QUALITY

TABLE 4A - Continued

(11)	(12A)	(12B)	(13A)	(13B)	(13C)	(13D)	(13E)	(14A)	(14B)	(15A)	(15B)
3U1820-30	18 20 26 -30 23 20 275.107 -30.389	2.78 -7.91	18 20 31 -30 22 52 275.129 -30.381	18 20 20 -30 22 52 275.084 -30.398	18 20 20 -30 23 53 275.129 -30.398	18 20 31 -30 23 53 275.129 -30.398	0.0006	250	1.5	ULINULAR CLUSTER: NGC6624 ?	SGR KR-4 (11) SGR 4 (13)  2U1820-30
3U1822-37	18 22 14 -37 11 24 275.56 -37.19	356.79 -11.79	18 21 55 -37 11 40 275.48 -37.13	18 21 14 -37 10 40 275.31 -37.10	18 22 36 -37 15 0 275.65 -37.25	18 23 17 -37 12 0 275.82 -37.20	0.0231	36.421.4			SGR 7 (13) SGR KR-6 (11) ?  2U1822-37
3U1822-0C	18 22 52 -0 2 10 275.716 -0.016	29.95 5.78	18 22 41 -0 0 50 275.67 0.014	18 22 26 -0 0 50 275.61 -0.014	18 23 2 -0 5 13 275.76 -0.087	18 23 17 -0 5 29 275.82 -0.058	0.0086	36.651.7			2U1822-00
3U1825-01	18 25 16 21 18 0 276.40 01.30	113.19 27.94	18 17 36 87 30 0 274.4 87.50	18 9 36 87 20 24 272.4 82.34	18 35 12 19 55 12 278.8 19.97	18 35 12 80 55 12 270.8 80.97	0.6900	2.750.3	3C390.3 (IN GALAXY) ?		2U1828-01
3U1837-23	18 37 0 -23 13 12 278.00 -23.22	10.41 -3.95	18 31 46 -23 7 40 277.94 -23.13	18 30 50 -23 11 24 277.71 -23.19	18 32 12 -23 19 40 278.05 -23.33	18 35 12 -23 16 12 278.80 -23.27	0.0960	6.940.9			
3U1837-05	18 32 10 -5 18 0 278.04 -5.30	76.36 1.78	18 30 14 -4 58 48 277.56 -4.98	18 30 24 -5 11 12 277.60 -5.22	18 34 24 -5 35 24 278.50 -5.59	18 34 0 -5 24 0 278.50 -5.40	0.1800	6.181.0			2U1833-05
3U1837-04	18 37 19 4 59 24 279.33 4.54	36.10 6.88	18 37 26 4 59 24 279.36 4.99	18 37 14 5 0 36 279.31 5.01	18 37 12 4 59 24 279.30 4.99	18 37 26 4 58 12 279.36 4.97	0.0012	270		102+36.3, SER KR-10 (11) ? SER KR-1 (12), SER 1 (13)	2U1836-05
3U1843-67	18 43 26 67 30 0 280.86 67.53	97.88 75.68	19 18 29 65 4 48 289.62 65.38	18 44 34 67 4 24 281.14 67.74	18 41 31 67 19 12 280.30 67.32	19 16 14 64 39 36 289.06 64.66	2.1000	3.520.4			2U1843-67

ORIGINAL PAGE IS  
OF POOR QUALITY



TABLE 4A--Continued

(1)	(2A)	(2B)	(3A)	(3B)	(3C)	(3D)	(3E)	(4A)	(4B)	(5A)	(5D)
3U1849-77	18 49 J -77 6 0 282.25 -77.13	317.47 -26.65	18 50 12 -76 36 0 281.03 -76.6	18 46 31 -77 0 0 281.03 -77.0	18 47 31 -77 36 0 281.08 -77.6	18 51 12 -77 12 0 282.80 -77.2	0.1500	3.0±0.5			2U1849-77
3U1901+03	19 1 41 3 1 12 285.42 3.02	37.14 -1.42	19 0 19 3 13 48 285.08 3.23	19 0 19 3 13 48 285.08 3.18	19 2 46 2 49 48 285.69 2.83	19 2 46 2 53 24 285.69 2.89	0.0335	87	4		2U1907+02
3U1904+07	19 4 48 67 0 J 286.2 67.0	97.83 23.56	19 2 0 67 18 0 285.5 67.3	19 0 0 67 0 0 285.0 67.0	19 33 36 64 48 0 293.4 64.8	19 20 0 66 12 0 290.0 66.2	1.1300	5±1			2U2012+62
3U1906+09	19 6 24 9 43 12 286.6 9.72	43.62 0.65	19 5 12 10 1 48 286.3 13.03	19 4 0 9 56 24 286.0 9.94	19 8 0 9 24 0 287.0 9.40	19 8 48 9 30 0 287.2 9.50	0.2200	7.4±1.4			
3U1908+00	19 8 7 0 31 12 287.03 0.52	35.67 -4.00	19 7 50 0 32 24 286.96 0.54	19 7 50 0 31 48 286.96 0.53	19 8 22 0 29 24 287.09 0.49	19 8 29 0 30 0 287.12 0.50	0.0020	199	3		AOL HR-1 (11) AOL 1 (13) 2U1908+00
3U1912+07	19 12 16 7 42 0 289.15 7.7	42.55 -1.65	19 17 17 7 57 0 289.37 7.95	19 18 55 7 57 0 289.73 7.95	19 8 0 7 27 0 287.0 7.45	19 18 48 7 27 0 289.7 7.45	0.7700	21.5±1.0			
3U1915-05	19 15 36 -5 16 49 288.90 -5.28	31.34 -8.32	19 14 2 -5 7 48 288.51 -5.13	19 13 43 -5 14 24 288.43 -5.24	19 17 34 -5 25 12 289.39 -5.42	19 17 53 -5 19 12 289.47 -5.32	0.1200	23	5?	STAR: 26 f AOL ?	2U1912-05
3U1921+43	19 21 41 43 23 48 290.42 43.48	75.54 13.01	19 23 50 43 24 36 290.96 43.41	19 21 2 43 45 0 290.26 43.75	19 19 29 43 33 36 289.87 43.56	19 22 17 43 12 36 290.57 43.21	0.2000	6.3±0.6		CLUSTER: ABELL 2319 ? (5)	2U1926+43

ORIGINAL PAGE IS  
OF POOR QUALITY

TABLE 4A--Continued

(11)	(12A)	(12B)	(13A)	(13B)	(13C)	(13D)	(13E)	(14A)	(14B)	(15A)	(15B)
3U1953+31	19 53 55 31 56 26 298.48 31.54	68.19 1.98	19 54 0 31 59 24 298.50 31.99	19 53 17 31 58 48 298.32 31.98	19 53 55 31 54 0 298.48 31.90	19 54 34 31 56 36 298.64 31.91	0.0127	63	5		2U1954+31
3U1956+65	19 56 0 65 0 0 299.0 65.0	91.92 18.20	19 54 0 68 36 0 291.0 68.5	19 53 17 31 58 48 298.32 31.98	19 53 55 31 54 0 298.48 31.90	19 54 34 31 56 36 298.64 31.91	2.8000	4.120.4			2U2006+59
3U1956+35	19 56 22 35 3 35 299.022 35.360	71.12 3.08	19 56 30 35 3 53 299.124 35.066	19 56 19 35 3 14 299.078 35.086	19 56 15 35 3 14 299.066 35.054	19 56 26 35 2 2 299.129 35.034	J.3313	1175	5	STAD: MNE276868 AT Q = 198 56M 288.843 B = +15° 03' 56" = 51	CYG K-1 (1.2) CYG L (13) + 2U1956+35
3U1956+11	19 56 48 11 36 0 295.2 11.6	51.30 -9.27	19 56 55 11 42 36 299.23 11.71	19 56 0 11 40 48 299.00 11.68	19 56 43 11 30 0 299.18 11.50	19 57 41 11 31 48 299.42 11.53	3.3669	12.4+5.5			
3U1957+40	19 57 12 40 36 0 299.33 40.63	76.14 5.85	19 55 41 40 36 24 293.95 40.44	19 55 2 40 40 12 298.16 40.57	19 58 38 41 14 24 299.66 40.24	19 59 7 40 31 48 299.78 40.53	J.2300	5.651.7		CY. A = 30405 (5)	2U1957+40
3U1959+89	19 59 16 -64 42 0 297.90 -64.70	325.86 -31.67	19 55 36 -68 27 0 293.9 -64.45	19 53 56 -69 3 0 298.4 -69.00	20 3 12 -73 57 9 300.8 -70.95	20 7 12 -70 45 0 301.8 -70.75	J.8700	2.342.4			2U1954+68
3U2010+40	20 13 13 43 47 6 307.639 40.745	79.34 3.71	20 30 11 40 48 27 307.636 40.805	20 30 27 40 47 38 307.613 40.794	20 30 35 40 45 50 307.645 40.764	20 30 40 40 46 34 307.666 40.776	J.3308	194	23		CYG K-3 (1.2) CYG L (13) + 2U2011+40
3U2041+75	20 41 55 75 25 12 313.48 75.47	109.36 19.48	20 31 36 77 6 0 307.3 77.1	20 23 48 76 2 0 307.2 76.7	20 50 0 73 54 0 312.5 73.9	20 54 0 74 24 0 313.5 74.4	1.2300	3.423.7			2U2041+75

ORIGINAL PAGE:  
OF POOR QUALITY

TABLE 4A—Continued

(1)	(2A)	(2B)	(3A)	(3B)	(3C)	(3D)	(3E)	(4A)	(5A)	(5B)
302052+97	20 52 24 47 55 12 313.1 472.97	87.85 2.09	21 5 12 48 48 0 316.3 48.8	20 54 0 48 48 0 313.5 48.9	20 40 48 47 0 0 310.2 47.0	20 50 24 47 0 0 312.6 47.0	3.1000	6.270.5		
302128+81	21 28 48 01 16 0 322.20 81.6	116.07 21.84	22 42 0 07 48 0 340.5 87.8	21 44 0 07 18 0 340.5 82.3	22 48 0 00 54 0 312.0 80.9	20 34 0 79 54 0 308.5 74.9	1.1000	1.590.3		202128+81
302129+87	21 29 58 47 1 48 322.49 47.01	91.60 -3.11	21 29 52 47 7 12 322.47 47.12	21 29 0 47 6 48 322.25 47.08	21 30 10 46 56 24 322.54 46.94	21 30 53 47 0 0 322.72 47.00	0.0269	11.600.5		202130+47
302131+11	21 31 12 11 49 12 322.8 11.02	65.55 -28.08	21 25 12 12 6 0 321.3 12.10	21 21 36 11 49 36 320.4 11.81	21 36 48 11 33 0 326.2 11.55	21 41 36 11 49 12 325.4 11.02	1.4300	4.190.4	GLIMPSE CLUSTER: M15 = NGC 7078 ?	
302142+30	21 42 35 30 5 13 325.64 38.07	87.32 -11.37	21 42 41 30 5 35 325.609 38.093	21 42 33 30 5 35 325.636 38.092	21 42 30 30 4 55 325.624 38.387	21 42 39 30 6 55 325.662 38.087	0.0001	540	STAR: CYG X-2 AT g 21h 42m 36s.91 b 38° 05' 27".9 + 202142+36	
302208+54	22 8 16 54 29 24 332.15 54.49	101.37 -1.14	22 9 3 54 42 36 332.25 54.71	22 7 2 54 28 12 331.76 54.47	22 8 10 54 15 36 332.04 54.26	22 10 14 54 30 36 332.56 54.51	0.1000	4.490.8		202208+54
302231+59	22 31 0 59 33 0 338.25 55.55	106.53 1.36	22 42 24 60 6 0 340.6 60.1	22 22 24 60 6 0 335.6 62.1	22 27 24 59 0 0 335.6 59.0	22 42 24 59 0 0 340.6 59.0	2.0000	4.791.4		
302321+58	23 21 13 58 33 23 350.131 52.526	111.75 -2.12	23 21 13 58 34 26 350.305 58.574	23 21 6 58 31 0 350.276 58.550	23 21 13 58 32 35 350.303 58.541	23 21 20 58 33 53 350.332 58.566	0.0004	5.541.0	(AS A = 3C 461)	(AS A (1.21) (AS A (3)
302346+26	23 46 1 26 13 3 356.53 26.53	105.49 -14.02	23 56 24 27 24 7 359.1 27.4	23 49 0 27 24 0 355.0 27.4	23 40 0 26 0 0 355.0 26.0	23 56 24 25 0 0 359.1 25.0	2.0000	7.041.2	(CLUSTER: ABELL 2634 ? ABELL 2634 ?	202321+58

TABLE 4B  
CATALOGS AND LISTS OF INTERESTING OBJECTS

1. Abell 1958	7. Kraus 1966
2. Arp 1966a	8. Markarian 1967, 1969a, b
3. Arp 1966b	9. Milne 1970
4. Becvar 1962	10. Terzian 1973
5. Bennett 1962	11. de Vaucouleurs and de Vaucouleurs 1964
6. Downes 1971	12. de Veny, Osborn, and Hanes 1972

variability, and a "counterparts" comment. The counterparts comment results from searching standard compilations of interesting objects which are listed following the table. Counterparts followed by a question mark (?) indicate either tentative identification or that the object is in or near the error region of the X-ray source. Counterparts with no question mark indicate more certain identification based upon particular properties of either the X-ray source or the counterpart object. We also have searched some of the previous X-ray literature, and under the "previous X-ray" comment we list back-references for the X-ray sources. This is intended to be not a complete literature survey but rather an aid in correlating the *Uhuru*

results with other observations. Again, comments with a question mark indicate possible correspondence. The numbers in parentheses following a comment refer to the list of references which follows the table.

f) For several sources which have been studied in detail we include a more detailed comment than allowed for in the catalog format. The table of annotations (table 5) follows the catalog. Sources for which there are annotations are indicated by a dagger (†) in the "previous X-ray" comment.

We would like to thank J. Fontes for her assistance in computer programming and data processing. We also appreciate the cooperation of the Information Processing Division of the Goddard Space Flight Center for their assistance in processing the bulk of our data.

We would also like to acknowledge the contributions of W. Liller, W. Forman, and C. Jones of the Harvard College Observatory with whom we have had several discussions regarding source identification.

This work was supported by NASA contract NAS5-11422.

TABLE 5

3U 0115-73.....	In SMC. Eclipsing binary, period 34895 ± 04045. Flat spectrum with 1.5-2.5 keV variable cutoff. Optical identification with Sanduleak star 160. <sup>1,2,3</sup>
3U 0316-41.....	Perseus cluster. Centered on NGC 1275 ~ 0.7 extent, implying an X-ray diameter of ~ 750 kpc. <sup>4,5</sup>
3U 0531+21.....	Time-averaged pulsed flux is about one-twelfth of the total X-ray flux. <sup>6</sup>
3U 0833-45.....	Centered on pulsar PSR 0833-45 and emitting pulsed X-radiation. <sup>7,8</sup>
3U 0900-40.....	Eclipsing binary, period 8495 ± 0401. Irregular variability on the time scale of hours. Flat spectrum with 2.2-4.4 keV cutoff. Optical identification with HD 77581. <sup>9,10,11,12</sup>
3U 1118-60.....	Cen X-3. Eclipsing binary, period 2908707. Pulsating with period 4.84239 s. Extended low states. <sup>13</sup>
3U 1228+12.....	Virgo cluster. Centered on M87. ~ 0.7 extent, implying an X-ray diameter of ~ 200 kpc. <sup>5,14</sup>
3U 1257+28.....	Coma cluster; ~ 0.6 extent, implying an X-ray diameter of ~ 1050 kpc. <sup>4,5</sup>
3U 1322-42.....	NGC 5128. Emission associated with unusual radio galaxy. Spectrum cutoff at 3.4 keV. <sup>15</sup>
3U 1543-47.....	Transient source first observed in 1971 August at 2000 counts s <sup>-1</sup> . Intensity in 1973 February about 20 counts s <sup>-1</sup> . Steep spectrum, no observed cutoff. <sup>16</sup>
3U 1617-15.....	Sco X-1. Variability on time scale of minutes and hours. Optical identification with 13th-mag irregular variable blue star. Correlated X-ray-optical variability. <sup>17,18</sup>
3U 1653+35.....	Her X-1. Pulsating, eclipsing binary, period 14700165. Pulsation period 1.2378 s. Long time variations with time scale of about 35 <sup>19</sup> . Optical identification with HZ Herculis. <sup>19,20,21</sup>
3U 1700-37.....	Eclipsing binary, period 344. Variability on time scale of minutes. Spectrum flat, cutoff 2.1-5.5 keV. Optical identification with O7f star HD 153919. <sup>22</sup>
3U 1735-28.....	GX 359+2. Transient source observed for one week during 1971 March. Not seen in April with an upper limit of 50 counts s <sup>-1</sup> . <sup>23</sup>
3U 1743-29.....	GCX. Extended source in the direction of the galactic center, ~ 2° extent. Location and size consistent with infrared and radio sources. Low-energy cutoff 2.7 keV. <sup>23,24</sup>
3U 1813-14.....	GX 17+2. Exponential spectrum with 2.0 keV cutoff. Coincides with weak variable radio source. <sup>25</sup>
3U 1956+35.....	Cyg X-1. Quasi-periodic fluctuation on the order of 0.1 s. Coincides with weak, variable radio source. Optical identification with HDE 226868, binary with 546 period. No X-ray modulation detected on this time scale. <sup>26,27,28,29</sup>
3U 2030+40.....	Cyg X-3. X-ray intensity not correlated with large radio flares. Intensity exhibits a 4h8 ± 0h02 periodicity. <sup>30,31</sup>
3U 2142+38.....	Cyg X-2. No X-ray optical correlations yet observed. Both intensities vary by a factor of ~ 2 on time scales of minutes. Optical identification with 14th-mag irregular variable star. <sup>32,33</sup>

REFERENCES TO TABLE 5.—(1) Leong *et al.* 1971; (2) Schreier *et al.* 1972a; (3) Liller 1972; (4) Forman *et al.* 1972b; (5) Kellogg *et al.* 1973a; (6) Bradt *et al.* 1969; (7) Kellogg *et al.* 1973b; (8) Harnden and Gorenstein 1973; (9) Forman *et al.* 1973; (10) Brucato and Kristian 1973; (11) Hiltner *et al.* 1972; (12) Ulmer *et al.* 1972; (13) Schreier *et al.* 1972b; (14) Gursky *et al.* 1972; (15) Tucker *et al.* 1973; (16) Matilsky *et al.* 1972; (17) Forman *et al.* 1971; (18) Sandage *et al.* 1966; (19) Giacconi *et al.* 1973; (20) Bahcall and Bahcall 1972; (21) Forman *et al.* 1972a; (22) Jones *et al.* 1973; (23) Kellogg *et al.* 1971b; (24) Hoffman *et al.* 1971; (25) Tananbaum *et al.* 1971a; (26) Tananbaum *et al.* 1972; (27) Hjellming and Wade 1971; (28) Webster and Murdin 1972; (29) Bolton 1972; (30) Hjellming *et al.* 1972; (31) Parsignault *et al.* 1972; (32) Tananbaum *et al.* 1971b; (33) Giacconi *et al.* 1967.

## REFERENCES

- Abell, G. O. 1958, *Ap. J. Suppl.*, No. 31, 3, 211.
- Arp, H. 1966a, *Atlas of Peculiar Galaxies* (Pasadena: California Institute of Technology).
- . 1966b, in *Galactic Structure*, ed. A. Blaauw and M. Schmidt (Chicago: University of Chicago Press).
- Bahcall, J. N., and Bahcall, N. A. 1972, *Ap. J. (Letters)*, **178**, L1.
- Becvar, A. 1962, *Atlas Coeli 1950.0* (Cambridge, Mass.: Sky Publishing Corp.).
- Bennett, A. S. 1962, *Mem. R.A.S.*, **68**, 163–172.
- Bolton, C. T. 1972, *Nature*, **235**, 271.
- Bradt, H., Burnett, B., Mayer, W., Rappaport, S., and Schnopper, H. 1971, *Nature*, **229**, 96.
- Bradt, H., Rappaport, S., Mayer, W., Nather, R. E., Warner B., MacFarlane, M., and Kristian, J. 1969, *Nature*, **222**, 724.
- Brucato, R. J., and Kristian, J. 1972, *Ap. J. (Letters)*, **173**, L105.
- de Vaucouleurs, G., and de Vaucouleurs, A. 1964, *Reference Catalogue of Bright Galaxies* (Austin: University of Texas Press).
- de Veny, J. B., Osborn, W. H., and Hanes, K. 1972, *Pub. A.S.P.*, **83**, 611–624; and private communication.
- Downes, D. 1971, *A.J.*, **76**, 305.
- Forman, W., Jones, C. A., and Liller, W. 1972a, *Ap. J. (Letters)*, **177**, L103.
- Forman, W., Jones, C., Tananbaum, H., Gursky, H., Kellogg, E., and Giacconi, R. 1973, *Ap. J. (Letters)*, **182**, L103.
- Forman, W., Kellogg, E., Gursky, H., Tananbaum, H., and Giacconi, R. 1972b, *Ap. J.*, **178**, 309.
- Forman, W., Kellogg, E., Gursky, H., Tananbaum, H., Giacconi, R., Bradt, H., Moore, G., Kunkel, W. E., Hiltner, W. A., Thomas, J., Warner, B., and Vanden Bout, P. 1971, *Bull. AAS*, **3**, 457.
- Fritz, G., Davidson, A., Meekins, J., and Friedman, H. 1972, *Ap. J. (Letters)*, **164**, L81.
- Giacconi, R., Gorenstein, P., Gursky, H., Usher, P. D., Waters, J. R., Sandage, A. R., Osmer, P., and Peach, J. V. 1967, *Ap. J. (Letters)*, **148**, L129.
- Giacconi, R., Gursky, H., Kellogg, E., Levinson, R., Schreier, E., and Tananbaum, H. 1973, *Ap. J.*, **184**, 227.
- Giacconi, R., Gursky, H., Kellogg, E., Schreier, E., and Tananbaum, H. 1971, *Ap. J. (Letters)*, **167**, L67.
- Giacconi, R., Murray, S., Gursky, H., Kellogg, E., Schreier, E., and Tananbaum, H. 1972, *Ap. J.*, **178**, 281.
- Gursky, H., Kellogg, E., Leong, C., Tananbaum, H., and Giacconi, R. 1971a, *Ap. J. (Letters)*, **165**, L43.
- Gursky, H., Kellogg, E., Murray, S., Leong, C., Tananbaum, H., and Giacconi, R. 1971b, *Ap. J. (Letters)*, **167**, L81.
- Gursky, H., Solinger, A., Kellogg, E. M., Murray, S., Tananbaum, H., Giacconi, R., and Cavaliere, A. 1972, *Ap. J. (Letters)*, **173**, L99.
- Harnden, F. R., and Gorenstein, P. 1973, *Nature*, **241**, 107.
- Hawkins, F. J., Mason, K. O., and Sanford, P. W. 1973, *Nature*, **241**, 109.
- Hiltner, W. A., Werner, J., and Osmer, P. 1972, *Ap. J. (Letters)*, **175**, L19.
- Hjellming, R. M., Hermann, M., and Webster, E. 1972, *Nature*, **237**, 507.
- Hjellming, R. M., and Wade, C. M. 1971, *Ap. J. (Letters)*, **168**, L21.
- Hoffman, W. F., Frederick, C. L., and Emery, R. J. 1971, *Ap. J. (Letters)*, **164**, L23.
- Hunter, J. H., and Lu, P. K. 1969, *Nature*, **223**, 1045.
- Jones, C., Forman, W., Tananbaum, H., Schreier, E., Gursky, H., Kellogg, E., and Giacconi, R. 1973, *Ap. J. (Letters)*, **181**, L43.
- Kellogg, E. 1970, AS & E Report ASE 2536.
- Kellogg, E., Gursky, H., Leong, C., Schreier, E., Tananbaum, H., and Giacconi, R. 1971a, *Ap. J. (Letters)*, **165**, L49.
- Kellogg, E., Gursky, H., Murray, S., Tananbaum, H., and Giacconi, R. 1971b, *Ap. J. (Letters)*, **169**, L99.
- Kellogg, E., Murray, S., Giacconi, R., Tananbaum, H., and Gursky, H. 1973a, *Ap. J. (Letters)*, **185**, L13.
- Kellogg, E., Tananbaum, H., Harnden, F. R., Gursky, H., Giacconi, R., and Grindlay, J. 1973b, *Ap. J. (Letters)*, **183**, 935.
- Kraus, J. D. 1966, *Radio Astronomy* (New York: Macmillan), pp. 429–438.
- Leong, C., Kellogg, E., Gursky, H., Tananbaum, H., and Giacconi, R. 1971, *Ap. J. (Letters)*, **170**, L67.
- Lewis, W., McClintock, J., Ryckman, S., and Smith, W. 1971a, *Ap. J.*, **166**, 169.
- Lewis, W. H. G., Ricker, G. R., and McClintock, J. E. 1971b, *Ap. J. (Letters)*, **169**, L17.
- Liller, W. 1972, *IAU Circ.*, No. 2469.
- Margon, B., Spinrad, H., Heiles, C., Troumassian, H., Harlan, E., Bowyer, S., and Lampton, M. 1972, *Ap. J. (Letters)*, **178**, L77.
- Markarian, B. E. 1967, *Astrofizika*, **3**, 55–68.
- . 1969a, *ibid.*, **5**, 445–459.
- . 1969b, *ibid.*, pp. 581–592.
- Markert, G. H., Clark, G. W., Lewis, W. H. G., Schnopper, H. W., and Sprott, G. F. 1973, *IAU Circ.*, No. 2483.
- Matilsky, T. A., Giacconi, R., Gursky, H., Kellogg, E. M., and Tananbaum, H. D. 1972, *Ap. J. (Letters)*, **174**, L53.
- Milne, D. K. 1970, *Australian J. Phys.*, **23**, 425–444.
- Oda, M., and Matsuoka, M. 1970, *Progr. Elementary Particle and Cosmic Ray Phys.*, **10**, 305.
- Parsignault, D. R., Gursky, H., Kellogg, E. M., Matilsky, T., Murray, S., Schreier, E., Tananbaum, H., Giacconi, R., and Brinkman, A. C. 1972, *Nature*, **239**, 123.
- Ricker, G. R., McClintock, J. E., Gerassimento, M., and Lewis, W. H. G. 1973, *Ap. J.*, **184**, 237.
- Sandage, A. R., Osmer, P., Giacconi, R., Gorenstein, P., Gursky, H., Waters, J., Bradt, H., Garmire, G., Sreekantan, B. V., Oda, M., Osawa, K., and Jugaku, J. 1966, *Ap. J.*, **146**, 316.
- Schreier, E., Giacconi, R., Gursky, H., Kellogg, E., and Tananbaum, H. 1972a, *Ap. J. (Letters)*, **178**, L71.
- Schreier, E., Gursky, H., Kellogg, E., Tananbaum, H., and Giacconi, R. 1971, *Ap. J. (Letters)*, **170**, L21.
- Schreier, E., Levinson, R., Gursky, H., Kellogg, E., Tananbaum, H., and Giacconi, R. 1972b, *Ap. J. (Letters)*, **172**, L79.
- Seward, F. 1970, "An Illustrated Catalog of Cosmic Ray Sources" (LRL Report UDID-15622).
- Tananbaum, H., Gursky, H., Kellogg, E., and Giacconi, R. 1971a, *Ap. J. (Letters)*, **168**, L25.
- Tananbaum, H., Gursky, H., Kellogg, E., Giacconi, R., and Jones, C. 1972, *Ap. J. (Letters)*, **177**, L5.
- Tananbaum, H., Kellogg, E., Gursky, H., Murray, S., Schreier, E., and Giacconi, R. 1971b, *Ap. J. (Letters)*, **165**, L37.
- Terzian, Y. 1973, "Pulsars" (Cornell University, private communication).
- Tucker, W., Kellogg, E., Gursky, H., Giacconi, R., and Tananbaum, H. 1973, *Ap. J.*, **183**, 357.
- Ulmer, M. P., Baity, W. A., Wheaton, W. A., and Peterson, L. E. 1972, *Ap. J. (Letters)*, **178**, L121.
- Webster, B. L., and Murdin, P. 1972, *Nature*, **235**, 37.